# PhD PROCEEDINGS

ANNUAL ISSUES OF THE DOCTORAL SCHOOL

FACULTY OF INFORMATION TECHNOLOGY & BIONICS

2018

PhD PROCEEDINGS

ANNUAL ISSUES OF THE DOCTORAL SCHOOL

FACULTY OF INFORMATION TECHNOLOGY & BIONICS
PÁZMÁNY PÉTER CATHOLIC UNIVERSITY

# PhD PROCEEDINGS

ANNUAL ISSUES OF THE DOCTORAL SCHOOL

FACULTY OF INFORMATION TECHNOLOGY & BIONICS

2018


PÁZMÁNY UNIVERSITY *e*PRESS
BUDAPEST, 2018

HU ISSN 2064-7271

Kiadja a Pázmány Egyetem eKiadó
Budapest, 2018

Felelős kiadó
Ft. Dr. Szuromi Szabolcs Anzelm O. Praem.
a Pázmány Péter Katolikus Egyetem rektora

The publication of this volume was supported by the European Union,
co-financed by the European Social Fund (EFOP-3.6.3-VEKOP-16-2017-00002.

Cover image by Áron Cserkaszky: *Circular camera array epipolar image of the test scene.*

# Contents

.

# Introduction

It is our pleasure to publish this Annual Proceedings again to demonstrate the genuine interdisciplinary research done at the Jedlik Laboratories by young talents working in the Roska Tamás Doctoral School of Sciences and Technology of the Faculty of Information Technology and Bionics at Pázmány Péter Catholic University. The scientific results of our PhD students show the main recent research directions in which our faculty is engaged. Thanks are also due to the supervisors and consultants, as well as to the five collaborating National Research Laboratories of the Hungarian Academy of Sciences, the Semmelweis Medical School and the University of Pannonia. The collaborative work with the partner universities, especially, Katolieke Universiteit Leuven, Politecnico di Torino, Technische Universität München, University of California at Berkeley, University of Notre Dame, Universidad de Sevilla, Universita di Catania, Université de Bordeaux, Universidad Autonoma de Madrid is gratefully acknowledged.

We acknowledge the many sponsors of the research reported here. Namely,

- the Hungarian National Research Fund (OTKA),
- the Hungarian Academy of Sciences (MTA),
- the National Research, Development and Innovation Office (NKFIH),
- the Gedeon Richter Co.,
- the Office of Naval Research (ONR) of the US,
- NVIDIA Ltd.,
- Verizon Computer Vision Group (Eutecus Inc.), Berkeley, CA,
- MorphoLogic Ltd., Budapest,
- Analogic Computers Ltd., Budapest,
- AnaFocus Ltd., Seville,

and some other companies and individuals.

Needless to say, the resources and support of the Pázmány Péter Catholic University is gratefully acknowledged.

Budapest, June 2018.

GÁBOR PRÓSZÉKY
Chairman of the Board of the Doctoral School

PÉTER SZOLGAY
Head of the Doctoral School

.

# PROGRAM 1
# BIONICS, BIO-INSPIRED WAVE COMPUTERS, NEUROMORPHIC MODELS

Heads: Tamás FREUND, György KARMOS, Zsolt LIPOSITS, Sándor PONGOR

# Altered protection against xenobiotics in the aged brain? – Functional changes of P-glycoprotein at the blood brain barrier.

Luca Anna BORS
(Supervisor: Franciska ERDŐ)
Pázmány Péter Catholic University, Faculty of Information Technology and Bionics
50/a Práter street, 1083 Budapest, Hungary
bors.luca.anna@itk.ppke.hu

Statement of originality – *This proceedings report describes the work of the doctoral student during the academic year 2017/2018. Parts of this work might be under submission to scientific conferences and journals.*

## Summary

We investigated the structural and functional changes of the blood-brain barrier (BBB) that occurs with advancing age. Although the fact of these alterations was already known [1], [2], the exact background of the increased leakage of the BBB is yet to discover. We categorized the results into two groups; the first one includes the structural alterations of the BBB, like the morphology of blood vessels in the brain and the other one is the collection of functional changes which include the effectiveness of the transporter proteins in BBB.

## Methods

With the help of multiple methods we studied the aging of BBB in rat models. The morphological differences of young and old brain capillaries were examined with light- and electronmicroscopy in fixated rat brains. The investigation of functional changes was focused on the activity and number of P-gp, one of the efflux transporters of the BBB. Two substrates of this transporter were used; [99mTechnetium]-2-methoxy-isobutyl-isonitrile as a radioactive tracer for SPECT imaging and quinidine for dual- and triple-probe microdialysis experiments. The biological samples of microdialysis were analyzed with HPLC-MS/MS. In our study, Wistar rats were used as model animals for healthy aging.

## Results and discussion

The histology showed that the capillaries of the brain are going through significant changes even in healthy aging. The wall of the blood vessels and the basal membrane were thickened, the number of tight junctions and P-gp transporter proteins were decreased while the astorcyte endfeet count and the staining of GFAP was increased in aged brains. SPECT and microdialysis results also showed that the BBB does not block out xenobiotics and drugs in aged rats as much as in young adults. These two methods also showed that the elimination of P-gp substrates slows down in old brain. Another finding was the different pharmacokinetics of young and middle-aged animals in response to pre-treatment of PSC-833, a second generation P-gp inhibitor. The inhibition of P-gp was significant in young rats while there was much less difference between the brain concentration of substrates in the aged pre-treated and non-treated groups.

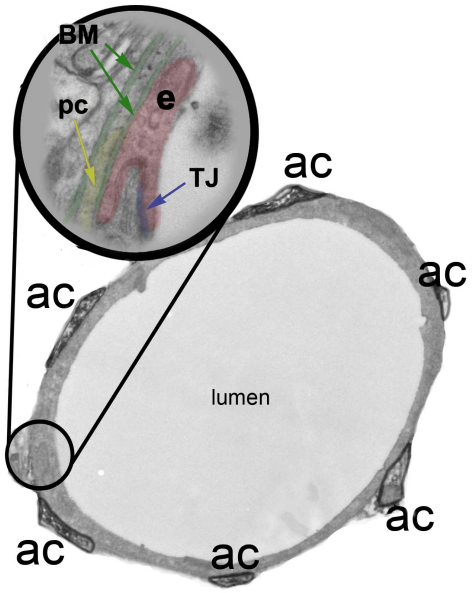


Fig. 1. Drawing of the blood-brain barrier, illustrates the capillary and its cellular environment. ac: astrocyte, pc: pericyte, e: endothelial cell, BM: basal membrane, TJ: tight junction

## References

[1] F. Erdő, L. Denes, and E. de Lange, "Age-associated physiological and pathological changes at the blood-brain barrier: A review.," *J Cereb Blood Flow Metab.*, vol. 37, no. 1, pp. 4-24, 2017.

[2] E. Beéry, Z. Rajnai, T. Abonyi, I. Makai, S. Bánsághi, F. Erdő, I. Sziráki, K. Herédi-Szabó, E. Kis, M. Jani, J. Márki-Zay, G. K. Tóth and P. Krajcsi, "ABCG2 modulates chlorothiazide permeability–in vitro-characterization of its interactions.," *Drug Metab Pharmacokinet.*, vol. 27, no. 3, pp. 349-53, 2012.

L. BORS, "Altered protection against xenobiotics in the aged brain? - Functional changes of P-glycoprotein at the blood brain barrier." in *PhD Proceedings Annual Issues of the Doctoral School, Faculty of Information Technology and Bionics, Pázmány Péter Catholic University – 2018.* G. Prószéky, P. Szolgay Eds. Budapest: Pázmány University ePress, 2018, pp. 12–12. This research has been partially supported by the European Union, co-financed by the European Social Fund (EFOP-3.6.3-VEKOP-16-2017-00002).

# The role of secretin signaling in the regulation of GnRH neurons

Veronika CSILLAG
(Supervisors: Imre FARKAS, Zsolt LIPOSITS)
Pázmány Péter Catholic University, Faculty of Information Technology and Bionics
50/a Práter street, 1083 Budapest, Hungary
csillag.veronika@itk.ppke.hu

Reproduction is controlled by the hypothalamo-pituitary-gonadal (HPG) axis in mammals and its main central regulators, the hypophysiotropic gonadotropin-releasing hormone (GnRH)-expressing neurons.

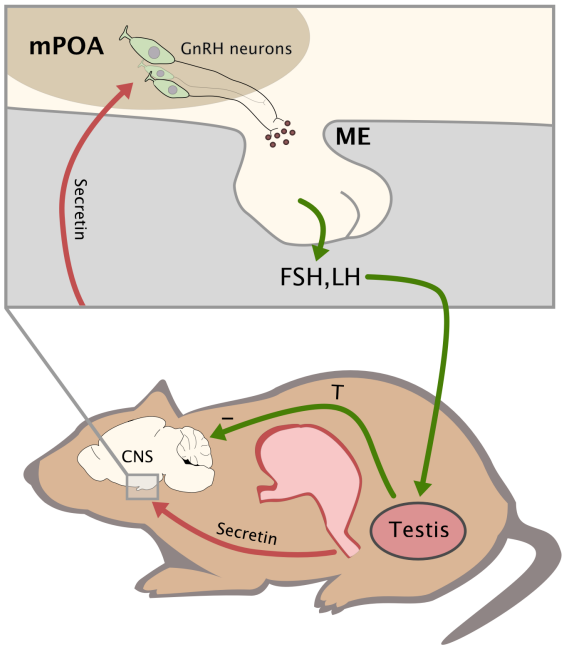


Fig. 1. Shematic figure of HPG axis in male mice. Fusiform GnRH neurons are located in the mPOA of the hypothalamus and their axons terminate in the median eminence (ME) where they secrete GnRH into the portal circulation. Red arrows show the relationship between secretin and the reproductive axis. Secretin is produced in the duodenum into the peripheral circulation, and after entering the CNS, it can affect GnRH neurons and reproduction.

Dysfunction of the reproductive axis can cause infertility. The HPG axis is affected by signalling from both the central nervous system and the periphery. Gut hormones are able to relay information about the energy homeostasis. These hormones are secreted from enteroendocrine cells, and majority of them are able to pass the blood brain barrier (BBB). Ghrelin which is an orexigenic hormone produced by the stomach, decreases the firing of GnRH neurons [1]. In contrast, glucagon-like peptide 1 (GLP-1) increases the activity of GnRH neurons [2]. Secretin is also a member of gut hormone family and it is released from the S-cells in the small intestine. It is a 27 amino-acid peptide which can pass the blood-brain barrier. Secretin receptor is a G-protein-coupled receptor, and it has been mapped in different regions of the brain, including the hypothalamus [3]. Since gonadotropin-releasing hormone (GnRH) neurons are the key regulators of the reproduction, any secretin-induced modulation of the GnRH neuronal system has a major impact on various events of reproduction. Therefore, the present study was undertaken to examine the putative, direct effects of secretin upon electric activity of GnRH neurons in male mice.

Whole cell patch clamp measurments on acute brain slices revealed the following results:

1) Secretin dose dependently increased the frequency of sPSCs in GnRH neurons, and the lowest effective concentration was 100nM.
2) Secretin (100nM) also elevated the frequency of mPSCs in the presence of TTX, which result shows direct effect of secretin in GnRH neurons.
3) Pretreatment with secretin antagonist eliminated the excitatory effect of secretin on mPSCs. It means, that secretin seems to affect the HPG axis via secretin receptors expressed in GnRH neurons.
4) Secretin application significantly depolarized the membrane potential in GnRH neurons, which is in accordance with the excitability of these neurons.

Changes in the frequency of mPSCs, but not in the amplitude indicate, that secretin may increase the probability of vesicular release of GABA from presynaptic terminals. GABA is the main excitatory neurotransmitter via $GABA_A$-receptors upon GnRH neurons of male mice. GABA can excite GnRH neurons because of the high intracellular $Cl^-$ level of the cells. In GnRH neurons, there are two retrograde signalization pathways wich can influence the presynaptic mechanisms. One is the retrograde endocannabinoid pathway and the other is the NO dependent retrograde signalling pathway [1], [2]. Nevertheless, which pathway is involved in the effect of secretin, requires further examinations in the subsequent year.

## Acknowledgements

The author wishes to acknowledge Dr. Imre Farkas and Prof. Zsolt Liposits for their excellent supervision.This research was supported by the National Science Foundation of Hungary (OTKA K100722, K115984).

## References

[1] Farkas, I., et al., Ghrelin decreases firing activity of gonadotropin-releasing hormone (GnRH) neurons in an estrous cycle and endocannabinoid signaling dependent manner. PLoS One, 2013. 8(10): p. e78178.
[2] Farkas, I., et al., Glucagon-Like Peptide-1 Excites Firing and Increases GABAergic Miniature Postsynaptic Currents (mPSCs) in Gonadotropin-Releasing Hormone (GnRH) Neurons of the Male Mice via Activation of Nitric Oxide (NO) and Suppression of Endocannabinoid Signaling Pathways. Front Cell Neurosci, 2016. 10: p. 214.
[3] 3. Toth, Z.E., et al., Distribution of secretin receptors in the rat central nervous system: an in situ hybridization study. J Mol Neurosci, 2013. 50(1): p. 172-8.

V. CSILLAG, “The role of secretin signaling in the regulation of GnRH neurons” in *PhD Proceedings Annual Issues of the Doctoral School, Faculty of Information Technology and Bionics, Pázmány Péter Catholic University – 2018.* G. Prószéky, P. Szolgay Eds. Budapest: Pázmány University ePress, 2018, pp. 13–13. This research has been partially supported by the European Union, co-financed by the European Social Fund (EFOP-3.6.3-VEKOP-16-2017-00002).

# Characterization of the CFTR chloride channel using *in silico* methods

Bianka Vivien FARKAS
(Supervisor:Tamás HEGEDŰS, Zoltán GÁSPÁRI)
Pázmány Péter Catholic University, Faculty of Information Technology and Bionics
50/a Práter street, 1083 Budapest, Hungary
farkas.bianka.vivien@itk.ppke.hu

Cystic fibrosis (CF) is a monogenic disease caused by the mutant variants of the cystic fibrosis conductance regulator (ABCC7/CFTR), a member of the ATP Binding Cassette (ABC) protein superfamily. The impaired function of CFTR chloride channel leads to a reduced chloride conductance in the epithelial cells, which results in disturbances of the salt and water homeostasis [1]. There are small molecule drugs, which partially rescue the protein folding and function, but their efficiency is marginal [2]. A detailed knowledge of the atomic resolution structure is required to develop drug molecules to treat CF more efficiently. Recent advances in single molecule cryo-electron microscopy (cryo-EM) methods enabled the determination of the full-length CFTR structures (human: hCFTR, zebrafish: zCFTR).

The CFTR protein has two transmembrane domains (TMD) consisting of six transmembrane helices (TH) and two cytosolic nucleotide binding domains (NBD) [3]. NBDs bind and hydrolyze the ATP molecules to generate conformational changes in the structure enabling the conductance of chloride ions through the cell membrane in the channel formed by the TMDs [4], [5]. For channel opening the phosphorylation of the intrinsically disordered R domain (RD) is required [6]. The recently determined zCFTR structure (PDBID:5W81) is determined in the active, ATP-bound, phosphorylated conformation, but it lacks an open channel for chloride permeation [7]. The stable closure may arise from the disturbed transmembrane helix 8 (TH8) and the loosely associated NBDs, which may result in the lack of required conformational changes to form an open channel. In addition, the degenerate ATP Site-1 is less compact compared to the Site-2, which is unexpected as Site-1 binds strongly the ATP-molecule according to experimental studies [5], [8].

Our main goal is to characterize the CFTR structure based on both experimental and homology models using *in silico* methods. We performed molecular dynamics simulations (MD) with the ATP-bound zCFTR structure embedded in a lipid bilayer to study the dynamics of the channel opening of and we analyzed the generated open conformations using channel detecting softwares (HOLE [9], CAVER [10]) to describe the properties of the chloride channel.

Our results suggest that the zCFTR conformation is either rare under physiological conditions or it could have been distorted due to the conditions required for cryo-EM structure determination. To overcome the lack of channel opening we generated a CFTR structural model with modified TH8 based on the MRP1 (PDBID: 6BHU) to correct the disruption in this transmembrane helix. The simulations of the remodeled CFTR show feasible channel opening events and a detailed analysis of the resulting conformations is in progress.

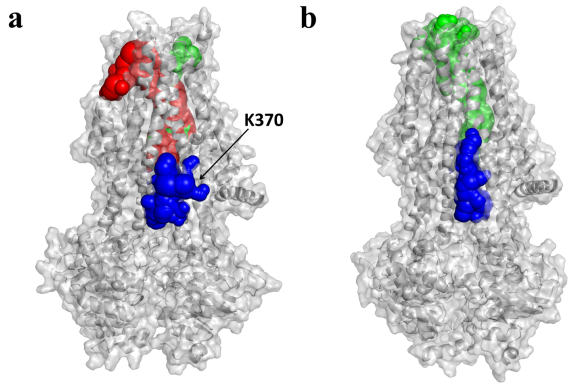


Fig. 1. Tunnels identified by CAVER in the simulations of the zCFTR (a) and in the simulations of the remodeled CFTR structures (b). Different tunnel clusters are labeled with different colors.

## REFERENCES

[1] J. R. Riordan, J. M. Rommens, B. Kerem, N. Alon, R. Rozmahel, Z. Grzelczak, J. Zielenski, S. Lok, N. Plavsic, and J. L. Chou, "Identification of the cystic fibrosis gene: cloning and characterization of complementary DNA," vol. 245, no. 4922, pp. 1066–1073.

[2] M. P. Boyle, S. C. Bell, M. W. Konstan, S. A. McColley, S. M. Rowe, E. Rietschel, X. Huang, D. Waltz, N. R. Patel, and D. Rodman, "A CFTR corrector (lumacaftor) and a CFTR potentiator (ivacaftor) for treatment of patients with cystic fibrosis who have a phe508del CFTR mutation: a phase 2 randomised controlled trial," vol. 2, no. 7, pp. 527–538.

[3] K. P. Locher, "Mechanistic diversity in ATP-binding cassette (ABC) transporters," vol. 23, no. 6, pp. 487–493.

[4] N. A. McCarty, "Permeation through the CFTR chloride channel," vol. 203, pp. 1947–1962.

[5] D. Muallem and P. Vergani, "ATP hydrolysis-driven gating in cystic fibrosis transmembrane conductance regulator," vol. 364, no. 1514, pp. 247–255.

[6] S. H. Cheng, D. P. Rich, J. Marshall, R. J. Gregory, M. J. Welsh, and A. E. Smith, "Phosphorylation of the r domain by cAMP-dependent protein kinase regulates the CFTR chloride channel," vol. 66, no. 5, pp. 1027–1036.

[7] Z. Zhang, F. Liu, and J. Chen, "Conformational changes of CFTR upon phosphorylation and ATP binding," vol. 170, no. 3, pp. 483–491.e8.

[8] L. Aleksandrov, A. A. Aleksandrov, X.-B. Chang, and J. R. Riordan, "The first nucleotide binding domain of cystic fibrosis transmembrane conductance regulator is a site of stable nucleotide interaction, whereas the second is a site of rapid turnover," vol. 277, no. 18, pp. 15419–15425.

[9] O. S. Smart, J. G. Neduvelil, X. Wang, B. A. Wallace, and M. S. P. Sansom, "HOLE: A program for the analysis of the pore dimensions of ion channel structural models," vol. 14, no. 6, pp. 354–360.

[10] M. Petřek, M. Otyepka, P. Banáš, P. Košinová, J. Koča, and J. Damborský, "CAVER: a new tool to explore routes from protein clefts, pockets and cavities," vol. 7, p. 316.

B. FARKAS, "Characterization of the CFTR chloride channel using in silico methods" in *PhD Proceedings Annual Issues of the Doctoral School, Faculty of Information Technology and Bionics, Pázmány Péter Catholic University – 2018.* G. Prószéky, P. Szolgay Eds. Budapest: Pázmány University ePress, 2018, pp. 14–14. This research has been partially supported by the European Union, co-financed by the European Social Fund (EFOP-3.6.3-VEKOP-16-2017-00002).

# Method development for the investigation of cell-cell interactions in *S. cerevisiae*

Tünde GAIZER
(Supervisor: Attila CSIKÁSZ-NAGY)
Pázmány Péter Catholic University, Faculty of Information Technology and Bionics
50/a Práter street, 1083 Budapest, Hungary
gaizer.tunde.eva@itk.ppke.hu

***Abstract*—Traditional investigations of microbial colony formation include mostly one strain at a time, however in their natural settings multiple, often genetically closely related strains live simultaneously. These mixed colonies provide opportunity to a great variety of interactions to occur. Besides the competition for nutrients, microbes can develop different strategies for better survival, like cooperation or competition. To better understand these kinds of interactions and their molecular background, we are developing a systems biological approach to investigate interactions between different strains of the budding yeast *Saccharomyces cerevisiae*.**

***Keywords*-systems biology, mathematical modelling, high-throughput genomics, yeast**

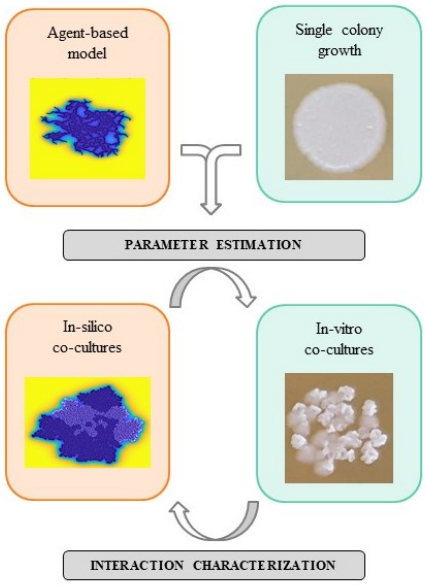


Fig. 1. Summary of research plan

## DISCUSSION

Cell-cell interactions have been shown to play fundamental role in many areas, including maintaining biodiversity [1], or in tumor formation [2]. The model organism investigated is the widely used *S. cerevisiae*. Several *S. cerevisiae* strains are used in the industry (wine, beer fermentation, as a chassis is pharma) and several laboratory strains are used as test organisms for basic research. Besides the general lab strains, a wide selection of natural isolates will be included in our studies. Some of these has been shown before to exhibit social interactions, such as cooperation and cheater control behavior [3]. Our approach is combining computational and experimental methods as shown on figure 1. For this purpose, an agent based mathematical model is developed to simulate yeast growth *in-silico* and experimental procedures are being developed that support parametrization of the model. Afterwards experiments will be carried out with mixed colonies both *in-vitro* and *in-silico*. Experimental environment is being developed taking into consideration the aspects required for differentiating strains next to each other and also screening large number of strains in the future.

## REFERENCES

[1] B. Kerr, M. A. Riley, M. W. Feldman, and B. J. M. Bohannan, "Local dispersal promotes biodiversity in a real-life game of rock-paper-scissors.", *Nature*, vol. 418, no. 6894, pp. 171–174, 2002.
[2] A. Csikász-Nagy, L. M. Escudero, M. Guillaud, S. Sedwards, B. Baum, and M. Cavaliere, "Cooperation and competition in the dynamics of tissue architecture during homeostasis and tumorigenesis," *Seminars in Cancer Biology*, vol. 23, no. 4. Elsevier Ltd, pp. 293–298, 2013.
[3] D. Rivero, L. Berná, I. Stefanini, E. Baruffini, A. Bergerat, A. Csikász-Nagy, C. De Filippo, and D. Cavalieri, "Hsp12p and PAU genes are involved in ecological interactions between natural yeast strains," *Environ. Microbiol.*, vol. 17, no. 8, pp. 3069–3081, 2015.

T. GAIZER, "Method development for the investigation of cell-cell interactions in S. cerevisiae " in *PhD Proceedings Annual Issues of the Doctoral School, Faculty of Information Technology and Bionics, Pázmány Péter Catholic University – 2018.* G. Prószéky, P. Szolgay Eds. Budapest: Pázmány University ePress, 2018, pp. 15–15. This research has been partially supported by the European Union, co-financed by the European Social Fund (EFOP-3.6.3-VEKOP-16-2017-00002).

# The investigation of the Fetal Breathing Movement using Synchronized Measurement of Phonocardiogram and Ultrasound Imaging

Márton Áron GODA
(Supervisor: Ferenc KOVÁCS)
Pázmány Péter Catholic University, Faculty of Information Technology and Bionics
50/a Práter street, 1083 Budapest, Hungary
goda.marton.aron@itk.ppke.hu

***Abstract*—The fetal breathing movement (FBM) is an important data according to its well-being, however, the measurement of them is circuitous because its appearance and inconvenient also for the mother. On this problem may help the extension of the fetal phonocardiographic monitoring (fPCG) when the same sensor head is applied on the maternal abdomen even for a long time at home.**

**The paper presents a two-step method to get information about the FBM through its sound signal and accomplishing these provides the reliability of FBM's carried out. The first step is the hypothetic features extraction, which is based on a multi-pass method. The second step uses the Support Vector Machine (SVM) in order to determine the real FBMs distinguishing their sounds from the other disturbing signals as hiccup, fetal body and limb movements or even additional noises of the mother.**

***Keywords*-keyword; fetal breathing movement, phonocardiography, time-frequency domain analysis, SVM**

Statement of originality: This report describes the work of the doctoral student during the academic year 2017/2018. Parts of this work might be under submission to scientific conferences and journals.

## I. Introduction

The list of non-invasive measurements of fetal monitoring is rather poor which therefore contains also the FBM being a part since [1] of the biophysical profile of the fetus. The first attempts to perceive this motion applied an ultrasonic scanner, as at the examinations of [2] validating the circadian rhythms and as well separating between gross body movements and breathing.

The ultrasound measurements were the most useful devices for fetal heart monitoring on an indirect way also proper for motion registration. That means, that the extension of the commercial Doppler CTG with a phase modulation the aid of which the complex motion of the fetus can be observed [3]. An interesting approach has been developed with pulsed B-scan ultrasound for tracking moving image parts in order to quantify of FBM by [4]. The system allowed detection of the wanted movements, however, its regular use was very inconvenient.

The application of the fetal phonocardiography (fPCG) on which broad scientific results, technical details and experiences are available [5].

## II. Methods and data processing

Because of the required high reliability of FBM selection a two-step method has been chosen. The essence of this is that in the first step a feedback, successive approximation procedure helps to determine those features, which at the second step as the input dataset of a Support Vector Machine (SVM) type classifier at further measurements reliably separates the breathing movements from others, generated either from the fetus or the mother.

Taking into account the available possibilities for analysing the rather complex and random-like FBM signal in question as second step for the classifying the Support Vector Machine (SVM) method seemed the most promising [6]. Due this may be guarantee the canceling of truncated breathing movements, hiccups, or other motions of the fetus with limb or body, or even the external noises including the maternal heart sounds.

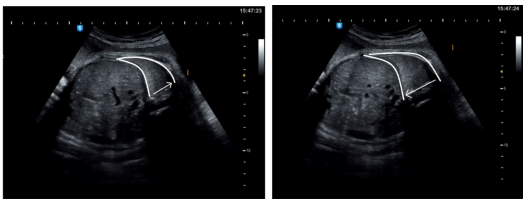

Fig. 1. The observation of motion on the sonographic image. The contraction and relaxation of the diaphragm is visible within 1.2 seconds, which is indicating a typical FBM episode.

## III. RESULTS

From more than 1000 former measured records after evaluating its content 100 pieces have been selected which all have more or less a joined part of fetal breathing. In order to validate our measurements further 50 measurements have been carried out with a simultaneous video recording of the well observed physical motions and acoustic sounds received from the maternal abdomen.

## References

[1] T. F. Baskett, *Gestational age and fetal biophysical assessment*, American Journal of Obstetrics and Gynecology, vol. 158,1988, pp. 332-334.

[2] J. Patrick, R. Natale, B. Richardson: *Patterns of human fetal breathing activity at 34 to 35 week's gestational age*, Amer. J. Obstet. Gynecol., vol. 132 (1978), pp. 507-513.

[3] K. Foulquiere et al.: *The Antepartum Assessment of Fetal Well-beingt*, IEEE Sympoium for Ultrasonics, 2000, pp. 1391-1394.

[4] A. J. Cousin, I. Rapoport, K. Campbell, J. E. Patrick: *Tracking System for Pulsed Ultrasound Images: Application to Quantification of Fetal Breathing Movements*, IEEE Transactions on Biomedical Engineering, 1983, pp. 577-587.

[5] F. Kovács et al.: *Extended Non-Invasive Fetal Monitoring by Detailed Analysis of Data Measured with Phonocardiography*, IEEE Trans. on Biomed. Eng. Vol. 58, No.1 (Jan. 2011) pp. 64-70.

[6] M. Á. Goda, P. Hajas: *Morphological Determination of Pathological PCG Signals by Time and Frequency Domain Analysis*, Computing in Cardiology - Vancouver, 2016, pp. 1133-1136.

M. GODA, "The investigation of the Fetal Breathing Movement using Synchronized Measurement of Phonocardiogram and Ultrasound Imaging" in *PhD Proceedings Annual Issues of the Doctoral School, Faculty of Information Technology and Bionics, Pázmány Péter Catholic University – 2018.* G. Prószéky, P. Szolgay Eds. Budapest: Pázmány University ePress, 2018, pp. 16–16. This research has been partially supported by the European Union, co-financed by the European Social Fund (EFOP-3.6.3-VEKOP-16-2017-00002).

# Stimulation and expansion of peripheral blood $\gamma\delta$ T cells

Anna HAJDARA
(Supervisor: Sarolta KÁRPÁTI, Miklós GYÖNGY)
Pázmány Péter Catholic University, Faculty of Information Technology and Bionics
50/a Práter street, 1083 Budapest, Hungary
hajdara.anna@itk.ppke.hu

***Abstract*—$\gamma\delta$ T cells represent a minor population of lymphocytes, however play an important role of immune surveillance and elimination of malignant cells. Unlike the conventional type of T cells carrying the $\alpha\beta$ T cell receptor (TCR), they respond to non-processed and non-peptidic antigens through MHC unrestricted mechanisms [1]. There are emerging evidences, that $\gamma\delta$ T cells can infiltrate solid tumors and play an important role in anti-tumor immune response. The metabolic changes in tumors can lead to increased accumulation and release of isopentenyl-pyrophosphate (IPP) that $\gamma\delta$ T cells can sense directly and this leads to their activation. Once activated, $\gamma\delta$ T cells contribute to the immune response with broad cytotoxic activity. In addition to their direct cytotoxic effect, their secretions of Th1 cytokines, such as IFN-$\gamma$ and TNF-$\alpha$ inhibit the tumor growth and promote the apoptotic pathway in tumor cells [2]. The role of $\gamma\delta$ T cells in carcinomas is extensively studied, but little is known about them in melanoma and other types of malignant skin diseases. In this manuscript, I demonstrate the methodology of $\gamma\delta$ T cell proliferation from isolated peripheral blood mononuclear cells (PBMCs) and the isolation of dermal fibroblasts from healthy controls according to our previous in house protocol. I use flow cytometry analysis to compare $\gamma\delta$ T cell ratio/numbers in zoledronic acid and interleukin-2 stimulated and unstimulated PBMCs. My results show, that $\gamma\delta$ T cells are present in the peripheral blood only in low numbers, but stimulation with zoledronic acid and interleukin-2 increases their ratio/numbers. These cells are double positive for the pan T cell marker CD3 and $\gamma\delta$ TCR. These results demonstrate that $\gamma\delta$ T cells can be expanded from PBMC with zoledronic acid (an FDA and EMA approved drug) and could be potential target for further experiments in melanoma and other malignant skin diseases.**

## Results

**After isolation and stimulation of PBMCs with high dose zoledronic acid and interleukine-2 the ratio/number of $\gamma\delta$ T cells was significantly increased. For optimization of CCK-8 proliferation assay normal dermal fibroblasts were used. CCK-8 - a colorimetric assay contains water soluble tetrazolium salt (WST-8) which is reduced by the dehydrogenase activites of cells to give an orange color formazan dye. Dermal fibroblasts from surgical specimen are more available in house, than PBMCs and further optimization will be conducted with them.**

## Conclusion

Our results indicate that the $\gamma\delta$ T cell proliferation protocol we use is adequate for further experiments and stimulation of PBMCs with zoledronic acid and interleukin-2 might be essential for the enrichment of $\gamma\delta$ T cells. Addition of markers for distinguishing $\delta1$ and $\delta2$ T cell subpopulations are needed for future experiments.

## Materials and Methods

### A. Cell isolation and stimulation

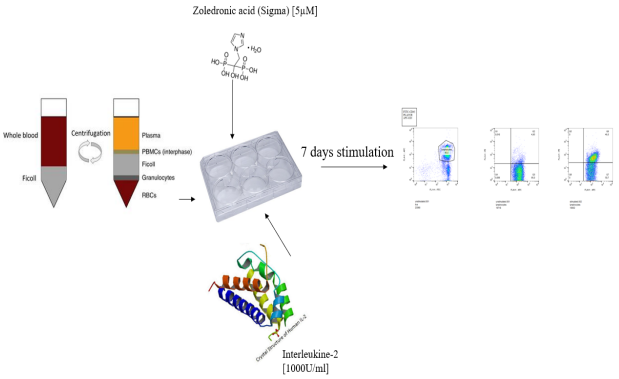


Fig. 1. Figure 1.: PBMC isolation and stimulation with high dose zoledronic acid and interleukine-2 leads to the expansion of $\gamma\delta$ T cells

## References

[1] C. Peters, D. Kabelitz, and D. Wesch, "Regulatory functions of $\gamma\delta$ T cells," Cell. Mol. Life Sci., no. 123456789, pp. 1–11, 2018.

[2] P. Vantourout and A. Hayday, "Six-of-the-best: Unique contributions of $\gamma\delta$ T cells to immunology," Nat. Rev. Immunol., vol. 13, no. 2, pp. 88–100, 2013.

A. HAJDARA, "Stimulation and expansion of peripheral blood $\gamma\delta$ T cells" in *PhD Proceedings Annual Issues of the Doctoral School, Faculty of Information Technology and Bionics, Pázmány Péter Catholic University – 2018.* G. Prószéky, P. Szolgay Eds. Budapest: Pázmány University ePress, 2018, pp. 17–17.
This research has been partially supported by the European Union, co-financed by the European Social Fund (EFOP-3.6.3-VEKOP-16-2017-00002).

# Ensemble-based assessment of the internal dynamics of small antifungal proteins

Máté HANDBAUER
(Supervisor: Zoltán GÁSPÁRI)
Pázmány Péter Catholic University, Faculty of Information Technology and Bionics
50/a Práter street, 1083 Budapest, Hungary
handbauer.mate@itk.ppke.hu

## I. Introduction

Small, cysteine-rich and cationic proteins with antimicrobial activity are produced by the most diverse organisms (e.g. bacteria, fungi, plants, insects, amphibians and humans). The ancestor of all industrial penicillin producing strains, the filamentous Ascomycete Penicillium chryosgenum Q176 secretes the extensively examined ([1] [2] [3]) protein PAF. The protein exhibits antimicrobial and antimycotic activity towards a variety of filamentous fungi, e.g. the often lethal Aspergillus infections that occur in humans (Aspergillus niger, A. fumigatus) and plant pathogenic molds (Botrytis cinerea) without toxic effects on mammalian cells. Therefore it may represent a considerable drug candidate against the aforementioned pathogens.

The pathogenesis of PAF on sensitive fungi involves G-protein coupled signaling followed by apoptosis.[1] The genome of this strain contains at least two gene with akin attributes. Such as the gene coding PAFB (and its shorter form sfPAFB) and the as thoroughly investigated AFP secreted by the filamentous ascomycete Aspergillus giganteus. [4]

Both PAF and AFP belong to a distinct group of cysteine-rich proteins, effectively inhibiting the growth of numerous plant-pathogenic and zoo-pathogenic filamentous fungi. Although they are close homologues there are substantial differences between the mode of action of the two. AFP is predominantly membrane and cell wall-based while PAF appears to be primarily receptor-based G-protein coupled apoptosis inducer. [1]

In order to understand the mode of action of PAF, there was an investigation on the surface-exposed loops of PAF by replacing one aspartic acid at position 19 in loop 2 that is potentially involved in active or binding, with a serine (Asp19 to Ser19) This PAFD19S (shortly D19S) is a noteworthy synthetic type of PAF. The analyses revealed that the overall structure of D19s is virtually identical with that of PAF. However, D19S showed slightly increased dynamics and significant differences in the surface charge distribution and showed that PAFD19S to be rather a two-state folder in contrast to the three-state folder PAF and a loss of antifungal activity by failing to trigger an intracellular Ca2+ response, all of which are closely linked to the antifungal toxicity of PAF. [3] The protein sfPAFB carries attributes beyond the antifungal protein properties, such as high stability, antiviral activity, and reversible denaturation.

By creating a structural ensemble of PAF, D19S, AFP and sfPAFB that represents the experimentally observed motions of the protein and using computational methods such as molecular dynamics (MD) may help to understand the mechanics behind these functions. I have applied MD simulations combined with experimental data derived from NMR measurements, and used Principal Component Analysis (PCA) in order to examine the dynamics of the molecules.

## II. Results

I performed calculations to explore the structural diversity of the disulfide-rich protein sfPAFB, its homologue PAF and the artificial protein D19S. I have used restrained molecular dynamics simulations. The MD run with MUMO method using $S^2$ and NOE restraints was simulated a 20 ns time-interval with a sampling in every 100 ps and 2 fs time-step in explicit solvent, at 298 K in 8 threads. Comparisons were made on the proteins with experimental data with CoNSEnsX+ for evaluation.

PCA was performed on the ensembles using local root-mean-square deviation (RMSD) on the aforementioned proteins and AFP using experimental and simulation-determined data. While the D19S showed a great change in both modes, the other molecules were showed dynamical motion mostly along mode 2. These motions where mainly in the ps-ns timescale. Sequence alignment including 54 sequences were also made.

## References

[1] G. Batta, T. Barna, Z. Gáspári, S. Sándor, K. E. Kövér, U. Binder, B. Sarg, L. Kaiserer, A. K. Chhillar, A. Eigentler, É. Leiter, N. Hegedüs, I. Pócsi, H. Lindner, and F. Marx, "Functional aspects of the solution structure and dynamics of PAF - A highly-stable antifungal protein from Penicillium chrysogenum," *FEBS Journal*, vol. 276, no. 10, pp. 2875–2890, 2009.

[2] d. Fizil, Z. G??sp??ri, T. Barna, F. Marx, and G. Batta, ""Invisible" Conformers of an Antifungal Disulfide Protein Revealed by Constrained Cold and Heat Unfolding, CEST-NMR Experiments, and Molecular Dynamics Calculations," *Chemistry - A European Journal*, vol. 21, no. 13, pp. 5136–5144, 2015.

[3] C. Sonderegger, Á. Fizil, L. Burtscher, D. Hajdu, A. Muñoz, Z. Gáspári, N. D. Read, G. Batta, and F. Marx, "D19S Mutation of the Cationic, Cysteine-Rich Protein PAF: Novel Insights into Its Structural Dynamics, Thermal Unfolding and Antifungal Function.," *PloS one*, vol. 12, p. e0169920, jan 2017.

[4] A. Rodríguez-Martín, R. Acosta, S. Liddell, F. Núñez, M. J. Benito, and M. A. Asensio, "Characterization of the novel antifungal protein PgAFP and the encoding gene of Penicillium chrysogenum," *Peptides*, vol. 31, pp. 541–547, apr 2010.

M. HANDBAUER, "Dynamic structural ensembles of small antifungal proteins" in *PhD Proceedings Annual Issues of the Doctoral School, Faculty of Information Technology and Bionics, Pázmány Péter Catholic University – 2018.* G. Prószéky, P. Szolgay Eds. Budapest: Pázmány University ePress, 2018, pp. 18–18. This research has been partially supported by the European Union, co-financed by the European Social Fund (EFOP-3.6.3-VEKOP-16-2017-00002).

# Characterisation of the Subunit Composition, Stochiometry and Structure of Calcium Channels Involved in Neurotransmission

Zita HARMAT
(Supervisor: Zoltán GÁSPÁRI)
Pázmány Péter Catholic University, Faculty of Information Technology and Bionics
50/a Práter street, 1083 Budapest, Hungary
harmat.zita@itk.ppke.hu

Glutamate receptors are one of the key players of synaptic transmission. By binding glutamate, they can modulate synaptic strength, inducing long term potentiation (LTP) or long term depression (LTD). By studying their three dimensional structures and interactions, more details about synaptic transmission and the general functioning of the central nervous system can be elucidated.

The $\alpha$-amino-3-hydroxy-5-methyl-4-isoxasole propionic acid (AMPA) receptors are ionotropic glutamate receptors. They are ligand gated ion channels regulating the entry of calcium ions and other cations into the neuron, thus causing excitatory synaptic transmission having L-glutamate as their primary ligand. They consist of four subtunits termed GluR1-GluR4 forming various heterotetramers depending on the brain region and exhibiting different functional properties [1].

The N-methyl-D-aspartate (NMDA) receptors are another type of ionotropic glutamate receptors. They are ligand-gated ion channels and along with AMPA receptors are playing a principal role in synaptic plasticity. They form heterotetramers from the combination of seven subunits: GluN1, GluN2A-GluN2D, GluN3A-GluN3B [2].

The kainate receptors are other subtypes of ionotropic glutamate receptors. They consist of five subunits: GluK1-5, forming heterotetramers from them. The subunit composition of the receptor greatly influences its ligand affinity. [3].

Unlike the aforementioned proteins, he metabotropic glutamate receptors (mGluR) are not ion channels. By ligand binding, they interact with GTP binding proteins, which are second messengers of cellular pathways, thus altering certain cellular processes such as gene transcription and glial-neuronal interaction. Eight mGluR subtypes exist throughout the central nervous system, termed mGluR1-mGluR8 [4].

I collected alltogether 335 structures from the PDB database [5]. From the STRING database [6] I collected the interacting partners of the subunits of these receptors.

Studying the interaction of glutamate receptors with the rest of the synaptic proteins is crucial for the understanding of the mechanism of synaptic transmission on an atomic level. According to the STRING databse, the 24 subunits of the four kind of human glutamate receptors form 929 collected interactions. The graph representation of the interactions with the proteins as nodes and the interactions as edges is a connected graph with many edges and meny circles. Looking at the density of the interactions the system seems to be robust and redundant, which means that even is one of the proteins are removed from the system, the other interactions still hold the system together. Looking at the interactions in more detail, as it is expected, most of the interactions are between the subunits of the same receptors, but there are many interactions between different receptor as well.

Comparing the STRING interactions with the interactions contained in the collected structures, only 2 of the STRING interactions are represented. These are interactions between are GluR2 and GluR4, GluR2 and GluR3. An example of the atomic level description of an interaction between the AMPA receptor subunit GluR2 and and a voltage dependent calcium channel Gamma 2 subunit (CACNG2, TARP $\gamma 2$) is depicted with PDB ID 5VOT [7]. The complex contains with quisqualate and the activated open conformation. The interaction surface is in the membrane-spanning regions. Some aromatic amino acids are involved in making the connection.

Although the scientific community has biochemically identified several interaction between glutamate receptor subunits and other proteins involved in synaptic function, determining the three dimensional structures of such complexes was only successfully carried out in a very few cases so far. Future work will be aimed at addressing the problem of the different nomenclature of the two databases, searching for more structures and three dimensional modelling of the protein complexes interacting with the glutamate receptors.

## References

[1] V. A. Derkach, M. C. Oh, E. S. Guire, and T. R. Soderling, "Regulatory mechanisms of AMPA receptors in synaptic plasticity," *Nature Reviews. Neuroscience*, vol. 8, pp. 101–113, Feb. 2007.

[2] E. S. Burnell, M. Irvine, G. Fang, K. Sapkota, D. E. Jane, and D. T. Monaghan, "Positive and Negative Allosteric Modulators of N-Methyl-d-aspartate (NMDA) Receptors: Structure-Activity Relationships and Mechanisms of Action," *Journal of Medicinal Chemistry*, Mar. 2018.

[3] M. Zhuo, "Cortical kainate receptors and behavioral anxiety," *Molecular Brain*, vol. 10, no. 1, p. 16, 2017.

[4] C. J. Blacker, C. P. Lewis, M. A. Frye, and M. Veldic, "Metabotropic glutamate receptors as emerging research targets in bipolar disorder," *Psychiatry Research*, vol. 257, pp. 327–337, Nov. 2017.

[5] H. M. Berman, J. Westbrook, Z. Feng, G. Gilliland, T. N. Bhat, H. Weissig, I. N. Shindyalov, and P. E. Bourne, "The Protein Data Bank," *Nucleic Acids Research*, vol. 28, pp. 235–242, Jan. 2000.

[6] L. J. Jensen, M. Kuhn, M. Stark, S. Chaffron, C. Creevey, J. Muller, T. Doerks, P. Julien, A. Roth, M. Simonovic, P. Bork, and C. von Mering, "STRING 8–a global view on proteins and their functional interactions in 630 organisms," *Nucleic Acids Research*, vol. 37, pp. D412–416, Jan. 2009.

[7] S. Chen, Y. Zhao, Y. Wang, M. Shekhar, E. Tajkhorshid, and E. Gouaux, "Activation and Desensitization Mechanism of AMPA Receptor-TARP Complex by Cryo-EM," *Cell*, vol. 170, pp. 1234–1246.e14, Sept. 2017.

Z. HARMAT, "Characterisation of the Subunit Composition, Stochiometry and Structure of Calcium Channels Involved in Neurotransmission" in *PhD Proceedings Annual Issues of the Doctoral School, Faculty of Information Technology and Bionics, Pázmány Péter Catholic University – 2018.* G. Prószéky, P. Szolgay Eds. Budapest: Pázmány University ePress, 2018, pp. 19–19. This research has been partially supported by the European Union, co-financed by the European Social Fund (EFOP-3.6.3-VEKOP-16-2017-00002).

# Insights to the ligand-binding of the third PDZ domain of PSD95 by molecular dynamics simulations

Anett HINSENKAMP
(Supervisor: Zoltán GÁSPÁRI)
Pázmány Péter Catholic University, Faculty of Information Technology and Bionics
50/a Práter street, 1083 Budapest, Hungary
anett.hinsenkamp@itk.ppke.hu

## I. SUMMARY

PSD-95 is the most abundant PDZ domain containing scaffold protein of the post synaptic density. It is responsible for the clustering of glutamate receptors and assembling macromolecular complexes essential for signal transduction. As a member of the MAGUK (membrane-associated guanylate kinases) protein family, PSD-95 contains three PDZ (PSD-95, Discs-large, ZO-1), one GK (Guanylate kinase) and one SH (SRC homology 3) domain.[5] PDZ domains are around 90 residue long, globular interaction motifs, typically binding the C-terminal peptides of their partner molecules.[3][4]

The third PDZ domain (PDZ3) of PSD-95 has an additional helix at its its carboxy terminus besides the conserved secondary structure elements characteristic of all PDZ domains. Truncation/phosphorylation of this helix leads to a decrease in the binding affinity of the CRIPT peptide even though it is not in direct contact with the binding site.[1] A detailed atomic-level model is necessary for describing the allostery mechanisms and the internal dynamics of binding.

Molecular dynamics simulation restrained with experimental data derived from NMR measurements result in ensembles resembling the intrinsic dynamics of protein molecules on a ns time scale.[10] Multiple ensembles of the third PDZ domain of PSD-95 were generated with a modified version of the open source GROMACS.4.5.5. package.[7] Simulations were carried out using published backbone and side-chain S2 NMR relaxation order parameters as restraints.[1] The correspondence of the resulting ensembles to the experimental parameters were assessed using the CoNSEnsX service.[2] The influence of the length of the simulations on the conformational space covered bythe different ensembles was evaluated. Free, complexed, full and truncated forms of PDZ3 were compared focusing on the conformational changes upon binding. Conformational entropy difference upon binding was calculated using multiple different methods available in the literature.[8][9]

The aim of this study is to obtain a comprehensive, atomic level model on the structural dynamics of PDZ3 and CRIPT peptide binding on a ns time scale.

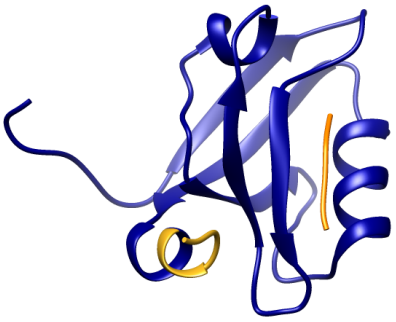

Fig. 1. Structure of the full PSD95 PDZ3 in complex with a section of CRIPT (orange). The additional helix displayed in yellow

## ACKNOWLEDGEMENTS

The research has been supported by the European Union, co-financed by the European Social Fund (EFOP-3.6.2-16-2017-00013).

## REFERENCES

[1] Chad M. Petit, Jun Zhang, Paul J. Sapienza, Ernesto J. Fuentes and Andrew L. Lee, "Hidden dynamic allostery in a PDZ domain", *PNAS*, Valume 106, Number 43, Pages 18249-18254, 2009.
[2] A.F.Ángyán, B. Szappanos, A. Perczel and Z. Gáspári, "Consensx: an ensemble view of protein structures and nmr-derived experimental data", *BMC Structural Biology*, Volume 10, 2010.
[3] Wei Feng and Mingjie Zhang, "Organization and dynamics of PDZ domain related supramodules int he postsynaptic density", *Nature Reviews Neuroscience*, Volume 10, Pages 87-99, 2009.
[4] Eunjoon Kim and Morgan Sheng, "PDZ domain proteins os synapses", *Nature Reviews Neuroscience*, Volume 5, Pages 771-781, 2004.
[5] J. Zhang, S. M. Lewis, B. Kuhlman and A. L. Lee, "Supertertiary Structure of MAGUK Core from PSD-95", *Structure*, Volume 21, Isuue 3, Pages 402-413, 1996.
[6] Harold D. MacGillavry, Yu Song, Sridhar Raghavachari, Thomas A. Blanpied, "Nanoscale scaffolding domains within the postsynaptic density concentrate synaptic AMPA receptors", *Neuron*, Volume 78, Pages 615-622, 2013.
[7] B. Hess, C. Kutzner, D. van der Spoel, and E. Lindahl, "Gromacs 4: algorithms for highly efficient, load-balanced, and scalable molecular simulation", /emphJournal of Chemical Theory and Computation, Volume 4,Pages 435-447, 2008.
[8] F.Fogolari, A. Corazza, S. Fortuna, M.A. Soler, B. VanSchouwen, G. Brancolini, S. Corni, G. Melacini and G. Esposito, "Distance-Based Configurational Entropy of Proteins from Molecular Dynamics Simulations", *PLOS ONE*, 10.1371, 2015.
[9] R. Grünberg, M. Nilges and J . Leckner, "Flexibility and Conformational Entropy in Protein-Protein Binding", *Structure*,Volume 14, Issue 4, Pages 683-693, 2006.
[10] A. F. Ángyán and Z. Gáspári, "Ensemble-Based Interpretations of NMR Structural Data to Describe Protein Internal Dynamics", *Molecules*, 18, Pages 10548-10567, 2013.

A. HINSENKAMP, "Insights to the ligand-binding of the third PDZ domain of PSD95 by molecular dynamics simulations" in *PhD Proceedings Annual Issues of the Doctoral School, Faculty of Information Technology and Bionics, Pázmány Péter Catholic University – 2018.* G. Prószéky, P. Szolgay Eds. Budapest: Pázmány University ePress, 2018, pp. 20–20. This research has been partially supported by the European Union, co-financed by the European Social Fund (EFOP-3.6.3-VEKOP-16-2017-00002).

# Calretinin-positive midline thalamic neurons convey arousal-related information

Kinga KOCSIS
(Supervisor: István ULBERT, DSc)
Pázmány Péter Catholic University, Faculty of Information Technology and Bionics
50/a Práter street, 1083 Budapest, Hungary
kocsis.kinga@itk.ppke.hu

The dorsal medial thalamus (DMT) has long been recognized as a key role-player in behavioural arousal ([1], [2]), its neurons exhibit diurnal and stress related cFos early gene expression in rodents ([3], [4], [5]). However, the cell-type specific thalamic population behind DMT-mediated arousal hasn't been elucidated. This thalamic region is tightly packed with calretinin(CR)-positive neurons ([6], [**?**]), so we aimed to identify whether CR is a reliable marker for testing arousal-related activities in the DMT. We previously examined the CR content and cFos expression of mouse DMT cells in diurnal cycle and stress-related conditions. The vast majority of cFos+ cells turned out to be CR+ in each case (Mátyás és Komlósi, under revision).

Since it has been previously shown that 10 Hz stimulation of DMT CR+ cells leads to arousal in sleeping mice, we focused on interrogating these neurons along spontaneous sleep/wake states in the upcoming experiments (Mátyás és Komlósi, under revision).

Fluorescent channelrhodopsin expressing virus (AAV-DIO-ChR2) was injected into the DMT of four CR(Calb2)-Cre mice. After 3 weeks of virus expression, four custom fabricated tungsten tetrodes were chronically implanted into the site of injection along with a multimode optic fiber. During recordings, the animals were let sleep in their homecage during their light phase. Electromyographic (EMG) activity was monitored. Optogenetic identification of CR+ single units was done at 1 Hz in order to evoke spiking only but not arousal.

Spike detection and principal component analysis-based automatic clustering were performed on the electrophysiological data. Short latency (<10ms) optogenetically evoked spiking was considered reliable to indicate direct light activation, which allowed the identification of the DMT/CR+ cell type. EMG onset was given as an indicator for heightened arousal. Z-scored peri-event time histograms (PETH) were defined for each cell around the detected EMG onsets.

Twenty out of 31 (64.5%) CR+ cells significantly increased their firing rate several seconds before the onset of EMG activity. 8 DMT/CR+ neurons (25.8%) elevated their activity at the onset of arousal. In comparison, among the non-tagged (putative CR-) neurons only 8/34 (23.5%) increased their firing prior to arousal (CR- versus CR+: Fisher's exact test, $p < 0.01$). At the population level, the activity of non-tagged DMT neurons showed significant changes only at the onset of the increased EMG signal not before and this activation took 1-2 seconds in comparison to the CR+ population where this elevation was over 10 seconds. These data show that DMT/CR+ cells selectively display predictive, arousal-related firing activity (Figure 1).

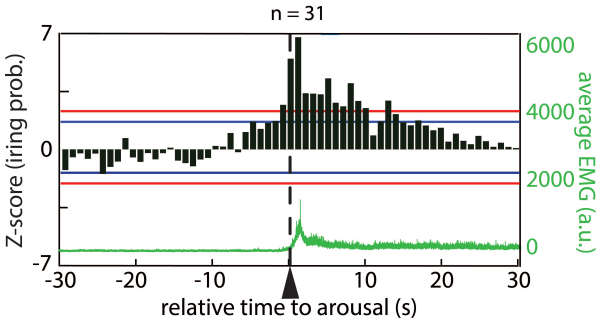


Fig. 1. Average activity changes of calretinin-positive dorsal medial thalamic neurons at sleep/wake transitions.

Relying on anatomical, behavioural and electrophysiological evidence, we have identified calretinin-containing neurons in mice as a key population in the DMT related to aroused behavioural states. DMT/CR+ cells are also good candidates to provide arousal-related information which is necessary to exhibit appropriate emotional responses. Taking my current data into account, spontaneous activation of DMT/CR+ neurons evokes biologically relevant arousal patterns and state transitions. The spontaneous activity of optogenetically tagged DMT/CR+ cells is tightly linked to the onset of EMG activity in animals arousing from sleep, CR+ thalamic cells often exhibit graded activation before the aroused state (movement) can be detected. However, the motor response is likely due to the top-down influence of the aroused forebrain on brainstem motor centers since DMT/CR+ cells have no direct descending projections.

## References

[1] G. Moruzzi and H. Magoun, "Brain stem reticular formation and activation of the EEG," *Electroencephalogr. Clin. Neurophysiol.*, vol. 1, no. 1-4, pp. 455–473, 1949.

[2] J. Hunter and H. H. Jasper, "Effects of thalamic stimulation in unanaesthetised animals," *Electroencephalogr. Clin. Neurophysiol.*, vol. 1, no. 1-4, pp. 305–324, 1949.

[3] M. Bubser, J. L. Scruggs, C. D. Young, and A. Y. Deutch, "The distribution and origin of the calretinin-containing innervation of the nucleus accumbens of the rat," *Eur. J. Neurosci.*, vol. 12, no. 5, pp. 1591–1598, 2000.

[4] M. A. Penzo, V. Robert, J. Tucciarone, D. De Bundel, M. Wang, L. Van Aelst, M. Darvas, L. F. Parada, R. D. Palmiter, M. He, Z. J. Huang, and B. Li, "The paraventricular thalamus controls a central amygdala fear circuit," *Nature*, vol. 519, no. 7544, pp. 455–459, 2015.

[5] F. H. Do-Monte, K. Quinõnes-Laracuente, and G. J. Quirk, "A temporal shift in the circuits mediating retrieval of fear memory," *Nature*, vol. 519, no. 7544, pp. 460–463, 2015.

[6] L. Winsky, P. Montpied, R. Arai, B. M. Martin, and D. M. Jacobowitz, "Calretinin distribution in the thalamus of the rat: Immunohistochemical and in situ hybridization histochemical analyses," *Neuroscience*, vol. 50, no. 1, pp. 181–196, 1992.

K. KOCSIS, "Calretinin-positive midline thalamic neurons convey arousal-related information" in *PhD Proceedings Annual Issues of the Doctoral School, Faculty of Information Technology and Bionics, Pázmány Péter Catholic University – 2018.* G. Prószéky, P. Szolgay Eds. Budapest: Pázmány University ePress, 2018, pp. 21–21. This research has been partially supported by the European Union, co-financed by the European Social Fund (EFOP-3.6.3-VEKOP-16-2017-00002).

# Determining parameters of neural models using numerical optimization methods

Máté MOHÁCSI
(Supervisor: Szabolcs KÁLI, Tamás FREUND)
Pázmány Péter Catholic University, Faculty of Information Technology and Bionics
50/a Práter street, 1083 Budapest, Hungary
mohacsi.mate@itk.ppke.hu

***Keywords*-neuronal modeling, model fitting, parallel optimization, algorithms, parallelization, python**

The detailed modeling of neurons is becoming an increasingly widespread method in neurobiological research. The currently available experimental data make it possible to create complex multicompartmental conductance-based neuron models. In principle, such models can approximate the behavior of real neurons very well. However, these models have many parameters and some of these parameters can not be directly determined in experiments. Therefore, we try to tune these values to bring the model's behavior as close as possible to the experimental data.

To determine the unknown parameters of the models in a systematic way, several software solutions have been developed recently, which implement various nonlinear metaheuristics. In our laboratory, we developed the software tool called Optimizer. [1] This framework uses search algorithms implemented in Python libraries to determine the parameters of single cell and network models. It includes a graphical interface, and provides a user-friendly option for adjustments and analysis. To determine model behaviour, Optimizer communicates with NEURON, a simulation program for modeling neurons. [2]

Different optimization problems can be solved efficiently with different methods. Optimizer already contains several popular optimization algorithms and was designed to be extensible with new methods. Our goal was to expand the repertoire of algorithms available in Optimizer, by including several new methods that proved effective in previous studies.

Multi-objective optimization assumes multiple target functions and attempts to find solutions that represent different tradeoffs between these objectives. We implemented several bio-inspired multi-objective searches from different libraries to find out their capabilities on neuronal tasks.[3] Moreover we also implemented a search distribution updating metaheuristic, the Natural Evolution Strategies. [4] These methods were integrated into the framework to give homogeneous output and be able to track through every generation.

All metaheuristic search methods require a large number of evaluations of models with different parameters, which makes the identification of best parameter values computationally resource-intensive. The Python language provides several options that use different methods for invoking parallel child processes, and their functionality and exploitation capabilities are required to integrate multiprocessor optimization into Optimizer. We managed to implement multiprocessing functions into the framework, which give the same solutions as the original implementation and provide substantial speedup.

In order to determine which of the specific optimization algorithms performs most effectively for different tasks, we systematically benchmarked the performance of algorithms. Initial testing indicated that the newly implemented algorithms can be used in this context, but their performance will need to be evaluated more carefully and further fine tuning of their implementation may be necessary.

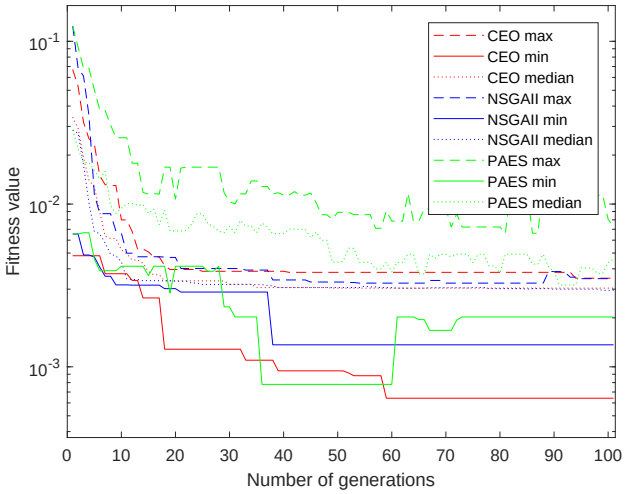


Fig. 1. Generation plot of a single-objective algorithm, the Simple Evolutionary algorithm (CEO) and multi-objective algorithms from the Inspyred package, Nondominated Sorting Genetic Algorithm (NSGA-II) and the Pareto Archived Evolutionary Strategy (PAES). The optimization is based on a Hodgkin-Huxley model, with 0.2mA input, optimized for 3 unknown parameters with 100 population size and 100 iteration. Fitness values calculated from Spike Count during stimuli, Action Potential amplitude and Action Potential width. The y-axis denotes the fitness values on a logarithmic scale and the x-axis denotes the generation number. For every generation the best (solid line), median (dotted line) and the worst of the population (dashed line) is shown on the figure.

## ACKNOWLEDGEMENTS

I would like to thank to my supervisor Szabolcs Káli, Sára Sáray and Márk Patrik Török for their help and support.

## REFERENCES

[1] P. Friedrich, M. Vella, A. I. Gulyás, T. F. Freund, and S. Káli, "A flexible, interactive software tool for fitting the parameters of neuronal models," *Frontiers in Neuroinformatics*, vol. 8, p. 63, 2014. [Online]. Available: https://www.frontiersin.org/article/10.3389/fninf.2014.00063

[2] N. T. Carnevale and M. L. Hines, *The NEURON Book*, 1st ed. New York, NY, USA: Cambridge University Press, 2009.

[3] S. Luke, *Essentials of Metaheuristics*, 2nd ed. Lulu, 2013, available for free at http://cs.gmu.edu/∼sean/book/metaheuristics/.

[4] D. Wierstra, T. Schaul, T. Glasmachers, Y. Sun, J. Peters, and J. Schmidhuber, "Natural evolution strategies," *J. Mach. Learn. Res.*, vol. 15, no. 1, pp. 949–980, Jan. 2014. [Online]. Available: http://dl.acm.org/citation.cfm?id=2627435.2638566

M. MOHÁCSI, "Determining parameters of neural models using numerical optimization methods" in *PhD Proceedings Annual Issues of the Doctoral School, Faculty of Information Technology and Bionics, Pázmány Péter Catholic University – 2018.* G. Prószéky, P. Szolgay Eds. Budapest: Pázmány University ePress, 2018, pp. 22–22. This research has been partially supported by the European Union, co-financed by the European Social Fund (EFOP-3.6.3-VEKOP-16-2017-00002).

# Investigation of Single-Unit Activity Using Hawkes Processes

György PERCZEL
(Supervisors: Loránd ERŐSS, László GERENCSÉR, Zsuzsanna VÁGÓ)
Pázmány Péter Catholic University, Faculty of Information Technology and Bionics
50/a Práter street, 1083 Budapest, Hungary
National Institute of Clinical Neurosciences, Department of Functional Neurosurgery
57. Amerikai street, 1145 Budapest, Hungary
perczel.gyorgy.miklos@itk.ppke.hu

***Keywords*-epilepsy; seizure prediction; stochastic point processes, maximum likelihood estimation**

*Statement of originality:*
*This report describes the work of the doctoral student during the academic year 2017/2018. Parts of this work might be under submission to scientific conferences and journals.*

Affecting 50 million people worldwide, epilepsy is one of the most frequent neurological diseases. It is characterized by recurrent seizure that appears to be resistant for pharmacological treatment in 30% of all cases. The unexpectedness of the seizures has a major influence on the patients quality of life (QoL) in multiple ways, as reviewed by [1]. It is thus straightforward that the ability of predicting epileptic seizures would greatly improve the patients QoL in multiple ways, especially in the case of drug resistant epilepsy. From the practical point-of-view, this would mean that given an observed brain-state related variable one is able to estimate the probability of a seizure to come in the following time-interval (prediction horizon) [2].

Recently, the use of action potentials (AP) of the neurons (single-unit activity, SUA) was also proposed as a substrate for seizure prediction [3], as this kind of signal can already be recorded from epileptic patients during invasive monitoring, see e.g. [4]. On this cellular scale of the brain, it has been observed that the firing properties of neurons show diverse changes at the seizure onset and a given nerve cell's firing pattern (sample path) shows a stereotypic change around it from seizure to seizure [3].

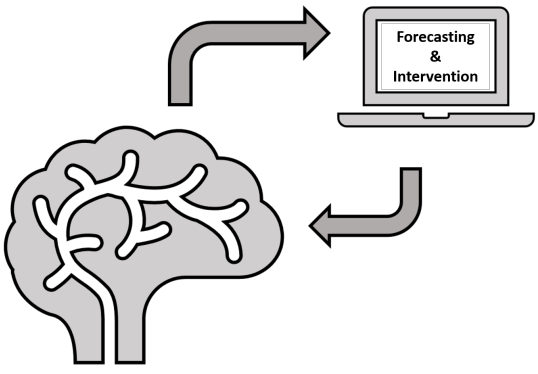


**Fig. 1: Basic concept of a closed-loop system**

We have implemented a simulation and maximum likelihood estimation (MLE) algorithm of the univariate Hawkes processes with exponential core function in a MATLAB environment, based on [5], [6]. The rational behind this was to give a brief characterization of the observed SUAs via the estimated parameters of the Hawkes process and possibly detect brain state dependent changes in the firing patterns of individual neurons (spike-trains). Asymptotic precision of the MLE is characterized by the confidence-ellipsoid. We used SUAs recorded from hippocampal brain slices of the rat to test the feasibility of the above algorithm implemented. In this way, a physiologically relevant region of the parameter-space was revealed.

## References

[1] A. Schulze-Bonhage and A. Kühn, "Unpredictability of Seizures and the Burden of Epilepsy," in *Seizure Prediction in Epilepsy: From Basic Mechanisms to Clinical Applications*, 2008, pp. 1–10.
[2] M. J. Cook, T. J. O'Brien, S. F. Berkovic, M. Murphy, A. Morokoff, G. Fabinyi, W. D'Souza, R. Yerra, J. Archer, L. Litewka, S. Hosking, P. Lightfoot, V. Ruedebusch, W. D. Sheffield, D. Snyder, K. Leyde, and D. Himes, "Prediction of seizure likelihood with a long-term, implanted seizure advisory system in patients with drug-resistant epilepsy: a first-in-man study." *The Lancet. Neurology*, vol. 12, no. 6, pp. 563–71, jun 2013.
[3] W. Truccolo, J. A. Donoghue, L. R. Hochberg, E. N. Eskandar, J. R. Madsen, W. S. Anderson, E. N. Brown, E. Halgren, and S. S. Cash, "Single-neuron dynamics in human focal epilepsy," *Nature Neuroscience*, vol. 14, no. 5, pp. 635–641, 2011.
[4] E. Tóth, D. Fabó, L. Entz, I. Ulbert, and L. Eross, "Intracranial neuronal ensemble recordings and analysis in epilepsy," *Journal of Neuroscience Methods*, vol. 260, pp. 261–269, 2016.
[5] A. G. Hawkes, "Spectra of some self-exciting and mutually exciting point processes," *Biometrika*, vol. 58, no. 1, pp. 83–90, apr 1971.
[6] T. Ozaki, "Maximum likelihood estimation of Hawkes' self-exciting point processes," *Annals of the Institute of Statistical Mathematics*, vol. 31, no. 1, pp. 145–155, 1979.

Gy. PERCZEL, "Investigation of Single-Unit Activity Using Hawkes Processes" in *PhD Proceedings Annual Issues of the Doctoral School, Faculty of Information Technology and Bionics, Pázmány Péter Catholic University – 2018.* G. Prószéky, P. Szolgay Eds. Budapest: Pázmány University ePress, 2018, pp. 23–23. This research has been partially supported by the European Union, co-financed by the European Social Fund (EFOP-3.6.3-VEKOP-16-2017-00002).

# HippoUnit: a Python test suite for the automatized validation of models of hippocampal neurons

Sára SÁRAY
(Supervisors: Szabolcs KÁLI, Tamás FREUND)
Pázmány Péter Catholic University, Faculty of Information Technology and Bionics
50/a Práter street, 1083 Budapest, Hungary
Institute of Experimental Medicine of the Hungarian Academy of Sciences
43 Szigony street, 1083 Budapest, Hungary
saray.sara@itk.ppke.hu

***Keywords*-model validation, CA1 pyramidal cell, python, jupyter notebook**

Constructing anatomically and biophysically detailed data-driven computational models of the different neuronal cell types and running simulations on them is becoming a more and more popular process in the neuroscience community in getting to know the behaviour and understanding the function of these neurons in the brain. The published models usually try to capture some of the most important or interesting properties of the given neuron type, but it is usually unknown how they would behave in other situations.

To quantitatively evaluate the behaviour of models under different conditions, to explore the changes in model behaviour during parameter tuning and to compare models that were developed using different methods and for different purposes, we have developed a Python test suite called HippoUnit. Current validation tests cover somatic behavior and signal propagation and integration in apical dendrites of hippocampal CA1 pyramidal cell models. However some of its tests are applicable or can be adapted for other cell types.

HippoUnit is based on the SciUnit [1] framework. In SciUnit tests usually four main classes are implemented: the Test class, the Model class, the Capabilities (the interface between the model and the test) and the Score class. HippoUnit is built in a way that keeps this structure, with the difference that the model's implementation is not part of the package itself; instead, it has a ModelLoader Class to load and run simulations that mimic experimental protocols on neuronal models built in the NEURON simulator [2]. This modular structure makes it possible to easily extend the package with new validation tests.

HippoUnit has been added to the Software Catalog of the Brain Simulation Platform of the Human Brain Project (HBP) and its tests were among the first to be registered in the Validation Framework [3] developed in the HBP.

On the Brain Simulation Platform an online Use Case is available, which via a jupyter notebook shows how one can run the validation tests of HippoUnit on models that are the outputs of BluePyOpt [4] optimizations, and how the models and the test results can be registered in the Validation Framework. This will encourage the collaborative use of this tool.

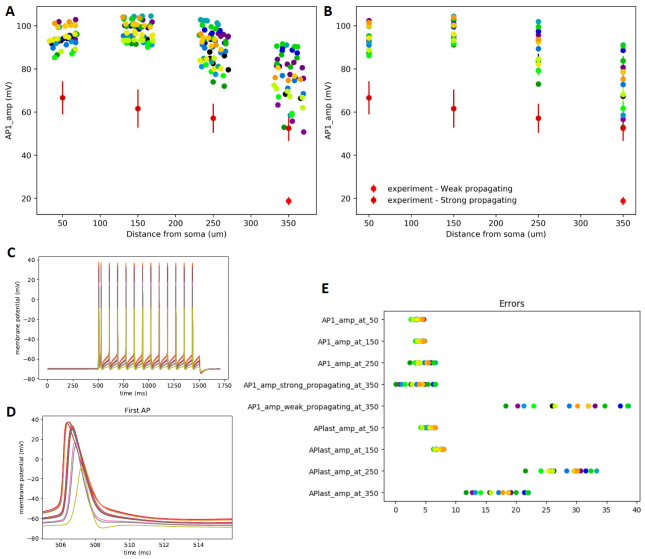


Fig. 1. Summary of some of the results of the Back-propagating AP Test run on CA1 pyramidal cell models that are the results of automatic parameter optimization using BluePyOpt [4] in the HBP. A: Amplitudes of the first back-propagating action potential measured at locations on the trunk at different distances from the soma on 17 different models (different colours) B: The mean of the amplitude values at given distance intervals. C: The spike train of an example model (CA1_pyr_cACpyr_mpg141217_A_idB_20170915111538) recorded at the different distances. D: Zoom to the first action potential of the spike train shown in C. E: The errors (Z-scores) of the evaluated features of the 17 models.

## ACKNOWLEDGEMENTS

Grants from the European Human Brain Project, the Széchenyi 2020 Program, the Human Resource Development Operational Program, the Program of Integrated Territorial Investments in Central-Hungary, and the European Structural and Investment funds are gratefully acknowledged. I thank Szabolcs Káli, Christian Rössert, Shailesh Appukuttan, Andrew Davison, Armando Romani, Mike Gevaert for their contribution.

## REFERENCES

[1] C. Omar and R. Gerkin, "Sciunit: A test-driven framework for formally validating scientific models against data," 2014, last accesed on: 23th April 2018. [Online]. Available: https://github.com/scidash/sciunit

[2] N. T. Carnevale and M. L. Hines, *The NEURON Book*, 1st ed. New York, NY, USA: Cambridge University Press, 2009.

[3] A. Davison and S. Appukuttan, "hbp-validation-client - a python package for working with the human brain project model validation framework," last accesed on: 25th April 2018. [Online]. Available: https://github.com/appukuttan-shailesh/hbp-validation-client

[4] W. Van Geit, M. Gevaert, G. Chindemi, C. Rössert, J.-D. Courcol, E. B. Muller, F. Schürmann, I. Segev, and H. Markram, "Bluepyopt: Leveraging open source software and cloud infrastructure to optimise model parameters in neuroscience," *Frontiers in Neuroinformatics*, vol. 10, no. 17, 2016. [Online]. Available: http://www.frontiersin.org/neuroinformatics/10.3389/fninf.2016.00017/abstract

S. SÁRAY, "HippoUnit: a Python test suite for the automatized validation of models of hippocampal neurons" in *PhD Proceedings Annual Issues of the Doctoral School, Faculty of Information Technology and Bionics, Pázmány Péter Catholic University – 2018.* G. Prószéky, P. Szolgay Eds. Budapest: Pázmány University ePress, 2018, pp. 24–24. This research has been partially supported by the European Union, co-financed by the European Social Fund (EFOP-3.6.3-VEKOP-16-2017-00002).

# Sequential auditory information processing

Beáta Tünde SZABÓ
(Supervisor: István WINKLER, István ULBERT)
Pázmány Péter Catholic University, Faculty of Information Technology and Bionics
50/a Práter street, 1083 Budapest, Hungary
szabo.beata.tunde@itk.ppke.hu

## Summary

In many situations in everyday life, we hear sounds from different sources while the number of sources is usually unknown. The task of the auditory system is to parse this complex mixture and determine the likely sources producing the incoming auditory signal. In his groundbreaking book, Bregman (1990) termed this process auditory scene analysis (ASA). As the incoming acoustic information does not fully specify the sources, ASA is an ill-posed problem. However, our brain solves this issue astonishingly well, while artificial systems struggle to cope with the problem. Further, the neural mechanisms by which our brain solves ASA are still unknown.Any mechanism that aims to solve the task of parsing the auditory scene needs to explore the relations across simultaneous and successive sounds. We also know, that as a part of solving ASA, the human auditory system processes sound patterns (sequences of acoustic events) very effectively. Acoustic patterns stand for temporally structured spectrally coherent sound-sequences, which can be segregated from other patterns or from the background noise. In this work we will focus on mechanisms enabling to process sequential patterns.

After discussing the sequential statistical learning paradigm and the results in the acoustic and visual domains relevant to our research [1], [3], [6], we present a pilot study testing sequential auditory information processing. We employed the statistical learning paradigm with non-linguistic, non-musical sound tokens. We use the notion sound token as a discrete isolated sound with a beginning and an end (e.g., a 400 ms long sound of a machine). Although many previous studies investigated sequential statistical learning of sounds, the statistics they are investigating (single-unit frequencies, transitional probabilities) were restricted. Further, only a few of them delivered non-linguistic and non-musical stimuli. We aim to extend the statistical learning paradigm beyond these types of stimuli in order to gain a deeper insight into the mechanisms of sequential auditory information processing. In the pilot experiments, we explored the utility of non-linguistic sound tokens in a sequential acoustic statistical learning paradigm. We tested how the complexity of the chunk sets (pair/triplet/quadruplet) affects their learning and whether there is some preference for the first/last part of the chunks. Figure 1 shows a snippet of the presented sound streams. We've found that the chunks of triplet and quadruplet size can be learned; chunks of two sounds (pairs) require further investigation. There appears to be a bias towards learning the first two elements of triplet chunks. This must be considered when investigating the embeddedness phenomenon.

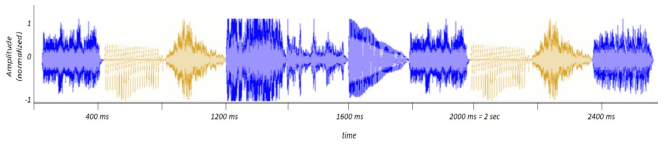


Fig. 1. Snippet from the sound training sequence's waveform. The highlighted tokens form a pair.

We also present a possible approach for modeling sequential auditory information processing by introducing sequentiality into a Bayesian non-parametric model [7]. When building a biologically inspired computational model for processing sequential auditory information, we can exploit unsupervised learning algorithms using non-parametric Bayesian methods. One of these methods is the Indian Buffet Process (IBP), which can be employed for inferring hidden causes [7]. In our case, hidden causes are the sources generating the sounds. Bayesian inference is an efficient mechanism for processing hierarchically structured information, and it compatible with human performance in many cases in the visual modality (e.g. [5]). The IBP model can provide inference to an unbounded number of hidden causes (i.e., the number of sound sources is not restricted in the model). For implementing sequentiality in the IBP model, we propose to use a sliding window and to represent the tokens' separation in time. By this approach one can gain different distributions for different time-windows, which then can be aggregated in a weighted manner. This computational model is in-line with the probabilistic computational framework [4] in which the distribution of the possible sound sources is represented in the model. This representation can then be compared to the model of the acoustic environment emerging in the human brain.

## References

[1] Aslin, R. N., and Newport, E. L. (2012). Statistical learning: From acquiring specific items to forming general rules. Current directions in psychological science, 21(3), 170-176.
[2] Bregman, A. S. (1990). Auditory Scene Analysis. The Perceptual Organization of Sound. Cambridge, MA: MIT Press.
[3] Fiser, J., and Aslin, R. N. (2002). Statistical learning of higher-order temporal structure from visual shape sequences. Journal of Experimental Psychology: Learning, Memory, and Cognition, 28(3), 458.
[4] Fiser, J., Berkes, P., Orbán, G., Lengyel, M. (2010). Statistically optimal perception and learning: from behavior to neural representations: perceptual learning, motor learning, and automaticity. Trends Cogn. Sci. 14, 119. doi: 10.1016/j.tics.2010.01.003
[5] Orbán, G., Fiser, J., Aslin, R. N., and Lengyel, M. (2008). Bayesian learning of visual chunks by human observers. Proc. Natl. Acad. Sci. U.S.A. 105, 2745–2750.
[6] Saffran, J. R., Aslin, R. N., and Newport, E. L. (1996). Statistical learning by 8-month-old infants. Science 274, 1926–1928. doi: 10.1126/science.274.5294.1926
[7] Wood, F., Griffiths, T., and Ghahramani, Z. (2012). A non-parametric Bayesian method for inferring hidden causes. arXiv preprint arXiv:1206.6865.

B. SZABÓ, "Sequential auditory information processing" in *PhD Proceedings Annual Issues of the Doctoral School, Faculty of Information Technology and Bionics, Pázmány Péter Catholic University – 2018.* G. Prószéky, P. Szolgay Eds. Budapest: Pázmány University ePress, 2018, pp. 25–25. This research has been partially supported by the European Union, co-financed by the European Social Fund (EFOP-3.6.3-VEKOP-16-2017-00002).

# Electrophysiological connection between sharp wave ripples generated in hippocampal CA3 region and dentate gyrus, in vitro

Csilla SZABÓ
(Supervisor: Lucia WITTNER)
Pázmány Péter Catholic University, Faculty of Information Technology and Bionics
50/a Práter street, 1083 Budapest, Hungary
szabo.csilla@itk.ppke.hu

Hippocampal sharp wave-ripples (SPW-Rs) and dentate spikes are thought to play a leading role in memory processes. In vitro population activities are generated in both the dentate gyrus (DG) and the CA3 region of the rodent hippocampus and are used as models of SPW-Rs. [2] [3] These events are well described, but the connection and propagation of these population bursts are not fully understood. SPW-Rs are characterized by a local field potential gradient (LFPg) transient, increased fast oscillatory activity and increased multiple unit activity (MUA). In vitro, these events are initiated in the CA3 and spread to the DG. [1] [5]

Local field potential gradient was recorded with a 24-channel laminar microelectrode (Pt/Ir, 50 $\mu$m intercontact distance) in rat ventral hippocampal slices. The electrode array was put perpendicularly to the cell layers (granule cell layer of DG, pyramidal cell layer of CA3 region).

The mu opioid receptor agonist DAMGO was used to affect the activity of parvalbumin-positive basket cells, while the acetylcholine receptor agonist carbachol (CCh) helped to examine the role of cholecystokinin (CCK) basket cells. The application of DAMGO significantly reduces the frequency of SPW-Rs. Further application of CCh blocks the remaining SPW-Rs activity. [1]

Current source density (CSD) and MUA analyses were used to determine the direction and the timing of SPW propagation. The role of excitatory and inhibitory circuits was examined with single unit clustering method.

Both independent and correlated occurrence of SPWs were recorded in the DG and the CA3 region of the rat hippocampus, in vitro. Population events either propagated from the DG to the CA3 region, or the opposite direction, but were also found to occur simultaneously. Multiple patterns of SPWs also occur simultaneously. During DAMGO application the amplitude of SPW-Rs increased, while its frequency decreased. CCh blocked the emergence of SPW-Rs. After the washout of both drugs, SPW-Rs returned with the initial frequency.

Results suggest that hippocampal SPWs can involve both the DG and the CA3 region simultaneously and spread from both regions to the other. It seems that both regions can drive the neuronal population of the other and might offer reverberating pathways to information processing.

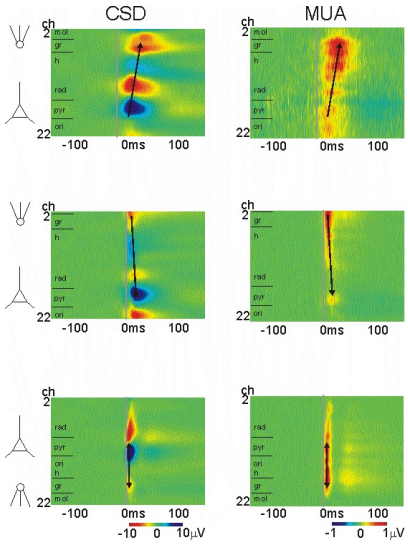


Fig. 1. Different patterns of SPA spreading according to CSD and MUA

## REFERENCES

[1] Hofer, K. T., Kandrács, Á., Ulbert, I., Pál, I., Szabó, C., Héja, L. and Wittner, L. (2015), The hippocampal CA3 region can generate two distinct types of sharp wave-ripple complexes, in vitro. Hippocampus, 25: 169–186. doi: 10.1002/hipo.22361

[2] Buzsáki G, Leung LW, Vanderwolf CH. 1983. Cellular bases of hippocampal EEG in the behaving rat. Brain Res 287:139-171

[3] Buzsáki G, 1989. Two-stage model of memory trace formation: A role foor 'noisy' brain states, Neuroscience 31:551-570

[4] Kubota D, Colgin LL, Casale M, BrucherFA, Lynch G. 2003. Endogenous waves in hippocampal slices. J Neurophysiol 89:81-89

[5] Colgin, L. L., Kubota, D., Brucher, F. a, Jia, Y., Branyan, E., Gall, C. M., Lynch, G. (2004). Spontaneous waves in the dentate gyrus of slices from the ventral hippocampus. Journal of Neurophysiology, 92(6), 3385–98. http://doi.org/10.1152/jn.00478.2004

Cs. SZABÓ, "Electrophysiological connection between sharp wave ripples generated in hippocampal CA3 region and dentate gyrus, in vitro" in *PhD Proceedings Annual Issues of the Doctoral School, Faculty of Information Technology and Bionics, Pázmány Péter Catholic University – 2018.* G. Prószéky, P. Szolgay Eds. Budapest: Pázmány University ePress, 2018, pp. 26–26. This research has been partially supported by the European Union, co-financed by the European Social Fund (EFOP-3.6.3-VEKOP-16-2017-00002).

# The Role of Extracellular Matrix Remodeling Enzymes in Dermal Stem Cell Function

Balázs SZÉKY
(Supervisor: Sarolta KÁRPÁTI, Miklós GYÖNGY)
Pázmány Péter Catholic University, Faculty of Information Technology and Bionics
50/a Práter street, 1083 Budapest, Hungary
szeba@digitus.itk.ppke.hu

***Abstract*—The extracellular matrix (ECM) plays a pivotal role in dictating stem cell fate. Proliferation, survival and differentiation of tissue resident stem cells are influenced by mechanisms facilitating ECM assembly and degradation. Structure, composition and mechanical forces of the ECM profoundly affect stem cell differentiation and regulated by ECM remodeling enzymes, such as matrix-metalloproteinases and transglutaminases. Transglutaminases are calcium-dependent protein-crosslinking enzymes catalizing the formation of isopeptide bonds between proteins. Eight different transglutaminase-coding genes are known to exist in the human genome, most of them have tissue specific expression. On the other hand, transglutaminase 2 or tissue transglutaminase (TG2, or TtG, gene ID: 7052) is expressed by minor cell subsets of diverse tissues. TG2 maintains tissue homeostasis and regulates stem cell fate not only by protein transamidation, but it also exerts signaling and scaffold protein functions. TG2 has widespread roles in wound healing, inflammation and cancer. It promotes drug-resistance, epithelial-to-mesenchymal transition, and stem cell-like properties of cancer cells, but it's role in normal stem cell homeostasis is still unknown. To understand functions of tissue transglutaminase in dermal stem cells, we isolated fibroblast cells from human dermis and melanoma, and analyzed tissue transglutaminase expression and Co-expression with stem cell markers. To assess the role of tissue transglutaminase in stem cell differentiation, we carried out in vitro differentiation assays.**

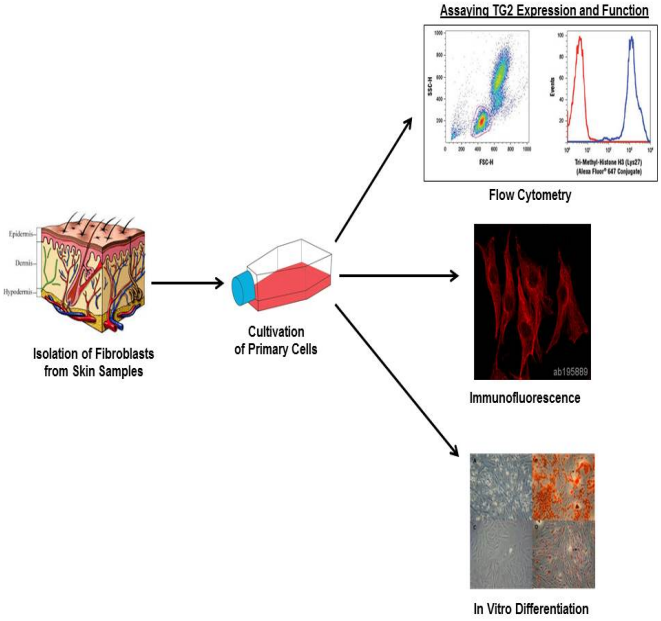


Fig. 1. Figure 1.: Research plan to analyze tissue transglutaminase functions in mesenchymal cells. Fibroblasts isolated from skin samples are cultivated as primary cells and used at low passage numbers in our experiments. In vitro assays are employed to analyze tissue transglutaminase expression (immunofluorescence), quantify tissue transglutaminase expressing stem cells (flow cytometry) and to assess tissue transglutaminase function in stem cell differentiation.

## REFERENCES

[1] Ayinde, O., Wang, Z. and Griffin, M. (2017). Tissue transglutaminase induces Epithelial-Mesenchymal-Transition and the acquisition of stem cell like characteristics in colorectal cancer cells. Oncotarget, 8(12).

[2] Chrobok, N., Sestito, C., Wilhelmus, M., Drukarch, B. and van Dam, A. (2016). Is monocyte- and macrophage-derived tissue transglutaminase involved in inflammatory processes?. Amino Acids, 49(3), pp.441-452.

[3] Condello, S., Sima, L., Ivan, C., Cardenas, H., Schiltz, G., Mishra, R. and Matei, D. (2018). Tissue transglutaminase regulates interactions between ovarian cancer stem cells and the tumor niche. Cancer Research, pp.canres.2319.2017.

[4] Eckert, R., Kaartinen, M., Nurminskaya, M., Belkin, A., Colak, G., Johnson, G. and Mehta, K. (2014). Transglutaminase Regulation of Cell Function. Physiological Reviews, 94(2), pp.383-417.

[5] Gattazzo, F., Urciuolo, A. and Bonaldo, P. (2014). Extracellular matrix: A dynamic microenvironment for stem cell niche. Biochimica et Biophysica Acta (BBA) - General Subjects, 1840(8), pp.2506-2519.

[6] Mousa, A., Cui, C., Song, A., Myneni, V., Sun, H., Li, J., Murshed, M., Melino, G. and Kaartinen, M. (2017). Transglutaminases factor XIII-A and TG2 regulate resorption, adipogenesis and plasma fibronectin homeostasis in bone and bone marrow. Cell Death and Differentiation, 24(5), pp.844-854.

[7] Myneni, V., Melino, G. and Kaartinen, M. (2015). Transglutaminase 2—a novel inhibitor of adipogenesis. Cell Death and Disease, 6(8), pp.e1868-e1868.

[8] Telci, D. (2006). Tissue transglutaminase (TG2) - a wound response enzyme. Frontiers in Bioscience, 11(1), p.867.

[9] Zemskov, E. (2006). The role of tissue transglutaminase in cell-matrix interactions. Frontiers in Bioscience, 11(1), p.1057.

B. SZÉKY, "The Role of Extracellular Matrix Remodeling Enzymes in Dermal Stem Cell Function" in *PhD Proceedings Annual Issues of the Doctoral School, Faculty of Information Technology and Bionics, Pázmány Péter Catholic University – 2018.* G. Prószéky, P. Szolgay Eds. Budapest: Pázmány University ePress, 2018, pp. 27–27. This research has been partially supported by the European Union, co-financed by the European Social Fund (EFOP-3.6.3-VEKOP-16-2017-00002).

# Filtration of MCF-7 human breast cancer cells in a microfluidic device

Ádám György SZÉLIG
(Supervisor: Kristóf IVÁN)
Pázmány Péter Catholic University, Faculty of Information Technology and Bionics
50/a Práter street, 1083 Budapest, Hungary
szelig.adam.gyorgy@itk.ppke.hu

Circulating tumor cells (CTCs) are defined as tumor cells present in the peripheral blood circulatory system. Cancer metastasis occurs when CTCs disassociate from the primary or secondary tumor, enter the circulation, and migrate to distant organs through the peripheral blood stream or lymphatic drainage and is the leading cause of death in patients with cancer. Clinical trials have shown that the presence and number of CTCs is predictive of survival in several types of cancer, including breast, prostate, colon, gastric, small and non-small cell lung carcinoma and melanoma [1]. Identification and characterization of CTCs offers an opportunity to understand the metastatic cascade, helps in the selection of the proper cancer treatment and enables the monitoring of treatment progression. An average-sized tumor may release an estimated million cells per day into the bloodstream; however, most of these cancer cells do not survive. The typical CTC concentration is approximately 1 CTC in 1 $mL$ of blood compared to $\sim 5 \cdot 10^9$ red blood cells and $\sim 7 \cdot 10^6$ leukocytes. To capture sufficient numbers of CTCs for reliable diagnosis many novel methods have been developed. Microfluidic technologies are an effective means to isolate and detect CTCs. Parameters in microfluidic devices can be precisely controlled at the cellular scale (e.g., channel dimensions, flow profile); this precise control facilitates capture efficiency and isolation purity. Furthermore, isolated CTCs can be manipulated to next-stage analysis (e.g., genetic analysis, drug screening, enzymatic reactions) or on-chip cell culturing as part of the cell separation process, speeding up the overall CTC characterization process and eliminating the intermediate procedures [2]. Microfluidic methods for CTC isolation are based on the physical and/or biological differences between CTCs and the background cells.

A variety of technologies have been developed to improve detection and capture of CTCs from peripheral blood. These technologies use one or more unique properties of CTCs that distinguish them from the surrounding normal blood cells: biological properties (surface protein expression, presence of mutations, expression of specific genes, viability, and invasion capacity) and/or physical properties (size, shape, density, electrical charges, deformability, inertia, optical properties and acoustic features). It is important to note that most of the current technologies that rely on isolating CTCs based on biological properties are based on epithelial cell adhesion molecule (EpCAM). The second most frequent approach is to isolate CTCs using the fact that most but not all of the tumor cells in the circulation are larger than most blood cells. Therefore, finely tuned filters can be manufactured that retain only tumor cells and let most of the blood cells go through.

When designing a microfluidic filtration device many important factors have to be taken into consideration like filter material, filter gap, filter width, channel width, density and distribution. Blood dilution, fixation and pressure will also influence the passage of blood through the filters and thereby the effectiveness of CTC isolation.

For the device design cross-flow filtration method was selected for its robustness and its capability of being less prone to clogging. It is a special type of cross-flow system with a chalice like filter array, where both lateral and vertical flows exist in the device.

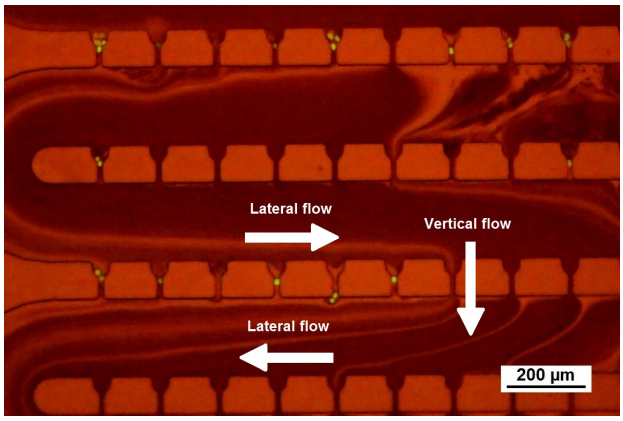


Fig. 1. Fluorescent image from EDTA treated blood sample spiked with CTCs. The captured tumor cells are blocked in the microcapillaries. The flow rate was 3 $ml/h$.

This device was successfully used to filter out CTCs with higher than 90% efficiency at lower flow rates using EDTA treated whole blood and whole blood treated with formaldehyde also. Figure 1 shows a fluorescent image of captured CTCs in EDTA treated blood at 3 $ml/h$.

Viability of the cells should be also examined and controlled in order to making further biological analysis steps possible. Progress towards understanding the heterogeneity and the complexity of CTCs in cancer could shed further light on the mechanisms of tumor metastasis. CTC populations are highly heterogonous in physical and biological properties. Thus CTC capture approaches that rely on a single property has its own limitation. Circumventing this problem microfluidic devices which combine several capture approaches on-a-chip can be fabricated.

## References

[1] F. Coumans, G. van Dalum, M. Beck and L. Terstappen, "Filtration Parameters Influencing Circulating Tumor Cell Enrichment from Whole Blood", *PLoS ONE*, vol. 8, no. 4, p. e61774, 2013.
[2] P. Li, Z. Stratton, M. Dao, J. Ritz and T. Huang, "Probing circulating tumor cells in microfluidics", *Lab on a Chip*, vol. 13, no. 4, p. 602, 2013.

Á. SZÉLIG, "Filtration of MCF-7 human breast cancer cells in a microfluidic device" in *PhD Proceedings Annual Issues of the Doctoral School, Faculty of Information Technology and Bionics, Pázmány Péter Catholic University – 2018.* G. Prószéky, P. Szolgay Eds. Budapest: Pázmány University ePress, 2018, pp. 28–28. This research has been partially supported by the European Union, co-financed by the European Social Fund (EFOP-3.6.3-VEKOP-16-2017-00002).

# A microfluidic cell cultivating device

Mihály SZÜCS
(Supervisor: Kristóf IVÁN)
Pázmány Péter Catholic University, Faculty of Information Technology and Bionics
50/a Práter street, 1083 Budapest, Hungary
szucs.mihaly@itk.ppke.hu

***Abstract*—Observing a cell culture under specific circumstances is a common element of many different protocols of drug research and cell biology.**

**However, the devices currently used for cell culturing are mostly outdated, and recent techniques are typically optimized towards a specific measurement, which makes them inconvenient in the field of fundamental research.**

**The aim of my work was to elaborate a device with different advantages compared to the traditional methods, while keeping the versatility. I considered microfluidic principles because of their numerous advantages.**

**As a result I created an early prototype. Its performance was compared to the conventional technique, and the results showed, that my device was suitable for mammalian cell growth.**

***Keywords*-cell culturing; microfluidics; stem cells**

## I. Introduction

*In vitro* cell cultivation has played a major role in most fields of biological and medical research, as well as in biotechnological applications. The most commonly used tools for this process are still the Petri dishes and traditional cell culture flasks.

Many cell cultivating solutions emerged in the last decades are mainly highly optimized for carrying out a single type of measurement, and cannot be used in other kinds of experiments. Another drawback of novel devices is that conventionally used protocols utilize traditional tools, thus laboratories are not always willing to try different methods.

Considering these I researched the possibility of a multipurpose cell cultivating device, which is compatible with conventional protocols, jet have significant advantages over the currently used tools.

## II. Microfluidic approach

Microfluidic devices manipulates small amounts of liquids using micro-channels with the width of $1 - 100\mu m$. The compact size is one of the great advantages of a microfluidic system, because it can minimize the required quantity of both the sample and the reagents. [1]

Beyond the minimization of reagents other possibilities of microfluidics are being utilized. In these micro-channels laminar flow is dominant. This phenomenon allows special fluid handling and separation methods opening up new possibilities.

## III. Cell culture in microfluidics

### A. Perfusion cell culture system

The main disadvantages of static cell cultures in Petri dishes, which are most commonly used, come from the need of manual intervention. In any case when manipulation of the cell culture is needed, the container has to be opened. This might be dangerous, particularly in case of long term cell cultures, because the culture can be contaminated. Other than contamination the composition of the cell culturing medium can also be changed by the metabolism of the cells. Evaporation can also change the concentration of the medium, and its quantity as well. The cells physiology can respond sensitively to such environmental changes, therefore solutions to these problems can greatly increase the effectiveness of the cell culture experiments.

Perfusion cell cultures can effectively get rid of most of the issues stated above. In these devices the cell culturing chamber is closed during the experiment, and the manipulation can be done by fluid inlets. In addition the extracellular conditions in these devices are more similar to the *in vivo* conditions.[2]

## IV. A multipurpose perfusion chamber

The aim of my research is to create a multipurpose perfusion chamber. My collaboration with biologists highlighted the need of a simple perfusion chamber to replace Petri dishes because of the disadvantages I mentioned before.

I created an early prototype, so I can define the direction of my further research based on the first experiments.

The device was tested with human mesenchymal stem cells. Before loading the cells the whole device as well as the used accessories were sterilized. The chamber was loaded with the prepared cell solution, and after a day of incubation the cell culture can be examined to confirm the survival and adhesion of cells to the glass surface.

## V. Results and discussion

During the test of the early prototype of a multipurpose cell culturing perfusion chamber only qualitative data was acquired jet. According to these experiences the prototype was overall successful.The applied protocol did not differ significantly from the original protocol with Petri dishes, so the goal to create a device that can replace traditional cell culturing tools was achieved.

The first design however has some flaws. I plan to continue my research by redesigning the device to correct these deficiencies.

## Acknowledgements

I gratefully acknowledge the support of my supervisor, Kristóf Iván, as well as the help of the other members of the Biomicrofluidic research group of the Pázmány Péter Catholic University. I am also grateful to the Molecular Cell Biology Research Group of the Hungarian Academy of Sciences for helping me by testing my devices.

## References

[1] G. M. Whitesides, "The origins and the future of microfluidics," *Nature*, vol. 442, no. 7101, p. 368, 2006.

[2] M. H. Wu, J. P. Urban, Z. Cui, and Z. F. Cui, "Development of pdms microbioreactor with well-defined and homogenous culture environment for chondrocyte 3-d culture," *Biomedical microdevices*, vol. 8, no. 4, pp. 331–340, 2006.

M. SZÜCS, "A microfluidic cell cultivating device" in *PhD Proceedings Annual Issues of the Doctoral School, Faculty of Information Technology and Bionics, Pázmány Péter Catholic University – 2018.* G. Prószéky, P. Szolgay Eds. Budapest: Pázmány University ePress, 2018, pp. 29–29. This research has been partially supported by the European Union, co-financed by the European Social Fund (EFOP-3.6.3-VEKOP-16-2017-00002).

.

# PROGRAM 2
# COMPUTER TECHNOLOGY BASED ON MANY-CORE PROCESSOR CHIPS, VIRTUAL CELLULAR COMPUTERS, SENSORY AND MOTORIC ANALOG COMPUTERS

Head: Péter SZOLGAY

# Dynamic thermal simulation of the CubeSat

Nawar AL-HEMEARY
(Supervisor: Gabor SZEDERKENYI)
Pázmány Péter Catholic University, Faculty of Information Technology and Bionics
50/a Práter street, 1083 Budapest, Hungary
al-hemeary.nawar@itk.ppke.hu

***Abstract*—Aerospace industry recognizes the importance of moving towards smaller, better, and cheaper spacecraft to support the community's increasing dependence on space-based technologies. PW-SAT is a CubeSat developed at Warsaw University of Technology. Because of the surface area and power are limited, passive thermal control was first selected for temperature regulation. Thermal mathematical model (TMM) with simulation results are presented in this paper to study the temperature variations and the thermal stability of the PW-SAT surface and the propellant tank. The concepts derived and evaluated within TMM can be used in a variety of other applications. The thermal simulation of the fuel tank has been done for several cases based on different variations of the satellite surface coating.**

***Keywords*-Keywords: CubeSat, PW-SAT, TMM, Thermal analysis, Passive control system.**

## I. Introduction

There has been a recent increase in emphasis on small satellites by governments and industry, attracted primarily by their low cost, mass, size, short development time and relative simplicity. The cost of sending vehicles and satellites into space together with the related large amount of work involved result in infrequent missions. Therefore, the engineers working on space systems usually do not get many opportunities for the practice of launch and flight operations. PW-SAT is a satellite developed for over a year by different teams at Warsaw University of Technology. The first version of the satellite was finished and delivered for launch during the year 2011. It is a CubeSat satellite, consistent with CubeSat Design Specification developed by California State Polytechnic. This standardized type of satellite poses limits on both the size and weight of the space segment. The size of this satellite cannot exceed roughly 10x10x10 $cm^3$ and a mass of 1kg. At present, PW-SAT hasn't flown with an onboard propulsion system, to provide attitude control or perform orbital maneuvers, thus there is a need to investigate the possibility to install propellant tank and perform the thermal simulations to obtain a starting point for adding propulsion system to PW-SAT. The thermal mathematical model of PW-SAT surface and fuel tank is responsible for predicting the transient thermal behavior of the fuel tank as well as the satellite faces through its orbital motion, with changing either the PW-SAT surface optical properties or the solar cell ratio which is attached to certain satellite surface depending on some feasible assumptions.

## II. SYSTEM DESCRIPTION AND ASSUMPTIONS

An important task in thermal modeling is the adequate consideration of PW-SAT surface and spherical fuel tank material properties as well as the formulation of appropriate initial and boundary conditions. The problem is to create a model, which is on the one hand simple enough to limit the expenditure, on the other hand detailed enough to give a proper description of the physical situation and relations.

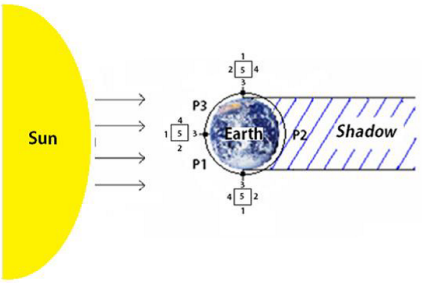


Fig. 1. PW-SAT orbital motion.

## III. Conclusion

A thermal mathematical model was constructed and studied for computing the surface and fuel tank temperatures of a PW-SAT. Several cases have been presented with different surface finishes and the results have shown that TMM accurately calculates the radiative heat that a PW-SAT will encounter in its assumed orbit. Initially, the PW-SAT surface has been built with 100 % aluminum 6061-T6, the corresponding results suggest that the surface and the fuel tank temperature would be too high. Thus, additional surface finishes have been taken into consideration. The first choice of the surface finish was to coat all of the satellite faces with magnesium oxide aluminum oxide paint, the results show that the temperature of the fuel tank was dropped, because of the increasing emissivity and decreasing absorptivity of the satellite surface. Further simulations were performed for the cases in which the faces were exposed to the sun covered partially with solar cells. The results indicate that the case (The satellite faces which are exposed to the sun during the orbit are covered with 30 % aluminum and 70 % solar cells) which delivers the most electrical power due to the higher percentage of the solar cell still satisfies the boundary conditions of the fuel tank and the satellite surface. The results also suggest that there is a possibility to install a fuel tank inside the PW-SAT and it will be the first step on adding propulsion system which can generate the thrust to this CubeSat.

N. AL-HEMEARY, "Dynamic thermal simulation of the CubeSat" in *PhD Proceedings Annual Issues of the Doctoral School, Faculty of Information Technology and Bionics, Pázmány Péter Catholic University – 2018.* G. Prószéky, P. Szolgay Eds. Budapest: Pázmány University ePress, 2018, pp. 32–32.
This research has been partially supported by the European Union, co-financed by the European Social Fund (EFOP-3.6.3-VEKOP-16-2017-00002).

# Analysis and file formats of circular light-fields

.

Aron CSERKASZKY
(Supervisor: Prof. Peter SZOLGAY)
Pázmány Péter Catholic University, Faculty of Information Technology and Bionics
50/a Práter street, 1083 Budapest, Hungary
cserkaszky.aron@itk.ppke.hu

## I. Summary

Linear data-structures have long been used in various processing techniques due to their relative ease of use and often low computational costs. This however is a hindrance for many applications with specific sampling requirements. In this paper we show the unique advantages of circular data-structures in the field light-field processing, with special considerations for light-field reconstruction.

Light-field is essentially a vector field of light rays with essential applications in the area of 3D visualization. The way light-fields are captured and stored determines the ray structure in the vector field. And this ray structure restricts the useful applications and available processing algorithms for the particular light-field. Choosing an efficient capturing setup to measure the rays we need for the processing algorithms, and then storing those captured rays in a useful structure is therefore essential for high quality results for any application.

Scene reconstruction is the task of computing the dense light-field from the sparse captured samples. The sparse samples often come from perspective cameras that capture rays from the position of the camera. This ultimately constrains the density of the captured light-fields in the spatial dimension. Often the cameras are arranged in a linear camera array, where cameras are placed along a straight line and the face in the same direction, that is orthogonal to the placement line. From the images of such a linear camera array we can assemble the epipolar image, that contains a specific line of each camera image in placement order. Fig. 1 shows such an epipolar image with three differently colored objects at different depths. Many methods of scene reconstruction exploit the linear relation between object depth and line slope in the epipolar image.

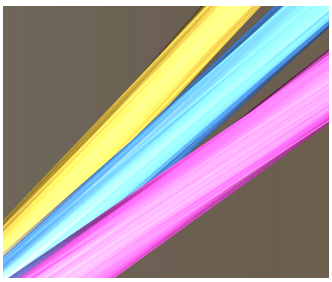

Fig. 1. Linear camera array epipolar image of the test scene indicating the three objects at different depths.

Another problem in scene reconstruction is how to treat and combine data from multiple camera arrays, this is especially challenging for linear camera arrays as the only common point of two arrays is the intersection of their line, if that exists. There are no solutions to this problem to date, but we can use circular camera arrays to work around this.

Perspective cameras along a circle pointing towards the center do not benefit from the same properties as linear arrays in terms of their circular epipolar image, shown on Fig. 2. The formula describing the relation between object position and their respective curve in the circular epipolar image is far too complicated for the purposes of scene reconstruction. Most likely only the brute force search of the curves is the only possibly solution, with restrictively high computational cost even on massively parallel computing hardware.

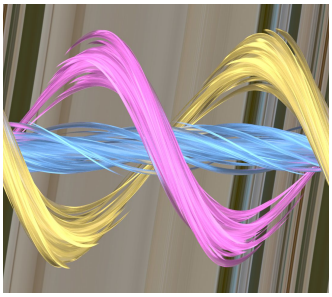

Fig. 2. Circular camera array epipolar image of the test scene.

Our proposed solution for reconstructing circular light-field is to slightly change their sampling structure from a normal perspective camera, to a camera that samples rays pointing to equidistant points along on the opposing side of the circle. The resampled image, after coordinate transformations exploiting the periodic properties of the circle, is shown on Fig. 3. In this representation the relation between the objects position and the curve is a pure sine with a fixed frequency. Exploiting this relation in scene reconstruction could achieve our goal of combining light-field information from multiple sides of a scene.

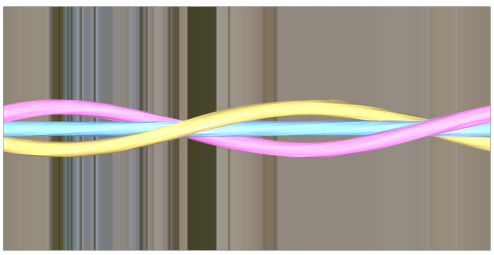

Fig. 3. Resampled test scene after coordinate transformation.

## Acknowledgements

This research is done as a part of ETN-FPI training network (project number 676401), which is funded under the H2020-MSCA-ITN-2015 call and is part of the Marie Sklodowska-Curie Actions Innovative Training Networks (ITN) funding scheme.

Á. CSERKASZKY, "Analysis and file formats of circular light-fields" in *PhD Proceedings Annual Issues of the Doctoral School, Faculty of Information Technology and Bionics, Pázmány Péter Catholic University – 2018.* G. Prószéky, P. Szolgay Eds. Budapest: Pázmány University ePress, 2018, pp. 33–33.
This research has been partially supported by the European Union, co-financed by the European Social Fund (EFOP-3.6.3-VEKOP-16-2017-00002).

# Technical review on Light Field Imaging and Capturing Systems

Subbareddy DARUKUMALLI
(Supervisor: Peter SZOLGAY)
Pázmány Péter Catholic University, Faculty of Information Technology and Bionics
50/a Práter street, 1083 Budapest, Hungary
darukumalli@itk.ppke.hu

***Abstract*—Light field imaging has been around for more than a hundred years, and at the time of this paper it is already widely used in the industry and about to enter the consumer market as well. Although cameras and even displays are indeed purchasable, the general appearance in home environment use case scenarios is to happen in the near future.The current state of light field technologies was enabled by the extensive research in the area and the numerous solutions that were proposed.**

***Keywords*-light field, camera capture systems, light Field Visualization.**

### *A. Scientific Literature Review*

The grand challenges of visualizing three-dimensional objects and scenes have motivated scientists in the past century, and their inspiration resulted in numerous solutions and technologies. French physicist Gabriel Lippmann is well-known for his contribution to color photography, for which he won the Nobel Prize in physics in 1908, but in the same year he also proposed the concept of integral imaging [1]. This is an autostereoscopic 3D imaging technique, which means it allows the binocular perception of depth without any additional viewing device, e.g., the special glasses we often use today for watching stereoscopic 3D television. The name of this technique is directly translated from "photographie integrale", but it can also be interpreted as "complete imaging" or as "complete photography", since the motivation was and still is the incomplete nature of 2D visual representation; the 3D world we live in simply cannot be fully embodied in a flat, 2D image.

With all these simplifications, we obtain a four-dimensional representation via a plenoptic function, commonly known as a 4D light field[2], but also often referred to as Lumigraph[3]. A light field is basically a 3D vector field, as it is a collection of 3D vectors, where a vector represents a ray of light. As described earlier, the intensity along a vector is defined to be constant. So a light field is a 3D vector field, however, it is important to note that the plenoptic function is not a vector function, because it returns a scalar value – this aforementioned light intensity – and not a vector. It could return a vector if we defined it in a way that it returns the values for the three prime colors (RGB), but we can simply have a separate function for each color.

A plenoptic representation of a scene evidently requires acquisition methods – i.e., visual capture techniques – in order to have something to visually reproduce. In case of Lippmann's integral imaging, the scene was captured from the position and orientation of each microlens. Since then, more than a hundred years have passed, and many new methods and techniques of scene capture have emerged and evolved, but for several, the principle remained the same. However, capturing the light field of a scene does not necessarily mean that it is immediately ready to be visualized by a light field display, especially since different capturing techniques may acquire different data, e.g., while some capture systems use one, single, fixed-position camera to capture the light field of the scene, in other systems the camera may move or there might be several cameras. The information obtained by the capture system must be suited to the display system in order to represent the scene, thus light field conversion is required. Also, in several scenarios, the reconstruction of the light field might be necessary, e.g., if a given point of view of the scene was not captured by the camera system but the display system needs it for appropriate visualization, or simply if the conversion technique relies on light field reconstruction. This paper provides a tutorial about the different light field capture systems, state-of-the-art light field and 3D reconstruction techniques, methods of light field conversion, and light field displays. Related to this paper is a recent publication by Ihrke[4], reviewing the past 25 years of digital light field imaging. Instead of historically reviewing the research carried out in light field imaging, the aim of our contribution is to present an easy-to-understand overview of the systems and methods in the aforementioned four areas of operation regarding light field, and thus to support the understanding of more complicated literature in the field.

*Acknowledgment*

The work in this paper was funded from the European Union's Horizon 2020 research and innovation program under the Marie Sklodowska-Curie grant agreement No 721383.

## REFERENCES

[1] G. Lippmann, "Epreuves reversibles. photographies integrals," *Comptes-Rendus Academie des Sciences*, vol. 146, pp. 446–451, 1908.
[2] M. Levoy and P. Hanrahan, "Light field rendering," in *Proceedings of the 23rd annual conference on Computer graphics and interactive techniques*. ACM, 1996, pp. 31–42.
[3] S. J. Gortler, R. Grzeszczuk, R. Szeliski, and M. F. Cohen, "The lumigraph," in *Proceedings of the 23rd annual conference on Computer graphics and interactive techniques*. ACM, 1996, pp. 43–54.
[4] I. Ihrke, J. Restrepo, and L. Mignard-Debise, "Principles of light field imaging: Briefly revisiting 25 years of research," *IEEE Signal Processing Magazine*, vol. 33, no. 5, pp. 59–69, 2016.

S. DARUKUMALLI, "Technical review on Light Field Imaging and Capturing Systems" in *PhD Proceedings Annual Issues of the Doctoral School, Faculty of Information Technology and Bionics, Pázmány Péter Catholic University – 2018.* G. Prószéky, P. Szolgay Eds. Budapest: Pázmány University ePress, 2018, pp. 34–34. This research has been partially supported by the European Union, co-financed by the European Social Fund (EFOP-3.6.3-VEKOP-16-2017-00002).

# A new compact self-referenced holographic setup tested on a fluorescent target

Márton Zsolt KISS
(Supervisor: Ákos ZARÁNDY)
Pázmány Péter Catholic University, Faculty of Information Technology and Bionics
50/a Práter street, 1083 Budapest, Hungary
kisma1@itk.ppke.hu

***Abstract*—We propose a new self-referenced holographic microscope setup based on a special bifocal lens. This setup can detect and visualize fluorescent objects. The new principle and the experimental results of the imaging are also presented.**

***Keywords*-self-referenced holography, fluorescent imaging**

## I. Introduction

The holographic technique is based on the interference phenomena so it is a requirement that the applied holographic setup provide smaller optical path differences than the coherent length of the applied light. That is why the used coherent length determines the construction of the holographic optical setup. When light with short coherence length is used, (fluorescent holography, white light holography, incoherent holography or self-referenced holography) only a special optical design can ensure the needed optical path difference. We can categorize the special setups by their basic optical element, which can be e.g. an interferometer (Linnik interferometer, Hariharan-Sen interferometer, Mach-Zehnder interferometer, or Michelson interferometer) or a multi- or bifocal optical element (Fresnel zone-plate, spatial light modulator or a bifocal lens).
TThe holographic setup presented in this article is a self-referenced fluorescence holographic microscope that is based on a ring-shaped bifocal lens. This creates a new shaped and a special structured in-line hologram. With the reconstruction of a fluorescent target I demonstrate in practice the applicability of this optical design.

## II. The ring-shaped bifocal lens at self-referenced holography

This optical element has an axial symmetry and double focuses. The concentric regions of the lens near and far from the axis have different focuses. Therefore this bifocal lens separates the wave field of a single point source in the space, and focuses them to two different places with its central and ring areas. As in this setup the divergence of the central beam is bigger than the divergence of the ring-shaped beam, the two separated beams will overlap each other in a region during the propagation. The cross-section of the union of the two beams is also ring-shaped. Hence the optical path difference is smaller than the coherence length of the fluorescent light the interference phenomena can be observed in this union. Capturing this cross-section of the united beams with a detector we get the digital self-referenced hologram.
The bifocal lens is placed at the back focal plane of an infinity corrected objective with a focus of 45 mm (NA=0.16). This is followed by an afocal optical system with an angular magnification of 0.2. The hologram is captured on the 1/4-th part of a Bayer-patterned CMOS sensor area that has a green color filter. The recorded hologram resolution is 640x480.

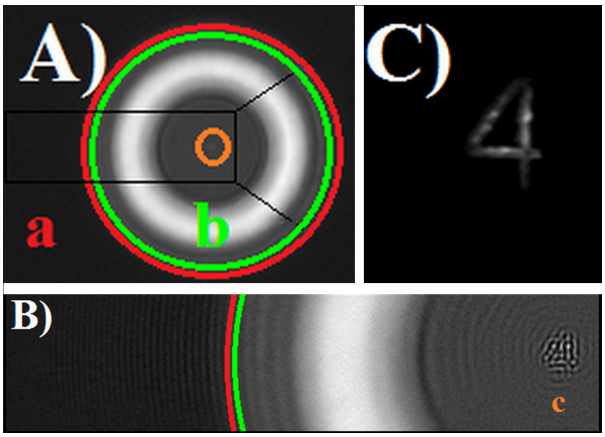


Fig. 1. A) is the reconstructed hologram (640x480). B) is a part of the reconstruction (377x90). C) is the common photo of the sample. a) is the area of the twin image. b) is the area of the zero order. c) is the image.

## III. The hologram reconstruction

The ring-shaped hologram reconstruction was fulfilled by using the angular spectrum method. Fig. 1/A shows the image of the whole reconstruction. Fig. 1/B delineates the separated orders (image, twin image and the zero order terms), while Fig. 1/C shows the photo of the sample object so it can be compared with that of the reconstruction. The similarity can be clearly seen.

## IV. Discussion and Conclusion

A new bifocal lens based self-referenced digital holographic microscope was introduced and constructed. This setup captured the self-referenced hologram of a fluorescent object. We got the image of the object from the hologram with reconstruction. This result demonstrates that the ring-shaped bifocal lens can be an alternative device to the interferometers, FZP, and SLM to build a self-referenced holographic setup. It is clear that its disadvantage is losing the low frequency components. But its benefits are the compact design, the insensitivity for vibrations, the advantages of the single-shot setups and its cheapness.

## V. Acknowledgement

This article was fully presented in: Digital Holography and Three-Dimensional Imaging, DH 2015. Digital Holography and Three-Dimensional Imaging, DH 2015 . Optical Society of America, Washington, DTh1A.7. ISBN 9781557529916 10.1364/DH.2015.DTh1A.7

M. KISS, "A New Compact Self-referenced Holographic Setup Tested on a Fluorescent Target" in *PhD Proceedings Annual Issues of the Doctoral School, Faculty of Information Technology and Bionics, Pázmány Péter Catholic University – 2018.* G. Prószéky, P. Szolgay Eds. Budapest: Pázmány University ePress, 2018, pp. 35–35. This research has been partially supported by the European Union, co-financed by the European Social Fund (EFOP-3.6.3-VEKOP-16-2017-00002).

# Growth-optimal portfolios and their approximations

Zsolt NIKA
(Supervisors: Miklós RÁSONYI and Péter SZOLGAY)
Pázmány Péter Catholic University, Faculty of Information Technology and Bionics
50/a Práter street, 1083 Budapest, Hungary
nika.zsolt@itk.ppke.hu

***Abstract*—One of the most used application areas of optimization theory in finance is portfolio optimization. In a simple approach an investor optimizes the expected value of his/her portfolio at a given time or at infinity. In the latter case a natural formulation of the problem is to maximize the growth of the value portfolio at each investment step and this is our aim in this article.**

**In the literature the problem is mostly worked out within non-parametric models. Our aim is to solve the optimization task when stock prices do show memory effect, i.e. their current prices depend in some way on their past prices. In general no solution exists for this (in parametric models). We are going to show a class of models where optimality can be proven and we will also give the necessary conditions for it.**

**The main focus of the paper is to present some approximations for the optimal procedure and how well they perform in our model class. Results will be demonstrated by numerical simulations.**

Keywords – growth optimal; investment strategy; semi-log-optimal; optimization theory; portfolio optimization

## I. Intorduction

A portfolio is a group of financial assets (like a stock or bond) held by an investor whose intention is to optimise some kind of benefit from this ownership. The most important property of a portfolio is its price or its expected price in the future, but it is not evident how to take it into consideration. To maximize its expected value (consider the price as a random variable) seems like an obvious idea, but this approach avoids addressing risk: given two portfolios with the same profit, we would choose the one with less risk. A practical approach is to maximise the expected logarithm of the portfolio value. While plain expectation is a generalization of arithmetic mean, the logarithm transforms it into geometric mean which is sensitive to the fluctuations in the future value, i.e. to the risk.

There exists a known approximation in the literature, called *semi-log-optimal portfolio*, when in each step a second order approximation of the growth is optimized (for theoretical results see [**?**], for application see [**?**]). We do not follow this terminology to avoid misconceptions because we use also first order approximation.

## II. Financial model

In the modelling of stock prices and the process of investment, we have the following assumptions:

- Investment is in discrete time, $t \in \mathbb{Z}$.
- Stock price ($S_t$) is a non-Markovian stochastic process, i.e. it has some kind of memory.
- Log-return of the price ($H_t := \log(S_t/S_{t-1})$) is stationary and ergodic.
- Log-return is modelled as a stochastic different equation, $H_t = F(H_{t-1}, Y_t, \varepsilon_t, \eta_t)$ for some real function $F$.
- Memory effect is included in the volatility of the log-return.
- The dynamics of the log-return is:
$$H_{t+1} = \alpha H_t + \sigma e^{Y_{t+1}}(\rho\epsilon_{t+1} + \sqrt{1-\rho^2}\eta_{t+1}), \quad (1)$$
Here $\varepsilon_t, \eta_t$ are i.i.d. noises. Initial value $H_0 = 0$. $Y_t = \sum_{j=0}^{\infty}(1+j)^{-b}\epsilon_{t-j}$.
- The time-evolution of the portfolio is:
$$W^{\pi}_{t+1} = W^{\pi}_t\left[(1-\pi_t)(1+r) + \pi_t e^{H_{t+1}}\right]. \quad (2)$$
The strategy of the investment is $\pi_t$ which should be optimized.
- A strategy $\pi^* = \{\pi^*_t\}_{t\in\mathbb{N}}$ that solve the equation
$$\max_{\pi} \liminf_{t\to\infty} \frac{1}{t} E[\log(W^{\pi^*}_t)] \quad (3)$$
is called *log-optimal strategy* in the infinite horizon long-run problem.

With this model we ensure that the log-return is stationary and ergodic, if $b < 0.5$.

## III. Approximations

Optimality can be achieved by maximizing the expected growth at every investment time, i.e. $\max_\pi \mathbb{E}[\log(W_t/W_{t-1})]$. Approximating the logarithmic function in the expected value leads to sub-optimal results, depending on how many terms we use in the Taylor-expansion. We are going to look at results in the case of first and second order approximation. As a benchmark model, we use constantly rebalancing portfolios: the log-optimal solution and its approximations are compared to a portfolio where the strategy function is constant in time.

## IV. Results

Table I shows results of a numerical simulation. Simulation can be regarded as daily investments and in this case the investment lasted for 16 years. The four portfolios (log-optimal, the two approximations and the constantly rebalancing) are compared by the value function, i.e. the objective function of the optimization procedure. Table I shows that the first and second order approximation is very close to the log-optimal solutions, but the constantly rebalancing portfolio's yield is poor. The advantage of the approximated portfolios is that they can be calculated as a function evaluation, while the log-optimal solution requires multidimensional numerical integration.

| Portfolio | Yearly interest |
|---|---|
| Log-optimal | 30.5% |
| 2nd order approx. | 30.3% |
| 1st order approx. | 29.0% |
| Constantly rebalancing | 5.8% |

TABLE I: Comparing the profitability of different portfolios (different investment strategies).

Zs. NIKA, "Growth-optimal portfolios and their approximations" in *PhD Proceedings Annual Issues of the Doctoral School, Faculty of Information Technology and Bionics, Pázmány Péter Catholic University – 2018.* G. Prószéky, P. Szolgay Eds. Budapest: Pázmány University ePress, 2018, pp. 36–36.
This research has been partially supported by the European Union, co-financed by the European Social Fund (EFOP-3.6.3-VEKOP-16-2017-00002).

# Antenna Design for Near-field Radio-frequency Devices

Áron PAPP
(Supervisor: György CSEREY)
Pázmány Péter Catholic University, Faculty of Information Technology and Bionics
50/a Práter street, 1083 Budapest, Hungary
papp.aron@itk.ppke.hu

## I. Summary

Radio-frequrency Identification (RFID) is widely used in logistic and supply chain, in sports race timing, conference attendee tracking, material management, access control, tool tracking, kiosks, library systems to just mention some of them. Now, it's time to introduce a application in the pharmaceutical industry.

Small animal telemerty systems are used to gather different types of information from the pharmaceutical experimental animals. Currently the most commonly collected information are ventricular and arterial pressure, temperature, SNA, low and high frequency biopotential, and tissue oxygen.

There are many vendors on the market producing implants for the mentioned problem, but their product has very high invasive impact on the animals, espacially on the small ones, line mice and rats. In order to achieve a high measurement frequency and a long measurement time, other manufacturers will add batteries to their circuits, which dramatically increase the size of the implants, and limits the measurement time in sum.

At the heart of our research is a system that gives more freedom to both the observed animal and the pharmaceutical researchers. The two problems are resolved at the same time, so we do not put a battery into the implant, instead we the device will be powered wirelessly. RFID technology is capable of solving both energy and communication alongside, but by not having this area of application the main cause of the technology, some of the emerging issues need to be solved.

We decided to use the high-frequrency range (13.56MHz). Low-frequency RFID systems were dropped because of the insufficient level of data transmission speed. The HF range on the other hand is less sensitive to obstacles than ultrahigh-frequency RFID systems and has a lower wavelength, which makes it possible to produce high-efficiency antennas in compliance with the given size requirements. As ferrite materials are available for 13 MHz frequency, HF RFID systems are typically using the electromagnetic near-field. This latter property allows the spatial limitation of a more potent magnetic field, which is indispensable for compliance with statutory regulations.

There are some other problems we needed to solve, mostly related to the size of the implant, but regarding cthe current article they are out of the scope. All the radio-frequency related issues are due to the field strength and the direction of the vector space. Increasing the field strength by using of amplifiers can simply be solved, the only limiting compliance is the spatial scope of the field (i.e. legal regulations). However, it is more difficult to solve the directional independence. It is not possible to achieve directional independence by simply increasing the number of antennas, because in this case the vector space of the resulting electromagnetic field is also stationary, as if it were generated by a single antenna.

This article presents a complete solution, that makes it impossible for a RFID tag with a 1-dimensional antenna to hide within a given space. Further solutions to achive direction independence are also repoted.

This research was supported by Pázmány Péter Catholic University (KAP17-61008- 1.2-ITK). The invaluable help of the multidisciplinary doctoral school at the Faculty of Information Technology of the Pázmány Péter Catholic University is gratefully acknowledged. The research has been partially supported by the European Union, co-financed by the European Social Fund (EFOP-3.6.3-VEKOP-16-2017-00002).

## References

[1] Vipul Chawla and Dong Sam Ha "An Overview of Passive RFID" Virginia Polytechnic Institute and State University [0163-6804/07/$20.00 © 2007 IEEE]
[2] Pavel V. Nikitin, K. V. S. Rao and Steve Lazar "An Overview of Near Field UHF RFID" 2007 IEEE International Conference on RFID, Gaylord Texan Resort, Grapevine, TX, USA, March 26-28, 2007
[3] Jose Luis Martinez Flores, Satya Sai Srikant, Bimal Sareen, Abhijit Vagga "Performance of RFID Tags in Near and Far Field" ICPWC 0-7803-8964-6/05/$20.00 IEEE 2005
[4] D. M. Dobkin, S. M. Weigand, and N. Iye, "Segmented Magnetic Antennas for Near-Field UHF RFID," Microwave Journal, vol. 50, no. 6, pp. 4, 2007.
[5] David J. Griffiths, "Introduction to electrodynamics – Fourth edition" ISBN-13: 978-0-321-85656-2, Pearson 2013.

Á. PAPP, "Antenna Design for Near-field Radio Frequency Devices" in *PhD Proceedings Annual Issues of the Doctoral School, Faculty of Information Technology and Bionics, Pázmány Péter Catholic University – 2018.* G. Prószéky, P. Szolgay Eds. Budapest: Pázmány University ePress, 2018, pp. 37–37. This research has been partially supported by the European Union, co-financed by the European Social Fund (EFOP-3.6.3-VEKOP-16-2017-00002).

# Global stability analysis of linear parameter varying systems via quadratic separator for uncertain constrained systems

Péter POLCZ
(Supervisor: Gábor SZEDERKÉNYI)
Pázmány Péter Catholic University, Faculty of Information Technology and Bionics
50/a Práter street, 1083 Budapest, Hungary
polcz.peter@itk.ppke.hu

***Abstract*—In this article, we compare our new results about global stability analysis of LPV systems first published in the conference contribution [1, Polcz, Kulcsár and Szederkényi, "Computation of rational parameter dependent Lyapunov functions for LPV systems," in Swedish Control Conference 2018] with the method proposed in [2, Iwasaki and Shibata, "LPV system analysis via quadratic separator for uncertain implicit systems", IEEE Transactions on Automatic Control, 2001]. Furthermore, we describe in brief the operations of [2]. This comparative evaluation clearly supports the applicability and versatility of our method presented in [1].**

***Keywords*-linear parameter varying systems, global stability, Lyapunov functions, linear matrix inequalities**

## I. Introduction

The computational construction of Lyapunov functions for dynamical system models caught a large amount of attention in the past few decades. Effective methods have been introduced to uncertain linear systems e.g. [2].

Based on frequency-domain rank-conditions and inequalities, the authors of [2] derived parameter dependent LMIs for the global stability of uncertain implicit systems. These results were applied for the global stability analysis of LPV systems in the linear fractional representation using rational Lyapunov functions (L.f.s) containing uncertain parameters.

Selecting a parameterized uncertain rational L.f. candidate, [3] used Finsler's lemma and affine annihilators to obtain polytopic parameter dependent LMIs ensuring the Lyapunov conditions. These results were further improved in our earlier papers e.g. [4], and successfully applied for different dynamical system models. The proposed method of [4] was adapted in [1] to prove global stability of LPV systems in the linear fraction representation (LFR).

### A. A brief comparison of the two approaches

In this article, we present in brief the approach of [2] for global stability analysis for LPV systems, where the authors construct an implicit system with an affine output zeroing constraint. Based on frequency-domain consideration, they proposed quadratically parameter dependent LMI conditions which ensure stable zeros and hence stable zero dynamics for an implicit LPV system for every possible value of the uncertain parameter $\varrho$ in a convex domain $\mathcal{R}$ with a bounded rate $\dot{\varrho}$. At the same time, the proposed LMIs generate a Lyapunov matrix $P$ inherently, which proves stable behaviour of the system for the whole state-space.

Differently from [2], in [1], we are looking for a parameterized L.f. given in a general quadratic form of the state variables and of rational (i.e. fractional) terms of the uncertain parameter values. Based on [3], we prescribe sufficient affine parameter dependent LMIs to ensure the Lyapunov conditions. If the LMIs do not depend on the state variables, global stability can be proven for any rational uncertain system in the linear fractional representation. Due to the polytopic nature of the LMIs proposed in [3] (and modified by [1]), it is enough to check their feasibility only in the corner points of the polytopic domain $\mathcal{R}$ of the uncertain parameters $\varrho$.

At first sight, the approaches are different in many aspects, however, we should note that the L.f. in both approaches are searched in the same structure.

## II. Discussion

In this work we compared our new method [1] for global stability analysis of LPV systems with a method already known from the literature [2].

In [1], we apply the dual stability conditions to reach global stability analysis of LPV systems under rational parameter dependence. The main idea behind the method proposed in [1] is to remove the possible state dependence from the generated parameter dependent LMI conditions, therefore, the feasibility of these new LMIs ensure global stability inside the preliminarily given bounded parameter domain.

Our approach is based on time domain consideration, while the method proposed by [2] uses frequency-domain rank conditions and inequalities to generate LMIs for the stability.

Both approaches has been tested on a second order LPV model of computational interest. A detailed comparative assessment of the two approaches can be found in [1].

## Acknowledgements

This research has been partially supported by the European Union, co-financed by the European Social Fund (EFOP-3.6.3-VEKOP-16-2017-00002). The research was also supported by Pázmány Péter Catholic University through the project KAP17-61005-1.1-ITK.

## References

[1] P. Polcz, B. Kulcsár, and G. Szederkényi, "Computation of rational parameter dependent lyapunov functions for LPV systems," in *Swedish Control Conference 2018 (Reglermöte 2018)*, (KTH Royal Institute of Technology and Stockholm University, Stockholm, Sweden), p. accepted, 2018.

[2] T. Iwasaki and G. Shibata, "LPV system analysis via quadratic separator for uncertain implicit systems," *IEEE Transactions on Automatic Control*, vol. 46, pp. 1195–1208, Aug. 2001.

[3] A. Trofino and T. J. M. Dezuo, "LMI stability conditions for uncertain rational nonlinear systems," *International Journal of Robust and Nonlinear Control*, vol. 24, no. 18, pp. 3124–3169, 2013. cited By 14.

[4] P. Polcz, T. Péni, and G. Szederkényi, "Improved algorithm for computing the domain of attraction of rational nonlinear systems," *European Journal of Control*, 2017.

P. POLCZ, "Global stability analysis of linear parameter varying systems via quadratic separator for uncertain constrained systems" in *PhD Proceedings Annual Issues of the Doctoral School, Faculty of Information Technology and Bionics, Pázmány Péter Catholic University – 2018.* G. Prószéky, P. Szolgay Eds. Budapest: Pázmány University ePress, 2018, pp. 38–38. This research has been partially supported by the European Union, co-financed by the European Social Fund (EFOP-3.6.3-VEKOP-16-2017-00002).

# Taking extensive advantage of the high capacity of convolutional neural networks

Mihály RADVÁNYI
(Supervisor: Kristóf KARACS, Péter SZOLGAY)
Pázmány Péter Catholic University, Faculty of Information Technology and Bionics
50/a Práter street, 1083 Budapest, Hungary
radmige@itk.ppke.hu

***Abstract*—The capacity of Convolutinal Neural Networks is enormous, and even if a network is specifically tailored for a given task, it has some extra potential that we can also turn to our advantage. Several trained networks are publicly available online for scientific and research purposes, but their commercial use is not allowed or at least limited. Similarly, from a commercial viewpoint a trained neural network can hold serious business value since it not only solves a concrete task, but in multiple level of abstractions it also reflects on the training data. In this paper I combine the hidden capacities of convolutional neural networks with some business related demands.**

***Keywords*-Convolutional Neural Networks; Network ownership; Hidden capacity; Machine learning**

## I. Introduction

Deep Neural Networks (see Fig.1) gained lot of attention and success recently in various fields on both scientific and commercial tasks and datasets. These datasets contain large amount of data, the network models deal with millions of parameters, thus training such neural networks are also time and energy consuming.

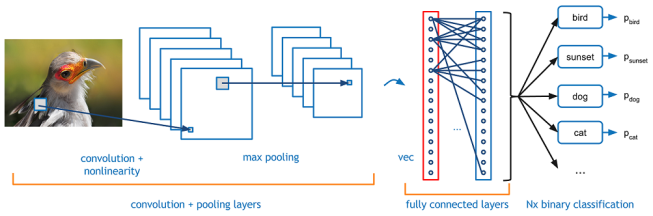


Fig. 1. A typical Convolutional Neural Network has several convolutional and pooling layers, converging into fully connected layers, all together with millions of trainable parameters. Such networks are capable of producing highly accurate classification results.

Besides the effort that goes into the training, many models are available online for research and scientific purposes such as the ones in Caffe Model Zoo [1], where commercial use is not allowed and fair use is asked. Similarly some datasets are also protected[1]. On the other hand a new business model can also evolve, where pre-trained networks are offered for sale. But once a network with all its trained parameters is sold, it can be easily copied and spread without limits.

Since Convolutional Neural Networks contain millions of parameters, a well designed network that is capable of solving an original task can be extended with a simple but robust extra part that helps their authentication. In this paper I present two different approaches for training a network to our special needs, and I show that the solution is very robust to both additive noise and parameter tuning.

[1]Model Zoo: http://caffe.berkeleyvision.org/

## II. Comparing Neural networks

In case multiple trainings are available for the same network architecture, a measure can be defined with that the different solutions are compared and proper distance metric of their weights can be calculated. This measure later can help differentiating independent solution. A sample task is shown in Fig.2 that is solved thousand of times since both the dataset and the different, high performing network architectures are widely available such as [2]. One may find $l^2$ *-norm* to be appropriate for comparing networks and use it as distance metric between learnt weights. To differentiate two solution not only the structure itself but comparison of the weights is also practical. In this paper I show how inefficient this measure can be, and how to imprint authorship more effectively.

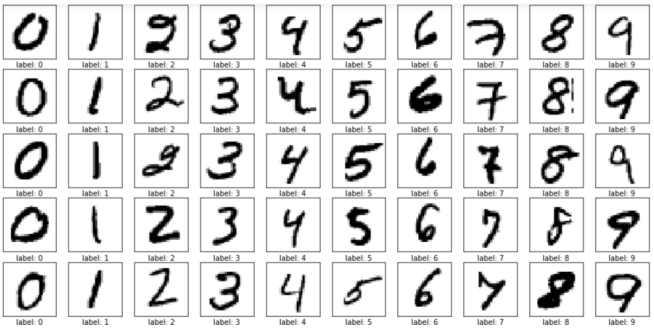

Fig. 2. MNIST is a commonly used dataset that contains 60'000 images of handwritten digits.

## III. Tailoring CNNs to our specific needs

Since the capacity of Convolutional Neural Networks is enormous, there always remain some hidden potential within the network that we can tailor for our specific needs. This is especially important in case our dataset or network have serious business value. In this paper I present a method that maximally takes advantage of the capacity and tolerance of Neural Networks by integrating specific parts that brings further benefits to the authors and network designers.

## References

[1] H. Zarrabi, M. Hajabdollahi, S. Soroushmehr, N. Karimi, S. Samavi, and K. Najarian, "Reversible image watermarking for health informatics systems using distortion compensation in wavelet domain," *arXiv preprint arXiv:1802.07786*, 2018.

[2] H. Larochelle and Y. Bengio, "Classification using discriminative restricted boltzmann machines," in *Proceedings of the 25th international conference on Machine learning*, pp. 536–543, ACM, 2008.

M. RADVÁNYI, "Taking extensive advantage of the high capacity of convolutional neural networks" in *PhD Proceedings Annual Issues of the Doctoral School, Faculty of Information Technology and Bionics, Pázmány Péter Catholic University – 2018.* G. Prószéky, P. Szolgay Eds. Budapest: Pázmány University ePress, 2018, pp. 39–39. This research has been partially supported by the European Union, co-financed by the European Social Fund (EFOP-3.6.3-VEKOP-16-2017-00002).

# Investigation of implementation opportunities of fast multipole methods on FPGA

Levente Márk SÁNTHA
(Supervisors: Zoltán NAGY, Ákos ZARÁNDY)
Pázmány Péter Catholic University, Faculty of Information Technology and Bionics
50/a Práter street, 1083 Budapest, Hungary
santha.levente.mark@itk.ppke.hu

***Abstract*—Fast multipole methods (FMMs) grew out of the fast Fourier transform method and they are powerful mathematical techniques to efficiently calculate pairwise interactions in physical systems, matrix-vector multiplication and summation [1]. It have been used for about 25 years. The advantage of this method is that the required time is of order $N$, where $N$ is the number of objects (atoms) that are interacting, instead of order $N^2$ like brute-force calculation of all pair interactions. It is regarded as among the top-10 algorithms of the 20th century [2].**

***Keywords*-FMM, Fast Multipole, FPGA**

## I. Introduction

The basic idea of FMM is that the influence of the distant atoms, that effects/fields smooth enough, can be modeled by a multipole. Figure 1 shows that. We concentrate the distant atoms in multipoles (empty circles) and we calculate only with these. Of course, the effects of near atoms (filled circles) are calculated directly.

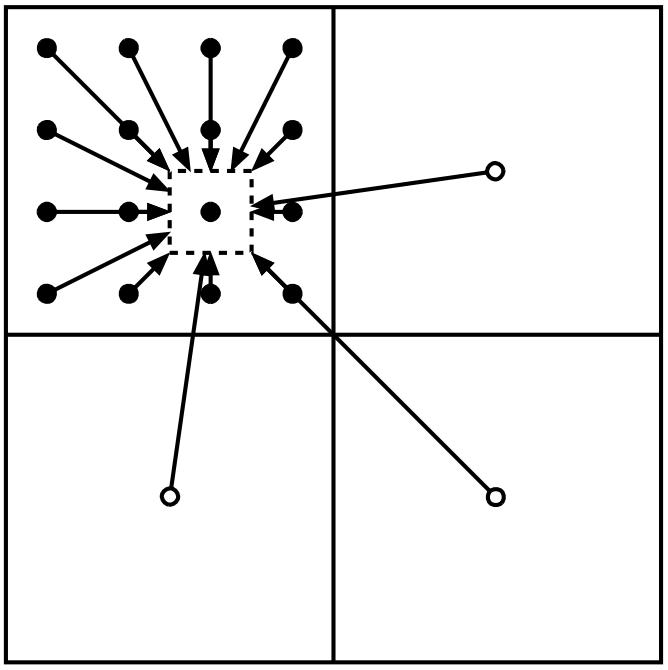

Fig. 1. The basic idea of FMM

There are several ways to create multipoles. In our implementation we are modeling a micro magnetic field and we use a $N * N$ grid. In the middle of the grids are the atoms. In each step, the size of the grid is reduced to quarter, halved both width and height, and we create a multipole in the middle of $2*2$ wide cell. We repeat this until we get a $4*4$ grid. After we got the multipoles, we start the calculation of the field.

## II. FPGA implematation

The FMM methods, despite their advantage, have some implementation, calculation difficulty. They are highly memory intensive tasks and therefore the normal PC implementations are not so satisfying. FPGAs are highly parallel programable logics with built in memories thus an optimized calculation hardware can be realized with them.

Our design can be seen on figure 2. On the left side the multipoles are calculated, and on the right the filed. The first and the last processing unit (PU) are different from the others because they interact with the atoms, not only with multipoles. The inner memory of the FPGA is used for the line buffers, this enables the pipeline process, and we use a traditional DDR main memory to store the different layers data. During the field calculation a downward PU need the data of the previous downward PU and the data of the multipole from the same layer (the same grid size).

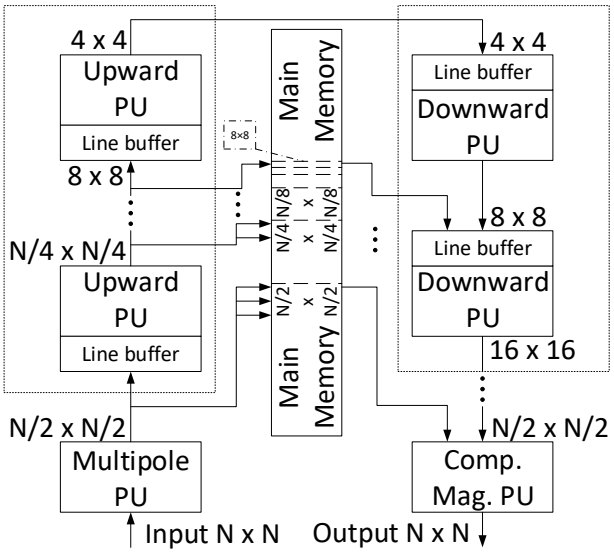


Fig. 2. The block diagram of the magnetic field calculator

## References

[1] Leslie Fredrick Greengard, *The Rapid Evolution of Potencial Field In particle Systems*, Yale University, 1987,
[2] *The Best of the 20th Century: Editors Name Top 10 Algorithms* SIAM News, 2000

L. SÁNTHA, "Investigation of implementation opportunities of fast multipole methods on FPGA" in *PhD Proceedings Annual Issues of the Doctoral School, Faculty of Information Technology and Bionics, Pázmány Péter Catholic University – 2018.* G. Prószéky, P. Szolgay Eds. Budapest: Pázmány University ePress, 2018, pp. 40–40. This research has been partially supported by the European Union, co-financed by the European Social Fund (EFOP-3.6.3-VEKOP-16-2017-00002).

# Performance evaluation of the Global Statistical and Principal Projected Edge Descriptor

Attila STUBENDEK
(Supervisor: Péter SZOLGAY, Kristóf KARACS)
Pázmány Péter Catholic University, Faculty of Information Technology and Bionics
50/a Práter street, 1083 Budapest, Hungary
stubendek.attila@itk.ppke.hu

***Abstract*—The comparison of shape descriptors strongly depends on the shape image type used in training and testing. In our research we developed a blob noise generation method for classification performance measure.**

***Keywords*-shape recognition; performance; comparison**

## I. Introduction

Shape is one of the most important local feature of an image besides color and texture. Contour-based shape features describe the shape based on its contour lines in various representation [1], [2], [3], [4]. Region-based techniques describe the shape based on every point of the shape and represent mainly global features of the shape. [5], [6], [7], [8].

### *A. The Global Statistical and Projected Principal Edge Descriptor*

The Global Statistical and Principal Projected Edge Descriptor (GSPPED) [9] is a combined shape descriptor built up from three parts:

1) a header including eccentricity and area fill ratio,
2) a region-based feature set based on the shape moments representing global properties,
3) a contour-based edge description employing Extended Projected Principal Shape Edge Distribution, based on the principle used by the PPED [10]. Edges are characterized by thresholding and projecting.

## II. Performance measurement on real-world images and in noisy environment

The description and the classification method in our research have been tested in the framework of the Bionic Eyeglass. The Bionic Eyeglass [11], [12] is a portable device to help blind and visually impaired people in everyday recognition tasks that require visual input.

Images were taken from live tests of the Hungarian Forint recognition task with the participation of visually impaired people. Images contained blobs from the banknotes, including portraits, numbers and several other patterns.

Based on these datasets, we observed that variations in the extracted shape images do not occur in pixel-level additions or removals but in joining with other blobs or in removal of some parts of the shape (also see Figure 1). To model this kind of noise, we added and removed several randomly generated blobs to and from the original shape. The total area of the blobs is given as a ratio ($\omega$) to the shape area. [13]

Our results highlighted the nature of GSPPED and AL-NN: the generalization capability of the AL-NN classification method using GSPPED is somewhat limited, but it is still comparable to other methods; at the same time, this combination provides outstanding discriminative power. [13]

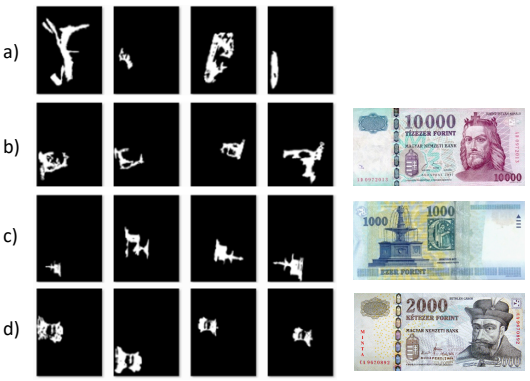


Fig. 1. Example shapes from the test set. Images were taken from Hungarian Forint Banknotes, and figures were extracted as shapes. Shapes vary a lot due to different lightning conditions.

## References

[1] S.A. Dubani, K.J. Breeding, R.B. McGhee, *Aircraft identification by moment invariants"*, IEEE Transactions on Computers, C-26:39-46, 1977.
[2] l.Gupta, M.D. Srinath, *Contour sequence moments for the classification of closed planar shapes*, Pattern Recognition, 20(3) p. 267-272, 1987.
[3] E. R. Davies, *Machine Vision: Theory, Algorithms, Practicalities*, Academic Press, New York, p. 171–191, 1997.
[4] A.C. Evans, N.A. Thacker, J.E.W. Mayhew, *Pairwise representation of shape*, Proceedings of the 11th IAPR International Conference on Pattern Recognition, vol. 1, Hague, Netherlands, p. 133-136, 1992.
[5] M. K. Hu, *Visual pattern recognition by moment invariant*, IRE Transactions on Information Theory, vol. 8, no. 2, pp. 179–187, 1962.
[6] H. S. Kim and H.-K. Lee, *Invariant image watermark using zernike moments*, IEEE Transactions on Circuits and Systems for Video Technology, 2003.
[7] A. Khotanzad and Y. H. Hong, *Invariant image recognition by Zernike moments*, IEEE Transactions on Pattern Analysis and Machine Intelligence, vol. 12, no. 5, pp. 489–497, 1990.
[8] C.-H. Teh and R. T. Chin, *On image analysis by the methods of moments*, IEEE Transactions on Pattern Analysis and Machine Intelligence, vol. 10, no. 4, pp. 496–513, 1988.
[9] A. Stubendek, K. Karacs, and T. Roska, *Shape description based on projected edges and global statistical features*, Proceedings of the International Symposium on Nonlinear Theory and Its Applications (NOLTA '14), 2014.
[10] M. Yagi, T. Shibata, *An Image Representation Algorithm Compatible with Neural-Associative-Processor-Based Hardware Recognition Systems*, IEEE Trans. Neural Networks, Vol. 14, No. 5, pp. 1144-1161, 2003.
[11] K. Karacs, A. Lázár, R. Wagner, D. Bálya, T. Roska, and M. Szuhaj, *Bionic eyeglass: an audio guide for visually impaired*, Proceedings of the IEEE Biomedical Circuits and Systems Conference Healthcare Technology, BioCAS '06, pp. 190–193, IEEE, London, UK, 2006.
[12] K. Karacs, M. Radvanyi, A. Stubendek, and B. Bezanyi, *Learning hierarchical spatial semantics for visual orientation devices*, Proceedings of the 10th IEEE Biomedical Circuits and Systems Conference, BioCAS 2014, pp. 141–144, Switzerland, 2014.
[13] A. Stubendek, K. Karacs *Shape Recognition Based on Projected Edges and Global Statistical Features*, Mathematical Problems in Engineering, vol. 2018, Article ID 4763050, https://doi.org/10.1155/2018/4763050 2018.

A. STUBENDEK, "Performance evaluation of the Global Statistical andPrincipal Projected Edge Descriptor" in *PhD Proceedings Annual Issues of the Doctoral School, Faculty of Information Technology and Bionics, Pázmány Péter Catholic University – 2018.* G. Prószéky, P. Szolgay Eds. Budapest: Pázmány University ePress, 2018, pp. 41–41. This research has been partially supported by the European Union, co-financed by the European Social Fund (EFOP-3.6.3-VEKOP-16-2017-00002).

# Structural analysis of an uncertain kinetic system model

Gergely SZLOBODNYIK
(Supervisor: Gábor SZEDERKÉNYI)
Pázmány Péter Catholic University, Faculty of Information Technology and Bionics
50/a Práter street, 1083 Budapest, Hungary
szlobodnyik.gergely@itk.ppke.hu

ABSTRACT

**In this paper, using some results from the field of uncertain kinetic systems, we examine the structural properties of a well-known deterministic kinetic model of the heterotrimeric G-protein cycle. It is shown that the examined G-protein network is not structurally uniqe from which its structural non-identifiability also follows.**

## I. G-PROTEIN NETWORK

Using the algorithms of [1] computing structurally different dynamically equivalent realizations of uncertain kinetic systems, we examine the structural properties a heterotrimeric G-protein network [2].

The model involves a so-called heterotrimeric G-protein containing three different subunits. In response to the extracellular ligand binding, the protein dissociates to G-$\alpha$ and G-$\beta\gamma$ subunits, where the active and inactive forms of the G-$\alpha$ subunit can also be distinguished.

The reaction network model involves the following species: $R$ and $L$ represent the receptor and the corresponding ligand, respectively, $RL$ refers to the ligand-bound receptor, $G$ is the G-protein located on the intracellular membrane surface, $G_a$ and $G_d$ denote the active and the inactive forms of the G-$\alpha$ subunit and $G_{bg}$ is the G-$\beta\gamma$ subunit.

The model can be characterized as a chemical reaction network $(Y, A_k)$, where the structures of the complexes and the reactions are defined by the complex composition matrix $Y \in \mathbb{R}^{7\times 10}$ and the Kirchhoff matrix $A_k \in \mathbb{R}^{10\times 10}$ as follows:

$$Y = \begin{bmatrix} 1&0&1&0&0&0&0&0&0&0\\ 0&0&1&0&0&0&0&0&0&0\\ 0&1&0&0&0&0&1&0&0&0\\ 0&0&0&1&0&0&1&0&0&0\\ 0&0&0&0&1&0&0&1&0&0\\ 0&0&0&0&0&0&0&1&1&0\\ 0&0&0&0&0&1&0&0&1&0 \end{bmatrix}$$

$$A_k = \begin{bmatrix} -0.4 & 0 & 0 & 0 & 0 & 0 & 0 & 0 & 0 & 4000\\ 0 & -14 & 0.322 & 0 & 0 & 0 & 0 & 0 & 0 & 0\\ 0 & 10 & -0.322 & 0 & 0 & 0 & 0 & 0 & 0 & 0\\ 0 & 0 & 0 & 0 & 0 & 0 & 0 & 0 & 1000 & 0\\ 0 & 0 & 0 & 0 & -11000 & 0 & 0 & 0 & 0 & 0\\ 0 & 0 & 0 & 0 & 11000 & 0 & 0 & 0 & 0 & 0\\ 0 & 0 & 0 & 0 & 0 & 0 & -0.01 & 0 & 0 & 0\\ 0 & 0 & 0 & 0 & 0 & 0 & 0.01 & 0 & 0 & 0\\ 0 & 0 & 0 & 0 & 0 & 0 & 0 & 0 & -1000 & 0\\ 0.4 & 4 & 0 & 0 & 0 & 0 & 0 & 0 & 0 & -4000 \end{bmatrix}$$

The kinetic system that is realized by the model is $\dot{x} = M \cdot \psi^Y = Y \cdot A_k \cdot \psi^Y$, i.e. $M = Y \cdot A_k \in \mathbb{R}^{7\times 10}$.

The computation of all possible reaction graph structures and the solution of the linear equations shows that the heterotrimeric G-protein cycle with the given parametrization is not just structurally but also parametrically unique. Thus the prescribed dynamics without uncertainty cannot be realized by any other set of reactions or different reaction rate coefficients using the given set of complexes.

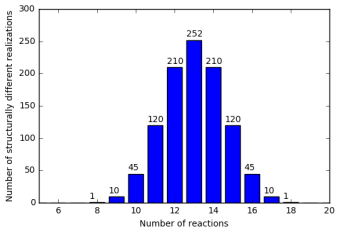


Figure 1: The number of structurally different realizations of the uncertain kinetic system of 1% relative parametric uncertainty with different number of reactions.

*Uncertainty defined with independent relative distance intervals*

We defined an uncertain kinetic system by introducing 1 % relative uncertainty around the nominal parameter values described in the previous section. By computing all possible reaction graph structures and the set of core reactions of this uncertain kinetic system, we obtained that all the reactions in the original G-protein cycle are core reactions. Moreover, in the dense realization there are 10 further reactions, and these can be present in the realization independently of each other. Consequently, the total number of different graph structures is $2^{10} = 1024$. Figure 1 shows the number of possible reaction graph structures with different number of reactions.

*Acknowledgement*

This research has been partially supported by the European Union, co-financed by the European Social Fund (EFOP-3.6.3-VEKOP-16-2017-00002). The research was also supported by Pázmány Péter Catholic University through the project PPKE KAP-1.1-16-ITK.

## REFERENCES

[1] B. Ács, G. Szlobodnyik, G. Szederkényi, *A computational approach to the structural analysis of uncertain kinetic systems*. Computer Physics Communication, Vol. 228., July 2018, Pages 83-95.

[2] T. M. Yi, H. Kitano, and M. I. Simon. A quantitative characterization of the yeast heterotrimeric G protein cycle. *Proc. Natl. Acad. Sci. USA*, 100(19):10764–10769, 2003.

G. SZLOBODNYIK, "Structural analysis of an uncertain kinetic system model" in *PhD Proceedings Annual Issues of the Doctoral School, Faculty of Information Technology and Bionics, Pázmány Péter Catholic University – 2018.* G. Prószéky, P. Szolgay Eds. Budapest: Pázmány University ePress, 2018, pp. 42–42. This research has been partially supported by the European Union, co-financed by the European Social Fund (EFOP-3.6.3-VEKOP-16-2017-00002).

.

# PROGRAM 3
# FEASIBILITY OF ELECTRONIC AND OPTICAL DEVICES, MOLECULAR AND NANOTECHNOLOGIES, NANO-ARCHITECTURES, NANOBIONIC DIAGNOSTIC AND THERAPEUTIC TOOLS

Head: Árpád CSURGAY

# Overview of tissue thermometry

Krisztián FÜZESI
(Supervisor: Dr. Miklós GYÖNGY)
Pázmány Péter Catholic University, Faculty of Information Technology and Bionics
50/a Práter street, 1083 Budapest, Hungary
fuzesi.krisztian@itk.ppke.hu

***Abstract*—There are several procedures in medicine where the intervention involves heating or cooling of tissue. Tissue thermometry methods are essential, as they make it available to track actual condition of a medical intervention, as the result of these treatments mainly related to the temperature distribution. The main aspects choosing between imaging modalities for thermometry are including patient safety, costs, availability, ease of use and compatibility with other devices. Also, sensitivity, tissue dependence and spatio-temporal resulution are imporant parameters. The three main techniques for deep tissue thermometry, which are computer tomography (CT), magnetic resonance imaging (MR) and ultrasound (US).**

## I. Introduction

There are a plethora of ablation methods, including radiofrequency-, microwave-, laser-, cryo-, and ferromagnetic ablation, irreversible electroporation and high intensity focussed ultrasound (HIFU) as well [1–3]. Using thermal information of the tissue the medical staff is able to judge which part of tissue remains healthy and which part suffer irreversible changes. The therapy could lead to instant cell death (necrosis), or initiating programmed cell death (apoptosis) – in both cases the goal is the destruction of undesirable tissue, which is in most of the cases a kind of tumor. Nowadays, minimally invasive – or if available – non-invasive techniques becoming more and more popular, thus for temperature measurement methods non-invasive techniques are favorable as well [4]. The three main techniques for deep tissue thermometry are computer tomography (CT), magnetic resonance imaging (MR) and ultrasound (US).

The advantages of CT are the compatibility with other devices, relatively low cost and general availability of CT machines. The disadvantage is, that the patient is exposed to ionizing radiation. The X-ray dose can be reduced with image reconstruction algorithms.

Magnetic resonance based techniques are precise tools of temperature monitoring, however the high cost, limited availability and difficulties in compatibility are obstructing their use.

In contrast to MR, US-based techniques have a relatively low cost. Spatial resolution of US is similar to CT and MR – both performing around some millimeter, however, US thermometry techniques are suffering from high tissue-dependence.

## II. Theoretical background of CT based thermometry

In computer tomography slices of the body are insonified with X-ray radiation. Data displayed based on measuring the linear attenuation coefficient of insonified materials. Applying a linear transformation, Hounsfield Units (HU) are extracted for each pixel. For increasing temperature the density, and parallel the CT number will decrease.

## III. Theoretical background of MR thermometry

In MR inaging, the resonance frequency of protons (PRF) is temperature dependent, while the temperature measurements are tissue independent, except fatty tissues. The PRF phase shift will be negative if the temperature is rising.

## IV. Ultrasound based approaches of thermometry

In ultrasound imaging, thermometry is usually carried out using the knowledge of the sound speed at ambient temperature inside tissues (generally assumed to be 1540 m/s in soft tissues. In US, similarly to MR imaging, fatty tissues introduce difficulties in temperature monitoring. In normal soft tissues sound speed is increasing parallel with temperature up to 50-60 °C, and the attenuation coefficient becoming lower simultaneously [5]. This trend turns to the reverse at higher temperatures, moreover, during the cooling back of the previously heated tissue, these values usually does not follow the course which was obtained during heating, due to the irreversible changes in treated tissues. In active US, where the region of interest (ROI) is irradiated with an US beam and the data obtained using backscattered signals. In passive US natural acoustic radiation of the body is recorded. Using mathematical models, the temperature map could be calculated. In optoacoustics, the thermoacoustic efficiency changes in a linear fashion, moreover temperature-dependent optoacoustic response was found to be independent of oxygen saturation of blood. [4]

## References

[1] M. Gyöngy, "Passive cavitation mapping for monitoring ultrasound therapy," 2010.

[2] Y. Zhou, "Noninvasive thermometry in high-intensity focused ultrasound ablation," *Ultrasound Quarterly*, vol. 33, pp. 253–260, dec 2017.

[3] E. Schena, F. Giurazza, C. Massaroni, Y. Fong, J. J. Park, and P. Saccomandi, "Thermometry based on computed tomography images during microwave ablation: Trials on ex vivo porcine liver," in *2017 IEEE International Instrumentation and Measurement Technology Conference (I2MTC)*, IEEE, may 2017.

[4] E. V. Petrova, H. P. Brecht, M. Motamedi, A. A. Oraevsky, and S. A. Ermilov, "In vivo optoacoustic temperature imaging for image-guided cryotherapy of prostate cancer," *Physics in Medicine & Biology*, vol. 63, p. 064002, mar 2018.

[5] J. Bamber and C. Hill, "Ultrasonic attenuation and propagation speed in mammalian tissues as a function of temperature," *Ultrasound in Medicine & Biology*, vol. 5, pp. 149–157, jan 1979.

K. FÜZESI, "Overview of tissue thermometry" in *PhD Proceedings Annual Issues of the Doctoral School, Faculty of Information Technology and Bionics, Pázmány Péter Catholic University – 2018.* G. Prószéky, P. Szolgay Eds. Budapest: Pázmány University ePress, 2018, pp. 44–44. This research has been partially supported by the European Union, co-financed by the European Social Fund (EFOP-3.6.3-VEKOP-16-2017-00002).

# Iterative Optimization Techniques for Limited Angle Computed Tomography

Janka HATVANI
(Supervisor: Miklós GYÖNGY)
Pázmány Péter Catholic University, Faculty of Information Technology and Bionics
50/a Práter street, 1083 Budapest, Hungary
hatvani.janka@itk.ppke.hu

***Abstract*—In order to decrease the amount of ionizing radiation in Computed Tomography examinations a couple of different techniques have been developed in the last decades, including limited angle imaging.This technique introduces ill-posedness to the reconstruction problem. A main group of the algorithms aiming to solve this problem incorporates prior knowledge as a regularization term to an iterative reconstruction algorithm. In this work two total-variation regularized algorithms, one using alternating direction method of multipliers, the other the simultaneous algebraic reconstruction technique were studied to support future work in this field.**

***Keywords*-limited angle CT, ADMM-TV, SART-TV**

## I. Introduction

To ease the danger of possible somatic and genetic injuries caused by Computed Tomography (CT) a couple of techniques have been applied. Either the electric charge can be decreased – leading to noise amplification and decrease in the contrast, or the number of projections can be reduced. There are two groups of algorithms used in the literature for solving the ill-posed limited angle reconstruction [1]. The first one improves existing full-view techniques, the second group uses some prior information like the surface of the subject, similar known images or sparseness in a given domain.

## II. Theory

The total variation (TV) is a commonly used prior assumption in medical imaging, meaning that the image is built up from piecewise constant regions A different prior usually used in CT reconstruction is the non-negativity of the image. Using these informations we can formulate our problem as

$$\min_f ||f||_{TV} \text{ such that } p_L = A_L \cdot f, f_(i) \geq 0 \qquad (1)$$

where $A_L$ is the system matrix, $p_L$ is the measured projections set, $f$ is the image to be reconstructed.

### A. ADMM-TV algorithm

One group of the techniques aiming to solve a constrained problem minimizes the corresponding augmented Lagrangian (AL) function with ADMM. With this technique we can transform our constrained problems.

$$\begin{aligned}\mathcal{L}(f,u,\lambda) =& \frac{1}{2}||p_L - W_L f||_2^2 + \tau||u||_{TV} + \\ & \lambda_u([\nabla_x \ \nabla_y]^T f - u) + \frac{\mu}{2}\left\|[\nabla_x \ \nabla_y]^T f - u\right\|_2^2\end{aligned}$$

such that

$$u = [u_x \ u_y]^T = [\nabla_x f \ \nabla_y f]^T \qquad (2)$$

This equation now can be solved alternately for $u$ andd $f$, as these subproblems have known solutions. [2] Here the non-negativity was included as a hard constraint.

### B. SART-TV algorithm

This technique uses the simultaneous algebraic reconstruction technique (SART). It gives a computationally efficient alternative as it can be parallelized. [3]. After a preset number of iterations of the SART algorithm the non-negativity is enforced, then the TV-regularization is realized with gradient descent. These steps are repeated until convergence.

## III. Discussion

To above algorithms were implemented in Matlab, and the ASTRA toolbox. The SART-TV algorithm proved to be computationally more efficient with the GPU-based SART algorithm, however it tended to oversmooth details which were visible with the ADMM-TV.

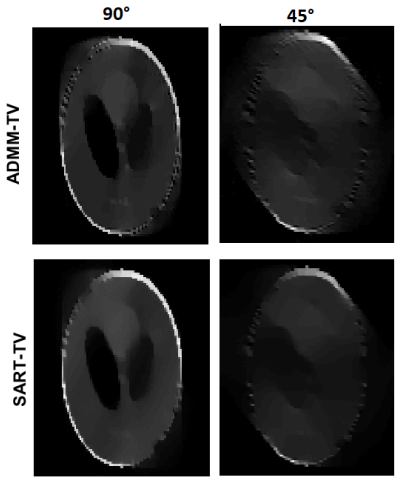


Fig. 1. Results on the Shepp-Logan phantom. The phantom was reconstructed from 90° and 45° angle range, 1-1 projection/degree.

## References

[1] W. Zhang, H. Zhang, L. Wang, A. Cai, L. Li, and B. Yan, "Limited angle ct reconstruction by simultaneous spatial and radon domain regularization based on tv and data-driven tight frame," *Nuclear Instruments and Methods in Physics Research Section A: Accelerators, Spectrometers, Detectors and Associated Equipment*, vol. 880, pp. 107–117, 2018.

[2] Z. Han-Ming, W. Lin-Yuan, Y. Bin, L. Lei, X. Xiao-Qi, and L. Li-Zhong, "Image reconstruction based on total-variation minimization and alternating direction method in linear scan computed tomography," *Chinese Physics B*, vol. 22, no. 7, p. 078701, 2013.

[3] J. Hatvani, "Applicability of computed tomography methods for tomosynthesis problems," in *PhD Proceedings Annual Issues of the Doctoral School, Faculty of Information Technology and Bionics, Pázmány Péter Catholic University – 2017*, pp. 48–48, 2017.

J. HATVANI, "Iterative Optimization Techniques for Limited Angle Computed Tomography" in *PhD Proceedings Annual Issues of the Doctoral School, Faculty of Information Technology and Bionics, Pázmány Péter Catholic University – 2018.* G. Prószéky, P. Szolgay Eds. Budapest: Pázmány University ePress, 2018, pp. 45–45. This research has been partially supported by the European Union, co-financed by the European Social Fund (EFOP-3.6.3-VEKOP-16-2017-00002).

# Resolution enhancement of ultrasound images using axial deconvolution

Ákos MAKRA
(Supervisor: Miklós GYÖNGY)
Pázmány Péter Catholic University, Faculty of Information Technology and Bionics
50/a Práter street, 1083 Budapest, Hungary
makra.akos@itk.ppke.hu

**Statement of originality: This report describes the work of the doctoral student during the educational years of 2016 – 2018. Parts of the work are adapted/taken verbatim from [1].**

## I. Introduction

Enhancement of image resolution in ultrasound images is key to help clinicians find early indicators of pathological lesions and has therefore long been of interest [2]–[4]. Image resolution enhancement relies on deconvolving the point spread function (PSF) of the imaging system out of the raw ultrasound image prior to envelope detection and other post-processing steps. Unfortunately, in most cases the PSF is spatially variant, complicating its estimation and subsequent use in deconvolution. The current work is driven by the realization that the PSF at a given coordinate can be decomposed into spatially invariant and variant components [5]–[7]. The aim of this work is to simultaneously increase both the axial and lateral resolution of B-mode ultrasound images by using axial deconvolution only.

## II. Methods

To show that the axial deconvolution can change the lateral resolution, 4 different B-mode images were considered, 2 simulations and 2 measurements. Two different methods were used for the deconvolution part. A classical Wiener filter approach and a custom Fourier domain method (called RAMP) was applied. Both of the methods were used along every A-line separately.

## III. Results

TABLE I
FWHM values in microns. Values in bold indicate best resolution. Table adapted from [1].

| | orig x | deconv x | RAMP x | orig z | deconv z | RAMP z |
|---|---|---|---|---|---|---|
| sparse | 290.0 | 399.8 | **222.1** | 27.8 | **18.0** | 18.7 |
| dense | 280.4 | 412.1 | **216.4** | 27.2 | **18.0** | 18.6 |
| phantom | 736.0 | **152.0** | 674.0 | 18.7 | **9.0** | 14.0 |
| skin | 723.4 | 576.0 | **521.0** | 111.7 | **39.7** | 127.1 |

Table I summarizes the resolution results obtained. Generally, it can be stated that both deconvolution approaches are able to improve lateral as well as axial resolution, though the RAMP filter tends to provide a better lateral resolution at the cost of a smaller improvement in axial resolution.

## IV. Conclusion

Using simulated and experimental data from two single element transducers (of 20, 35 MHz nominal frequencies), it was shown that axial deconvolution can simultaneously improve resolution in both directions. The results demonstrate a framework for improving axial and lateral resolution for ultrasound images that is unaffected by depth-dependent effects and that can balance the need for axial and lateral resolution improvement based on their relative values. The results also highlight the need to set deconvolution parameters correctly. For cases when the deconvolution only improves lateral resolution at the expense of axial resolution, this may still result in a reasonable trade-off given the typically worse lateral resolution. Since both deconvolution methods introduce noise, care needs to be taken to keep it under control. Future work aims to optimize deconvolution parameters (NSR and RAMP characteristics) according to pre-defined axial and lateral resolution improvement criteria.

## Acknowledgements

The author is thankful to *Gergely Csány* and *Dr. Klára Szalai* for their contribution to this work. The author would like to acknowledge the support of Pázmány Péter Catholic University KAP R&D and equipment grants (2014 – 2018), as well as Hungarian state funding PPKE ITK EFOP-3.6.2-16-2017-00013, 3.6.3-VEKOP-16-2017-00002. The author was supported by the Nation's Young Talent Scholarship of the Hungarian Ministry of Human Resources (NTP-NFTÖ-17).

## References

[1] Á. Makra, G. Csány, K. Szalai, and M. Gyöngy, "Simultaneous enhancement of B-mode axial and lateral resolution using axial deconvolution," *Proc. Mtgs. Acoust.*, vol. 32, no. 1, February 2018.
[2] Y. M. Benane, R. Lavarello, D. Bujoreanu, C. Cachard, F. Varray, J.-M. Escoffre, A. Novell, and O. Basset, "Ultrafast ultrasound imaging using a resolution and bandwidth enhancement technique," *International Ultrasonics Symposium (IUS,Washington,USA)*, 6–9 Sept. 2017.
[3] Y. M. Benane, R. Lavarello, D. Bujoreanu, C. Cachard, F. Varray, A. S. Savoia, E. Franceschini, and O. Basset, "Ultrasound bandwidth enhancement through pulse compression using a cmut probe," *International Ultrasonics Symposium (IUS,Washington,USA)*, 6–9 Sept. 2017.
[4] S. Chen and K. J. Parker, "Enhanced axial and lateral resolution using stabilized pulses," *Journal of Medical Imaging*, vol. 4 (2), pp. 027001–1 – 027001–11, Apr – Jun 2017.
[5] J. M. Mari, T. Blu, O. B. Matar, M. Unser, and C. Cachard, "A bulk modulus dependent linear model for acoustical imaging," *Journal of the Acoustical Society of America*, vol. 125, pp. 2413–2419, April 2009.
[6] J. A. Jensen, "A model for the propagation and scattering of ultrasound in tissue," *Journal of the Acoustical Society of America*, vol. 89, no. 1, pp. 182–190, 1990.
[7] M. Gyöngy and Á. Makra, "Experimental validation of a convolution-based ultrasound image formation model using a planar arrangement of micrometer-scale scatterers," *IEEE Transactions on Ultrasonics, Ferroelectrics, and Frequency Control*, vol. 62, pp. 1211–1219, June 2015.

Á. MAKRA, "Resolution enhancement of ultrasound images using axial deconvolution" in *PhD Proceedings Annual Issues of the Doctoral School, Faculty of Information Technology and Bionics, Pázmány Péter Catholic University – 2018.* G. Prószéky, P. Szolgay Eds. Budapest: Pázmány University ePress, 2018, pp. 46–46. This research has been partially supported by the European Union, co-financed by the European Social Fund (EFOP-3.6.3-VEKOP-16-2017-00002).

# Review of computer-aided melanoma diagnosis methods

Péter MAROSÁN
(Supervisor: Miklós GYÖNGY PhD)
Pázmány Péter Catholic University, Faculty of Information Technology and Bionics
50/a Práter street, 1083 Budapest, Hungary
marosan.peter@itk.ppke.hu

***Abstract*—Skin lesions have a huge variability regarding to how dangerous and malicious are they. While nevi are completely harmless, some other types of lesions like melanomas can cause serious problems. The lack of early detection and treatment of this kind of features can easily lead to medical complications, including death. Tendencies of the past years show that the number of subjects with malicious skin cancer is increasing. This article describes the main steps of the pipeline of computer-aided melanoma diagnosis (CAD) such as pre-processing, segmentation, feature extraction and classification. After a general description of the CAD process and its methods, the main steps are also presented on three different but significant imaging modalities: dermoscopy, ultrasound-based imaging and smartphone-based photography.**

***Keywords*-CAD; diagnosis; melanoma; skin cancer; dermoscopy; ultrasound; smartphone**

## I. Introduction

Malignant melanoma is one of the most dangerous types of skin cancer. Early detection and treatment of malicious skin cancer is indispensable and vital because metastasis can leads to death. Worldwide tendencies show that the number of patients suffering from malicious melanomas increasing in every single year. To help doctors and dermatology experts with the growing number of subjects one remarkably effective, sufficiently robust and accurate computer-aided diagnosis tool is required which is able to analyse and interpret the type of the occurring skin lesions.

## II. The CAD pipeline

Skin-lesion-related CAD has a characteristic pipeline which describe the whole process (Figure 1): Pre-processing of the acquired image data has a great impact on the further processes. Noise filtering methods are indispensable steps of the framework, numerous lesion segmentation methods requires smooth and homogeneous images. The consecutive task in the pipeline is to differentiate the region of the interest (ROI) from the background, making a robust and precise segmentation of the skin lesion. Having the exact borders of the ROI is a prerequisite of making a medical diagnosis about the properties and type of the examined lesion. The step of feature extraction stands for creating an informative description about the lesions themselves which can help to differentiate the classes from each other. Classification of various kind of lesions can be done with the help of the extracted features.


Fig. 1. Melanoma CAD pipeline

## III. Diagnostic modalities

The above-described CAD pipeline and its main steps can be applied for different imaging modalities such as dermoscopy, ultrasound imaging and smartphone photography.

### A. Dermoscopy

Most of the demoscopy-based segmentation methods are thresholding-, edge- or region-based techniques. Saliency map based segmentation algorithms are also effective ways to differentiate the lesion itself from the background.

The most significant approaches of classification are based on the ABCDE features. Other descriptors like shape and symmetry features, global and local colour, amplitude, orientation histograms or Gabor-filters are also good choices for robust classification. Supervised and deep learning algorithms gives promising results too.

### B. Ultrasound

Ultrasound-based automatic segmentation algorithms use prior information of skin tissue, significant reduction of speckle noise and thresholding or clustering methods. Semi-automatic algorithms usually requires some seed points from the user and this can help to find its borders with the help of more accurate and precise algorithms like level-set methods [1] or active contour model based procedures.

Differential diagnosis uses acoustical, textural and shape features, linear support vector machine classifier to differentiate skin lesions. [2] At the side of feature extraction, deep neural networks were also tried out and gives some promising results.

### C. Smartphone based melanoma diagnosis

Smartphone-based melanoma diagnosis is challenging because the images are acquired under loosely-controlled environmental conditions and smartphones result memory and computation constrains. The first problem can be handled by deep neural network methods. Esteva et al. created a powerful and highly effective tool by using 1.41 million pre-training and training images make classification robust to photographic variability. [3]

## References

[1] B. Sciolla, P. Delachartre, L. Cowell, T. Dambry, and B. Guibert, "Improved boundary segmentation of skin lesions in high-frequency 3d ultrasound," *Computers in biology and medicine*, vol. 87, pp. 302–310, 2017.

[2] K. Andrėkutė, G. Linkevičiūtė, R. Raišutis, S. Valiukevičienė, and J. Makštienė, "Automatic differential diagnosis of melanocytic skin tumors using ultrasound data," *Ultrasound in Medicine and Biology*, vol. 42, no. 12, pp. 2834–2843, 2016.

[3] A. Esteva, B. Kuprel, R. A. Novoa, J. Ko, S. M. Swetter, H. M. Blau, and S. Thrun, "Dermatologist-level classification of skin cancer with deep neural networks," *Nature*, vol. 542, no. 7639, p. 115, 2017.

P. MAROSÁN, "Review of computer-aided melanoma diagnosis methods" in *PhD Proceedings Annual Issues of the Doctoral School, Faculty of Information Technology and Bionics, Pázmány Péter Catholic University – 2018.* G. Prószéky, P. Szolgay Eds. Budapest: Pázmány University ePress, 2018, pp. 47–47.
This research has been partially supported by the European Union, co-financed by the European Social Fund (EFOP-3.6.3-VEKOP-16-2017-00002).

# In vitro validation of sharp wave related dendritic events in hippocampal GABAerg interneurons

Zsolt MEZRICZKY
(Supervisor: Balázs RÓZSA)
Pázmány Péter Catholic University, Faculty of Information Technology and Bionics
50/a Práter street, 1083 Budapest, Hungary
mezriczky.zsolt@itk.ppke.hu

Hippocampus and its specific oscilatory pattern is responsible for the formation and recall of the long term and spatial memory. Cell assemblies synchronize their activity and stabilize themselves as a functional network during SWR [1]. It also has an important role in navigation: in rest state SWRs recall the place field information and stabilize the information as a map to the future [2]. SWRs related input activity in pyramidal cells and interneurons appears not only on the soma, but also in the dendrites [3] and shows nonlinear Ca2+ responses [4]. This dendritic integration is summing and create "hot-spots". The synchronous activity of this synaptic inputs create regenerative dendritic potentials, "spikes".

The dendritic regenerative signals coupled with SWR activity were investigated in vitro [5]. Dendrites of parvalbumin (PV) containing interneurons in hippocampus can generate regenerative Ca2+ dSpikes related to the SWR activity, which independent to the soma. Spikes can be distinguish to the somatic dependent according spatial spreading of the Ca2+ responses. But this study focused on the apical dendrites.

In vivo two-photon three-dimensional acousto-optical measurements allow fast volume scanning. With this technique we can image different layers or a complete neuron with the whole dendritic arborization. Our group is already using this type of microscope to investigate the SWR related dendritic events in hippocampal PV neurons. We found evidence about SWR related regenerative dSpikes in vivo, but the identification of this events are complicated. DSpikes related Ca2+ curves propagate towards to soma with decreasing amplitude, contrary to the BAPs. These inputs evoke excitatory postsynaptic potentials (EPSP) in the soma. In some cases we also fund evidence of SWR doublets in different time delays and it may cause potentiated Ca2+ response in an appropriate temporal distance.

I determined the spatial spreading of elicited BAPs on the basal dendrites. The amplitude of decreasing BAPs showed decreased Ca2+ responses on the proximal part of the dendrites. The distance dependent spreading shows the same decreasing as in vivo measurements and independent to the number of the evokeded BAP. This Functional distance can help us to distinguish the BAP to regenerative events. In contrast to the BAP the SWR associated regenerative events shows increasing Ca2+ signals in the direction of lateral zone [5]. Thus outside of the BAP spread, regenerative events are predicted.

Rarely appearing SWR doublets shows potentiation in Ca2+ signals in vivo [6]. The time dependence of the potentiation can be examined in vitro. The validation of this events need temporarily shifted optogenetic stimuli. Different temporal distances between the stimuli shows different Ca2+ signals. The increasing time delay between the stimuli induce decreased

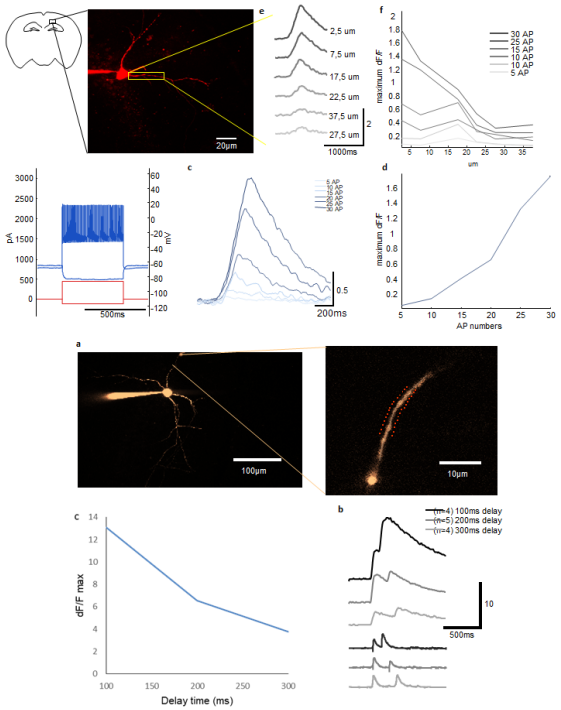


Fig. 1. In vitro validation of different dendritic events

Ca2+ response in the distal part of basal dendrites. The CA1 inputs form medial enthorinal cortex (MEC) had important role in the originating of different SWR bursts (doublets, triplets...) and so in long range replay during navigation [7].

## REFERENCES

[1] Buzsák G. Neural syntax: Cell assembles, synassambles and readers. 2010. Neuron, 68: 362-385
[2] Colgin L. Rhytms of the hippocampal network. 2016. Nature Rewievs Neuroscience. volume 17, pages 239–249
[3] Buzsaki G, Silva F L. High frequency oscillations in the intact brain. Prog. Neurobiol., 98 (2012), pp. 241-249
[4] Katona G, Kaszás A, Turi G F, Hájos N, Tamás G, Vizi E S, Rózsa B. Roller Coaster Scanning reveals spontaneous triggering of dendritic spikes in CA1 interneurons. Proc. Natl. Acad. Sci. USA, 108 (2011), pp. 2148-2153
[5] Chiovini B, Turi GF, Katona G, Kaszás A, Pálfi D, Maák P, Szalay G, Szabó MF, Szabó G, Szadai Z, Káli S, Rózsa B. Dendritic spikes induce ripples in parvalbumin interneurons during hippocampal sharp waves. 2014. Neuron. 82(4):908-24
[6] Davidson, T.J., Kloosterman, F., and Wilson, M.A. (2009). Hippocampal replay of extended experience. Neuron 63, 497–507.
[7] Yamamoto J1, Tonegawa S2. Direct Medial Entorhinal Cortex Input to Hippocampal CA1 Is Crucial for Extended Quiet Awake Replay. 2017. Neuron. 96(1):217-227

Zs. MEZRICZKY, "In vitro validation of sharp wave related dendritic events in hippocampal GABAerg interneurons" in *PhD Proceedings Annual Issues of the Doctoral School, Faculty of Information Technology and Bionics, Pázmány Péter Catholic University – 2018.* G. Prószéky, P. Szolgay Eds. Budapest: Pázmány University ePress, 2018, pp. 48–48. This research has been partially supported by the European Union, co-financed by the European Social Fund (EFOP-3.6.3-VEKOP-16-2017-00002).

.

# PROGRAM 4
# HUMAN LANGUAGE TECHNOLOGIES, ARTIFICIAL UNDERSTANDING, TELEPRESENCE, COMMUNICATION

Head: Gábor PRÓSZÉKY

# The usage of adaptive neuron-based controllers in automated guided vehicles

Máté LŐRINCZ
(Supervisor: András OLÁH)
Pázmány Péter Catholic University, Faculty of Information Technology and Bionics
50/a Práter street, 1083 Budapest, Hungary
lorincz.mate@itk.ppke.hu

***Abstract*—In this paper two different neuron-based speed controllers are proposed and compared for an AGV-like application. One of them is a classical single-neuron PID (SN-PID) implementation and the other is a sensor-based neuron (SBN). The two neuron-based solutions have a novel weight-training algorithm which runs continuously and is based on a modified Delta learning rule. The paper presents the general behaviour, and the stability properties of the proposed control methods under different actuator characteristics and conditions. A simple, distributed-controlled RC car has been built using the MSP430 and CC1101 based Amber 8423 module. The performance analysis shows that the modified Delta learning rule has excellent stability and SBN method exceeds the SN-PID in most cases.**

## I. Introduction

Automated Guided Vehicles (hereinafter referred to as AGV) have huge and growing importance in intralogistics. In a typical AGV system, the vehicles have bound path, the allowed error is below a few centimeters. If a vehicle is too far apart from the designated route, it must stop immediately and it needs human intervention to continue its tasks. Because AGV-s have huge operational area and they operate with minimal human supervision, human intervention is expensive and slow.

To provide smooth and reliable tracking method, AGV-s need stable speed controllers. The most common speed-tracking algorithms (as almost every controllers in industry) are PID-based, but Fuzzy-based controllers are also used.

This paper demonstrates two speed-tracking methods implemented by single neurons. The SN-PID (single neuron PID) is an adaptive low-computing PID controller which uses only the momentary error, the derivative of the error and the integral of the error. The other, novel control method namely the SBN (sensor based neuron) is also based on a single neuron but in contrast to the SN-PID method, SBN method utilises different measured signals beside the error signal input. (In most industrial or civilian applications there are lots of different sensors monitoring the equipment which are unused by PID-based controllers.) In this paper we will show that using different sensors instead of the error as only input can stabilise the system faster.

## II. Implementing the exemplary system

The exemplary system is implemented by a rebuilt RC car and an Amber 8423 module. The steer angle and speed reference can be controlled via a Qt-based application. The remote control application can also monitor and plot the weights of the adaptive controlling neuron implemented inside the vehicle. The vehicle has no built-in speedometer, the speed is measured by a very noisy, acceleration-based sensor which raw measures have to be evaluated by the remote control application. (The sensor measures the centrifugal acceleration.) The application uploads the calculated, noisy speed, the reference speed and the desired steering angle to the car twice in every second. From these data the car calculates the fill factor of the drive engine, which is controlled by a 300Hz square signal.

## III. Tracking the speed with two different single neuron controllers

This paper demonstrates and compares two different single neuron based controllers, namely SN-PID and SBN. Both of them have the same, modified Delta learning rule, but they use different kind of inputs..

## IV. Performance analysis

The speed tracking capability of the RC car was tested with SN-PID and SBN. Both algorithms had to control the speed during multiple circles based on the noisy, delayed, acceleration-based sensor. Because the used sensor is not reliable on alternating curved road sections, the testlayout had a constant radius. In the first part of the test, the car had to maintain $0.8m/s^2$ centrifugal acceleration and in the second part, it had to maintain $1.2m/s^2$ centrifugal acceleration. (Constant centrifugal force during a circular path means constant speed.)

According to the measures, the long-term stability is similar between SN-PID and SBN, but SBN has shorter transient.

M. LŐRINCZ, "The usage of adaptive neuron-based controllers in automated guided vehicles" in *PhD Proceedings Annual Issues of the Doctoral School, Faculty of Information Technology and Bionics, Pázmány Péter Catholic University – 2018.* G. Prószéky, P. Szolgay Eds. Budapest: Pázmány University ePress, 2018, pp. 50–50. This research has been partially supported by the European Union, co-financed by the European Social Fund (EFOP-3.6.3-VEKOP-16-2017-00002).

# Processing sensor data utilizing machine and deep learning techniques

György SZÖVÉRDFFY
(Supervisor: András OLÁH)
Pázmány Péter Catholic University, Faculty of Information Technology and Bionics
50/a Práter street, 1083 Budapest, Hungary
szoverdffy.gyorgy@itk.ppke.hu

## I. Deep learning

Deep learning is considered to be a subcategory within machine learning. Deep learning can be supervised, semi-supervised and unsupervised. The basics of the concept are to mimic the learning procedure of ourselves made possible by the connection of neurons in our nervous system and our brains. The concept has been proposed long ago when computational capacity was one of the limitations it encountered. Since then a wide variety of neural network structures have been utilized with great success. Some of the well-known types are:

- FFNN (Feed Forward Neural Network)
- RNN (Recurrent Neural Network)
- CNN (Convolutional Neural Network)

An FFNN's consecutive layers are only connected to each other.

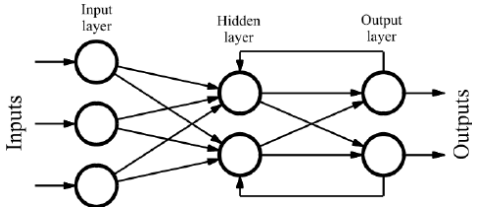


Fig. 1. Sample of a recurrent neural network.

Figure 1 shows that instead of strictly forward connections it is allowed to have connections pointing to a previous layer. Several papers have investigated and shown that RNNs are applicable in the analysis of time-dependent data, which is in the case of this article sensor data.

Convolutional neural networks have proven to be exceptionally useful in processing visual imagery or any kind of data which can be described with matrices.

## II. Frameworks

In the recent years, various frameworks have been developed to support the construction of neural networks. As it was mentioned before machine and deep learning methods require huge amounts of hardware capacity. This fact encouraged the developers of these frameworks to delegate the computations to GPUs because of their architectural design which consists of significantly more cores than regular CPUs. Some of the most notable frameworks: ***TensorFlow, NVIDIA Caffe, Caffe 2, PyTorch, Theano, Cognitive Toolkit***. Most of them are developed in Python and support multi-GPU execution. For further research open source frameworks are mandatory for extensive customization if needed. TensorFlow and NVIDIA Caffe stands out from the supply, the first is maintained and developed by Google which guarantees fine quality, on the other hand, NVIDIA Caffe hence the name is developed by NVIDIA which is one of the leading manufacturers of GPU hardware.

## III. Applications

As the title of the paper suggests these computer learning techniques would be utilized in processing measurement data from several types of sensors. It is important to note that data involved in this case is spatio-temporal which means both the time and the place of the measurement is of great value. One possible field is application is biometric identification. For example identifying the owner of a mobile phone based on the gestures during picking up the phone. The intensity of these gestures can be measured thanks to the numerous sensors hidden inside the hardware such as gyroscope. Storing every measurement data allows neural networks to identify these gestures, furthermore to determine whether the owner was the source or not. The other important field is so called smart grid systems. The problem here relies in the load of the electrical grid. In general the supplied energy is in balance with the consumed. However, occasionally there are documented events when consumption becomes suddenly a lot higher than the supplied energy or even the opposite.

## IV. Further discussion

Further reading is planned while experimenting with neural networks in TensorFlow most likely. Experiments are needed in the desire of achieving optimized neural networks. There are well known difficulties in the construction of a neural network like there is no exact recipe for making one for a certain task. Other difficulty is the inability to detect faulty or unnecessary points of the network. With these disadvantages listed, attempts to shrink the size of a network without hindering it's capacity and efficiency proves to be quite challenging. The reason behind optimizing neural networks is the fact that huge networks still take huge amounts of time to train, not to mention the hardware needs which make it close to impossible to be implemented on an embedded system or any kind of mobile platform.

## References

[1] *Deep learning* I. Goodfellow, Y. Bengio, A. Courville, 2016.
[2] *Recurrent neural network based user classification for smart grids* K. Tornai, A. Oláh, R. Drenyovszki, L. Kovács, I. Pintér, J. Levendovszky, 2017, IEEE Power & Energy Society Innovative Smart Grid Technologies Conference (ISGT), Paper 8086043.
[3] *Deep learning based consumer classification for smart grid* K. Tornai, A. Oláh, R. Drenyovszki, L. Kovács, I. Pintér, J. Levendovszky 2017, Smart grid inspired future technologies: second EAI International Conference, Springer Verlag, 2017. pp. 132-141.

Gy. SZÖVÉRDFFY, "Processing sensor data utilizing machine and deep learning techniques" in *PhD Proceedings Annual Issues of the Doctoral School, Faculty of Information Technology and Bionics, Pázmány Péter Catholic University – 2018.* G. Prószéky, P. Szolgay Eds. Budapest: Pázmány University ePress, 2018, pp. 51–51. This research has been partially supported by the European Union, co-financed by the European Social Fund (EFOP-3.6.3-VEKOP-16-2017-00002).

.

# PROGRAM 5
# On-board Advanced Driver Assistance Systems

Head: Csaba REKECZKY

# NP-complete optimization with continuous-time dynamics

Dóra Eszter BABICZ
(Supervisors: Csaba REKECZKY, András HORVÁTH)
Pázmány Péter Catholic University, Faculty of Information Technology and Bionics
50/a Práter street, 1083 Budapest, Hungary
babicz.dora.eszter@itk.ppke.hu

NP complete problems are efficiently (polynomial time) checkable, but the worst-case complexity of finding a solution is exponential on Turing machines [1]. Because every NP-complete problem can be transformed into a Boolean satisfiability (*k*-SAT) in polynomial time, it increases the relevance of solving these types of problems [2]. Boolean satisfiability problems are a type of constraint satisfaction problems and are considered to be one of the hardest. Converting an NP-complete problem to a Boolean satisfiability (*k*-SAT) problem - can be done in polynomial time. *k*-SAT problems contain conjunctive normal formulas of variables in which every conjunction contains *k* number of variables. It was shown in [3] that *k*-SAT problems can be solved with analogue dynamics, avoiding local traps, and also in polynomial time, but with an exponentially increasing power consumption.

The definition of the *k*-SAT problem is the following: there are given *N* Boolean variables $x_i \in \{0, 1\}$ and a propositional formula $\mathcal{F}$ which is a conjugation form of *M* constraints $C_i$. Each constraint is a disjunctive form of *k* variables $x_i$ or their negations $\bar{x_i}$. Solving this kind of problem means finding an assignment of the variables where all clauses (constraints) are satisfied.

The form of the dynamics used in the circuits are very similar to regular cellular neural network dyanmics and are the following:

$$\frac{\mathrm{d}x_i(t)}{\mathrm{d}t} = -x_i(t) + \sum_j w_{ij} f(x_j(t)) + u_i \qquad (1)$$

where $x_i$ is the state value (activation potential) of the cell, *f(x)* is the output function of the neuron (usually sigmoid), $u_i$ is the input or bias of the neuron and $w_{ij}$ are connection weights between cells $i$ and $j$.

The Continuous-time recurrent neural network can be defined on a bipartite graph with two type of nodes/cells. One is called the "*s*-type" and represents the variables of *k*-SAT. Their state value will be denoted by $s_i$, *i*=1,...,*N* and the output function is defined as the following:

$$f(s_i) = \frac{1}{2}(\mid s_i + 1 \mid - \mid s_i - 1 \mid) \qquad (2)$$

The output of $f(s_i)$ = 1 is assigned to $x_i$ Boolean variable when it is $TRUE$ ($x_i$ = 1) and if the variable is $FALSE$ ($x_i$ = -1), then $f(s_i)$ = -1, but between these two extrema, any continuous value is allowed, meaning *f*($s_i$) $\in$ [-1,1]. The self-coupling parameter will be a fixed value $w_{ii}$ = *A* and the input is $u_i$ = 0 $\forall i$.

The other type of the cells represent the constraints of *k*-SAT with value $a_m$, *m*=1, ..., *M* and with the output function of:

$$g(a_m) = \frac{1}{2}(1 + \mid a_m \mid - \mid a_m - 1 \mid) \qquad (3)$$

The "*a*-type" cells determine the impact of a clause at a given moment on the dynamics of the state (*s*) variables. When the clause is true, then *g*($a_m$) = 0 and *g*($a_m$) = 1 if it is false. For these cells the self coupling $w_{mm}$ = *B* and the input is $u_m$ = *u* = 1 - *k* where k is the number of variables in the clause, in this case $k = 3$.

The dynamics fulfill the following requirements:

- They have continuous-time dynamics
- All states, constraints and variables remain bounded
- The derivative of the dynamics is zero if and only if the formula is satisfied
- Starting from a chosen initial condition the system converges to a solution without getting trapped

The proof of the last two points along with a more detailed description can be found in [4]. An example problem in conjunctive form is the following:

$$(\neg A_1 \vee A_2 \vee V) \wedge (A_1 \vee \neg A_2 \vee V) \wedge (A_1 \vee A_2 \vee \neg V) \wedge (\neg A_1 \vee \neg A_2 \vee \neg V) \wedge (\neg C \vee H \vee G) \wedge (D \vee H \vee F)$$

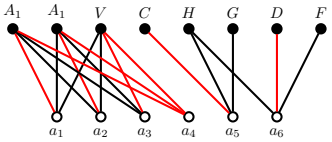


Fig. 1. Bipartite graph of the example problem

## REFERENCES

[1] Michael, R. Garey, and S. Johnson David. "Computers and intractability: a guide to the theory of NP-completeness." WH Freeman and Co., San Francisco (1979).
[2] Cook, Stephen A. "The complexity of theorem-proving procedures." Proceedings of the third annual ACM symposium on Theory of computing. ACM, 1971.
[3] Ercsey-Ravasz, Maria, and Zoltan Toroczkai. "Optimization hardness as transient chaos in an analog approach to constraint satisfaction." Nature Physics 7.12 (2011): 966-970.
[4] Molnar, Botond, Zoltan Toroczkai, and Maria Ercsey-Ravasz. "Continuous-time neural networks without local traps for solving Boolean satisfiability." Cellular Nanoscale Networks and Their Applications (CNNA), 2012 13th International Workshop on. IEEE, 2012.

D. BABICZ, "NP-complete optimization with continuous time dynamics" in *PhD Proceedings Annual Issues of the Doctoral School, Faculty of Information Technology and Bionics, Pázmány Péter Catholic University – 2018.* G. Prószéky, P. Szolgay Eds. Budapest: Pázmány University ePress, 2018, pp. 54–54.
This research has been partially supported by the European Union, co-financed by the European Social Fund (EFOP-3.6.3-VEKOP-16-2017-00002).

# Brick Segmentation In Archaeological Masonry Walls Using Point Cloud Data

Yahya IBRAHIM
(Supervisor: Csaba BENEDEK)
Pázmány Péter Catholic University, Faculty of Information Technology and Bionics
50/a Práter street, 1083 Budapest, Hungary
ibrahim.yahya@itk.ppke.hu

***Abstract*—3D Laser Scanning is being increasingly applied in archaeology and heritage sites due to its numerous advantages. The literature shows the value of making a point cloud segmentation in the 3d point cloud data taken in archaeological sites. The algorithms applied in this field are limited and done only by 2d image processing algorithms. This paper proposes a new algorithm that focused on automatic processing of point clouds to segment the bricks in the archaeological masonry walls that take a shape of cylinder. The algorithm depends on the density and color information of the 3D point cloud. The method is tested on the point cloud of four different walls and the results of the brick detection are presented. The initial results are promising.**

***Keywords*-brick segmentation; archaeological masonry walls; 3D point cloud segmentation**

## I. Introduction

In the last decade, machine vision techniques have been increasingly used in order to assist the process of cultural heritage documentation, preservation, and restoration. Typically the objective of studied algorithms is a general structural damage detection which use segmentation and classification methods in bricks detection. Most of the previous work done in this field is limited and mostly done by means of image processing, and only for a wall that formulates flat plane.
Noelia et. al. [1] present an automatic image-based delineation algorithm to objectivize and standardize the analysis and decision process, that leads to determine the degree of protection of built heritage. Riveiro et. al. [2] present a color-based algorithm that automatically segments masonry structures, this method is based on an improved marker-controlled watershed with good results in a flat plane.

## II. Proposed Method

Masonry is a heterogeneous material that consists of units (bricks, stone, etc.) and joints (mortar, dry, etc.). An algorithm focused on automatic processing of point clouds was developed. This algorithm may be summarized in three main steps: First, data pre-processing. The objectives of this step are: finding the best fitting surface to all points in the point cloud, and then projecting these points to a 2D dimension coordinate (finding the color image and the depth image). Second, depth image analysis: calculate, as good as possible, the marker that represents the mortar between the bricks. In the depth image, a cell consists of 2D rectangle in multi-scale dimensions is selected, 10 different scales are selected. The best obtained result was by choosing the points that less than the ( ($y_{max}$ - $y_{min}$) / 2) to represent the marker of the mortar at each scale. The final marker is selected by choosing the points which have been selected in 7 different scales. Third, color image processing: by useing the achieved marker to make a good bricks segmentation. Before applying the watershed algorithm, we convert the rgb values to hsv (hue, saturation, and value), so we can untangle the effect of the variability of the surface light because of the difference in lighting parts of bricks and mortar. Figure (1) represents the result by applying the watershed on the hue channel of the image by using the obtained marker.

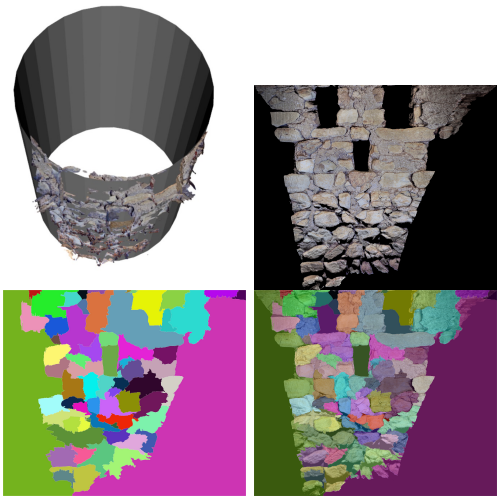

Fig. 1. The obtained surface that fits the wall (top- left), the obtained color image of the wall (top-right), the watershed algorithm result (down)

## III. Conclusion and Further work

The results above show the success of the proposed algorithm to segment the bricks in masonry wall in our provided data. Future work will focus on testing the algorithm on other data, increasing the accuracy of the segmentation step, finding a way to compute the accuracy of the algorithm and comparing it with the state-of-the-art algorithms proposed in this field of study.

## Acknowledgment

This work was supported by the National Research, Development and Innovation Fund (grants NKFIA K-120233 and KH-125681), and by the Széchenyi 2020 Program (grants EFOP-3.6.2-16-2017-00013 and 3.6.3-VEKOP-16-2017-00002).

## References

[1] N. Oses, F. Dornaika, and A. Moujahid, "Image-based delineation and classification of built heritage masonry," *Remote Sensing*, vol. 6, no. 3, p. 1863–1889, 2014.
[2] B. Riveiro, B. Conde-Carnero, H. González-Jorge, P. Arias, and J. Caamaño, "Automatic creation of structural models from point cloud data: The case of masonry structures," *ISPRS Annals of Photogrammetry, Remote Sensing and Spatial Information Sciences*, vol. II-3/W5, p. 3–9, 2015.

Y. IBRAHIM, "Brick Segmentation In Archaeological Masonry Walls Using Point Cloud Data" in *PhD Proceedings Annual Issues of the Doctoral School, Faculty of Information Technology and Bionics, Pázmány Péter Catholic University – 2018.* G. Prószéky, P. Szolgay Eds. Budapest: Pázmány University ePress, 2018, pp. 55–55. This research has been partially supported by the European Union, co-financed by the European Social Fund (EFOP-3.6.3-VEKOP-16-2017-00002).

# Improving image quality during SPECT imaging using artificial intelligence

Ákos KOVÁCS[1, 2]
(Supervisor: Dr. András HORVÁTH[1], Dr. Tamás BÜKKI[2])
[1]Pázmány Péter Catholic University, Faculty of Information Technology and Bionics
50/a Práter street, 1083 Budapest, Hungary
[2]Mediso Kft.
3 Laborc street, 1037 Budapest, Hungary
kovacs.akos@itk.ppke.hu

***Abstract*—SPECT (Single Photon Emission Computed Tomography) technology, which is a medical imaging technique, has been an important part of the diagnosis of certain disease groups for decades. Improving image quality during SPECT imaging using artificial intelligence can help in diagnostics, and can reduce the required radiopharmacon dosage of the measurement. [1]**

**In my first half year of my PhD I have implemented multiple reconstruction softwares for image reconstruction in C++, CUDA and MATLAB. I have experimented with various neural networks in TensorFlow and made preliminary steps for a noise filtering artificial network implementation for SPECT. [2]**

***Keywords*-medical imaging; SPECT; AI; artificial intelligence;**

## I. Summary

There are many possible entering steps into the SPECT processing pipeline with artificial intelligence. One can correct the measurements with filtering, or simulating measurements for missing angles. There are several possibilities to improve reconstruction. First of all we can replace traditional methods with trained neural networks. Reconstruction softwares have many parameters and an AI could select them automatically. Filtering reconstructed volumes, segmentation and lesion detection are all feasible for neural networks and all can be necessary for an appropriate diagnosis.

During my studies including my MSc. and the first half year of my PhD I have implemented 3 different reconstruction softwares. Neural networks can improve each methods performance, so the target area can specify which software should we use. These softwares are:

- Ray driven ML-EM reconstruction software in C++ with CUDA acceleration
- FBP optimized for Mediso SPECT Camera Systems
- ML-EM based reconstruction software with rotational projectors in MATLAB with optional GPU acceleration

## II. Preliminary results for image regression with UNET architecture

With my U-NET implementation, which is capable of image regression I have preliminary results. Results on the training set can be seen on Fig. 1, and on the test set Fig. 2. First column is the reconstructed slice with my own FBP algorithm. The second column is the enhanced version with the U-NET like neural network. The third column represents the ideal phantom, which was used during simulation. The network is trained only on 928 slice extracted from reconstructed 3D volumes.

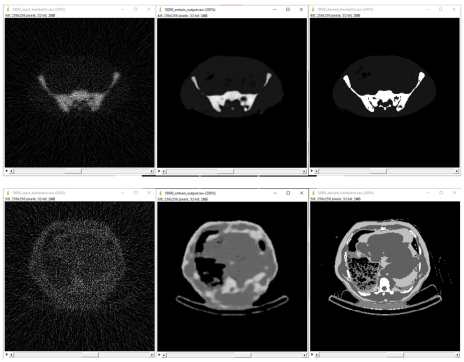

Fig. 1. Preliminary image regression results on training data. First column is the reconstructed slice with my own FBP algorithm. The second column is the enchanced version with the U-NET like neural network. [3] The third column represents the ideal phantom, which was used during simulation.

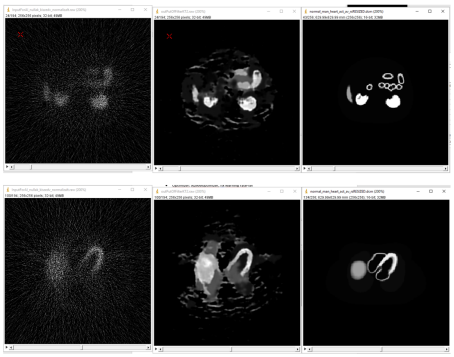

Fig. 2. Preliminary image regression results on test data. Columns are the same as in Fig 1.

The preliminary results are encouraging, but more sophisticated developments are required.

## References

[1] M. N. Wernick and J. N. Aarsvold, *Emission Tomography: The Fundamentals of PET and SPECT*. Elsevier, Dec. 2004. Google-Books-ID: R5slur_hdfEC.

[2] M. Abadi, P. Barham, J. Chen, Z. Chen, A. Davis, J. Dean, M. Devin, S. Ghemawat, G. Irving, M. Isard, M. Kudlur, J. Levenberg, R. Monga, S. Moore, D. G. Murray, B. Steiner, P. Tucker, V. Vasudevan, P. Warden, M. Wicke, Y. Yu, and X. Zheng, "TensorFlow: A system for large-scale machine learning," *arXiv:1605.08695 [cs]*, May 2016. arXiv: 1605.08695.

[3] O. Ronneberger, P. Fischer, and T. Brox, "U-Net: Convolutional Networks for Biomedical Image Segmentation," *arXiv:1505.04597 [cs]*, May 2015. arXiv: 1505.04597.

Á. KOVÁCS, "Improving image quality during SPECT imaging using artificial intelligence" in *PhD Proceedings Annual Issues of the Doctoral School, Faculty of Information Technology and Bionics, Pázmány Péter Catholic University – 2018.* G. Prószéky, P. Szolgay Eds. Budapest: Pázmány University ePress, 2018, pp. 56–56. This research has been partially supported by the European Union, co-financed by the European Social Fund (EFOP-3.6.3-VEKOP-16-2017-00002).

# Challenges in sensor fusion

Lóránt KOVÁCS
(Supervisor: Ákos ZARÁNDY)
Pázmány Péter Catholic University, Faculty of Information Technology and Bionics
50/a Práter street, 1083 Budapest, Hungary
kovacs.lorant@itk.ppke.hu

## I. Introduction

The use of autonomous vehicles require that the controller system is always aware of the vehicle's surroundings, at all kind of weather-, road- and traffic conditions. The vehicle has to be able to respond to the change in its environment as quickly as it can, and as the safety requirements set. This requires a hardware, capable of both collecting the sensor data and processing them with the fusion algorithm. This algorithm has to be designed and developed with respect to both its time- and safety critical attributes.

## II. Sensor selection and placement

To observe the vehicle surroundings in different light conditions, the use of sensors with different modalities is implied.

The cameras are the most sensitive for the changing weather and light conditions: dawn, rain, snow, etc. Radars work well in poor visibility conditions. Lidars give the possibility to measure the objects size.

With the use of multiple sensors from the different modalities, and by placing them properly on the vehicle, the rest of the vehicle neighbourhood can be observed. As the autonomous driving is a safety critical application, the duplication of the most important sensors might be required. The forward looking sensors could be considered for this, as they look towards the travelling direction of the vehicle. While the sideways and rearward looking devices are responsible only for getting information on the overtaking and overtaken vehicles.

Proper sensor placement ensures the coverage of the vehicle surroundings with good spatial and time coverage, and also at different environmental conditions. As the lidars have 3D imaging capability, this can be exploited with high efficiency either on the roof of the car, or at the vehicle corners. Considering a truck or any heavy duty vehicle, the corner alignment can be achieved easily by placing the lidars on the rear view mirrors. The cameras should be mounted as high as possible to have a better view of the world below the horizon. The selected location is usually near the top edge of the windscreen on the front. On the side, there are two approaches either placement of the cameras on the mirrors, or on the door pillars. The radars are placed around the car at the height of the bumper. Depending on the radar type, to cover the sides of the car, it might be required to have multiple radar sensors.

## III. Data collection

Both for the sensor fusion algorithm development, and for the algorithm evaluation, it is required to collect measurement data from real traffic scenarios. A vehicle is needed, fully equipped with the sensor set described above. For exact measurement, the sensors have to be calibrated, and their placement parameters are needed in a common coordinate system, fixed to the vehicle.

Having the parameters of the physical setup of the measurement vehicle, there is a need for an installed data collection hardware with proper software. This has to be capable of recording all the sensor signals with synchronized time.

The recorded data is organized on the top level by the measurement scenario, and by sensors on the bottom. This gives the possibility to handle, process and evaluate the concurrently recorded signals in a proper environment.

## IV. Data fusion algorithm

The publicly available automotive radars usually do not provide interface to get access to the raw detection data of their radar sensors. The only published and available sensor information is based on objects, and their properties: track, position, speed, and sometimes object class and size. This is the so called *track-to-track sensor fusion*.

Houenou et al. described an association method in [1]. The implementation and later the evaluation of this algorithm is in progress. Their solution is splitted into two main parts.

The sensor specific layer is responsible for handling the sensor specific data. Including resampling and even tracking. The output of this layer is universal, all the sensor dependent parameters are removed. From here, all sensor data have the same properties, independent of their originating sensor.

The fusion layer works from universal sensor packages at every timestamp. The tracks are merged, associated. The generated meta-tracks are predicted, resulting system tracks as a result of the fusion algorithm.

For improving this approach [2] and [3] are worthy an extensive evaluation.

## Acknowledgements

This research has been partially supported by the European Union, co-financed by the European Social Fund (EFOP-3.6.3, VEKOP-16-2017-00002). This study was supported by the *Foundation for the Hungarian Vehicle-technical higher education*. We are grateful to fellow engineers for their support: László Lindenmaier, Ádám Szöllősi, Balázs Gál, Viktor Tihanyi and Huba Németh.

## References

[1] A. Houenou, P. Bonnifait, V. Cherfaoui, and J. F. Boissou, "A track-to-track association method for automotive perception systems," *IEEE Intelligent Vehicles Symposium, Proceedings*, pp. 704–710, 2012.

[2] D. Müller, J. Pauli, M. Meuter, L. Ghosh, and S. Müller-Schneiders, "A generic video and radar data fusion system for improved target selection," in *IEEE Intelligent Vehicles Symposium, Proceedings*, pp. 679–684, IEEE, jun 2011.

[3] C. Lundquist, *Sensor Fusion for Automotive Applications*. PhD thesis, Linköping University, 2011.

L. KOVÁCS, "Challenges in sensor fusion" in *PhD Proceedings Annual Issues of the Doctoral School, Faculty of Information Technology and Bionics, Pázmány Péter Catholic University – 2018.* G. Prószéky, P. Szolgay Eds. Budapest: Pázmány University ePress, 2018, pp. 57–57. This research has been partially supported by the European Union, co-financed by the European Social Fund (EFOP-3.6.3-VEKOP-16-2017-00002).

# Applying Deep Learning on Geographic Information Data Analysis

Balázs NAGY
(Supervisor: Csaba BENEDEK)
Pázmány Péter Catholic University, Faculty of Information Technology and Bionics
50/a Práter street, 1083 Budapest, Hungary
nagy.balazs@itk.ppke.hu

***Abstract*—In this paper we take two different scene understanding problems related to Geographic Information Data Analysis and we propose deep convolutional neural network (CNN) based methods to solve them. Our aim is to demonstrate how flexible and efficient the CNN based feature extraction and learning on computer vision tasks without any handcrafted features and complex model or rule based approaches. First we introduce a 3D CNN to segment complex urban environment point cloud data obtained by a mobile laser scanning system (MLS) into 9 different classes. Secondly we propose an U shaped network to segment buried man made structures on archaeological sites obtained by a soil radar.**

***Keywords*-deep learning; GIS; point cloud; archaeology**

## I. Introduction and Related Work

Scene segmentation is a complex and great challenge in computer vision applications. In general, the objective is to assign a label to each part of the given scene, then the label map can serve as an input of further processing steps such as object detection and classification. The segmentation process turn the original data into a label map, which separates the different type of regions into two or more classes.

To segment the scene, most traditional approaches use predefined, handcrafted features, such as intensity, rgb values, edge contours, or texture information. Furthermore they also use expert priors such as different constraints and models to the shape, the neighborhood and the dimensions of the target object. These predefined rules and limitations make it harder to adopt the method to different segmentation problems, where the target objects or the data quality are slightly different from the original problem.

Contrary deep CNN methods extract different features from the input data, and during the training session they optimize for the best feature selections, which give the best segmentation result with the smallest loss. Since they do not use any handcrafted features the models can adopt much easier and we can use the networks to solve different tasks.

We propose a 3D CNN to segment complex urban environment point cloud data obtained by a mobile laser scanning system (MLS) into 9 different classes and we use an U shaped network to perform a binary segmentation to detect buried man made structures on archaeological sites obtained by a soil radar. We demonstrate that with a bit of structure modification CNN are able to manage different type of segmentation problems without any predefined features and rules.

## II. Proposed Approaches

We built a CNN network to handle the $phantom$ effects and the model segments MLS point cloud scenes into 9 different classes ($wall$, $vegetation$, $pole$, $car$, $ground$, $wire$, $streetfurniture$, $phantom$ and $pedestrian$). Fig. 1 demonstrates the qualitative results of the proposed segmentation and Tab. I presents the quantitative results.

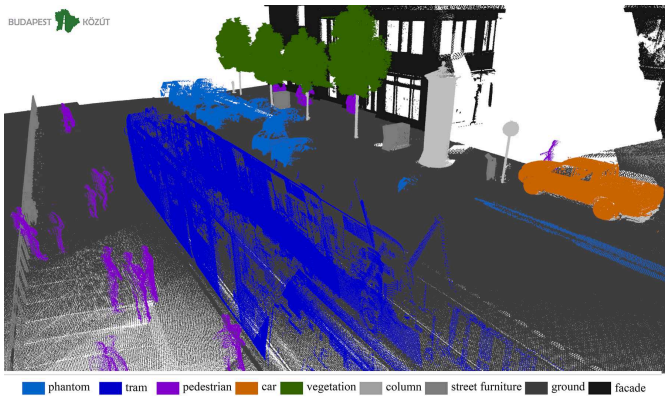


Fig. 1. Labeling result of the proposed 3D CNN based scene segmentation approach (test data provided by Budapest Közút Zrt.).

TABLE I
Quantitative evaluation of the proposed $C^2$-CNN approach for the 7 challenging classes, and comparison with OG-CNN.

| Class | OG-CNN | | | Proposed $C^2$-CNN | | |
|---|---|---|---|---|---|---|
| | Pr % | Rc % | F-r % | Pr % | Rc % | F-r % |
| Phantom | 85.3 | 34.7 | 49.3 | 84.3 | 85.9 | **85.1** |
| Pedestrian | 61.2 | 82.4 | 70.2 | 85.2 | 85.3 | **85.2** |
| Car | 56.4 | 89.5 | 69.2 | 86.4 | 88.7 | **87.5** |
| Vegetation | 72.4 | 83.4 | 77.5 | 98.2 | 95.5 | **96.8** |
| Column | 88.6 | 74.3 | 80.8 | 86.5 | 89.2 | **87.8** |
| Tram/Bus | 91.4 | 81.6 | 86.1 | 89.5 | 96.9 | **93.0** |
| Furniture | 72.1 | 82.4 | 76.9 | 88.8 | 78.8 | **83.5** |
| Overall | 75.3 | 75.5 | 75.4 | 88.4 | 88.6 | **88.5** |

Note: Voxel level Precison (Pr), Recall (Rc) and F-rates (F-r) are given in percent

We introduce a method to detect buried archaeological structures obtained by a soil radar. We can represent the output of the radar as a gray scale image where the width of the image is denoted to the length of the scanned area while the height is represents the scanning depth. On each pixel position the values are depend on the depth and the material properties. Our goal is to perform a pixel wise binary segmentation where the foreground is the valid archaeological objects and structures.

### A. Acknowledgment

The authors would like to thank Budapest Közút Zrt (Road Management Department) for the provision of the Riegl VMX-450 MLS test data. This work was supported by the János Bolyai Research Scholarship of the Hungarian Academy of Sciences and by the National Research, Development and Innovation Fund (NKFIA K 120233).

B. NAGY, "Applying Deep Learning on Geographic Information Data Analysis" in *PhD Proceedings Annual Issues of the Doctoral School, Faculty of Information Technology and Bionics, Pázmány Péter Catholic University – 2018.* G. Prószéky, P. Szolgay Eds. Budapest: Pázmány University ePress, 2018, pp. 58–58. This research has been partially supported by the European Union, co-financed by the European Social Fund (EFOP-3.6.3-VEKOP-16-2017-00002).

# Using neural networks to domain-to-domain transformation

Franciska Sára RAJKI
(Supervisor: Dr. András HORVÁTH)
Pázmány Péter Catholic University, Faculty of Information Technology and Bionics
50/a Práter street, 1083 Budapest, Hungary
rajki.franciska.sara@itk.ppke.hu

***Abstract*—Neural networks became widely popular in the last few years in every science field. They reached breakthrough results in image processing, linguistics etc. However, one of their biggest unsolved problem is, that we can not look inside the "black-box". There is no information about how a decision was made, we only receive the result. Humans classify based on similarities and differences with known objects. I tried to force this strategy to a neural network, to help us understand the reasoning behind decisions.**

## I. Summary

I tried three different networks to perform domain-to-domain transformation; an autoencoder, a U-net[1] (the U-net arcitecture can be seen on Fig 1. ) and a simple convolutional network. The first mentioned worked the best. I implemented an autoencoder neural network which performs a domain-to-domain transformation. An autoencoder is a neural network that is trained to attempt to copy its input to its output (A typical autoencoder structure can be seen on Fig 2.). Internally, it has a hidden layer h that describes a code used to represent the input. The network may be viewed as consisting of two parts: an encoder function h=f(x) and a decoder that produces a reconstruction r=g(h). Autoencoders are designed to be unable to learn to copy perfectly. Usually they are restricted in ways that allow them to copy only approximately, and to copy only input that resembles the training data. Because the model is forced to prioritize which aspects of the input should be copied, it often learns useful properties of the data.[2]

This network is capable of classification and the decisions are interpretable to humans. The constructed network worked properly on the MNIST dataset. The next step is to train the network on more complex databases, where it is more complicated to examine distribution. We still need to find the ultimate best parameters which work properly with any type of datasets. In particular, receptive field size has an important role in the transformation. A unit in convolutional networks only depends on a region of the input. This region in the input is the receptive field for that unit.[3]

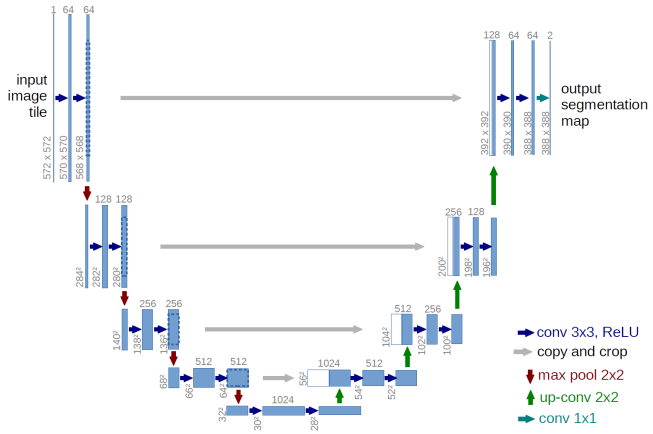


Fig. 1. U-net architecture[1], the networks structure conatins lateral connection between layers, which help the structure to graps elements and features with different resolution.

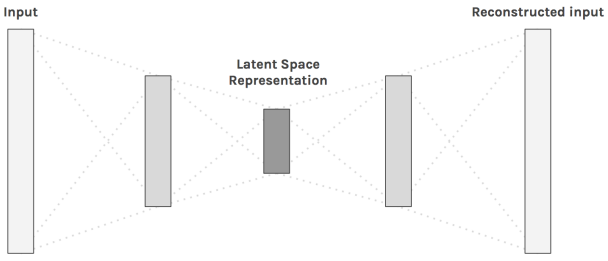


Fig. 2. Autoencoder architecture: an autoencoder forces a lower embedded dimension of the data which ensure optimal reconstructability of the original input data. An autoencoder architecture can also be considered as a non-linear version of the Principal component analysis. (PCA)

## References

[1] O. Ronneberger, P. Fischer, and T. Brox, "U-Net: Convolutional Networks for Biomedical Image Segmentation," *arXiv:1505.04597 [cs]*, May 2015. arXiv: 1505.04597.

[2] I. Goodfellow, J. Pouget-Abadie, M. Mirza, B. Xu, D. Warde-Farley, S. Ozair, A. Courville, and Y. Bengio, "Generative Adversarial Nets," in *Advances in Neural Information Processing Systems 27* (Z. Ghahramani, M. Welling, C. Cortes, N. D. Lawrence, and K. Q. Weinberger, eds.), pp. 2672–2680, Curran Associates, Inc., 2014.

[3] W. Luo, Y. Li, R. Urtasun, and R. Zemel, "Understanding the Effective Receptive Field in Deep Convolutional Neural Networks," *arXiv:1701.04128 [cs]*, Jan. 2017. arXiv: 1701.04128.

F. RAJKI, "Using neural networks to domain-to-domain transformation" in *PhD Proceedings Annual Issues of the Doctoral School, Faculty of Information Technology and Bionics, Pázmány Péter Catholic University – 2018.* G. Prószéky, P. Szolgay Eds. Budapest: Pázmány University ePress, 2018, pp. 59–59. This research has been partially supported by the European Union, co-financed by the European Social Fund (EFOP-3.6.3-VEKOP-16-2017-00002).

# Simulation of an Analogue Circuit Solving Constraint Satisfaction Problems

Dóra Eszter BABICZ, Csaba REKECZKY and András HORVÁTH
Pázmány Péter Catholic University, Faculty of Information Technology and Bionics
50/a Práter street, 1083 Budapest, Hungary

babicz.dora.eszter@itk.ppke.hu

***Abstract*—In this paper we present PSPICE [1] simulation of an analogue circuit, which is capable of solving NP-complete optimization problems in *k*-SAT form [2].**

## I. Introduction

Constraint satisfaction problems are one of the most difficult problems in optimization and a circuit, which can solve such problems with low power-consumption could be used in various areas. These problems pose a significant and important challenge, because almost every difficult, non-polynomial time optimization problem can be formulated and derived back to an NP-complete problem. For this reason a number of algorithms have been developed, which are able to approximate the optimal solution, but at present, all known algorithms which are not using problem specific heuristics for NP-complete problems are superpolynomial in time, and it is unknown whether faster algorithms can be achieved or not. It was shown in [4] that *k*-SAT problems can be solved with analogue dynamics, avoiding local traps, and also in polynomial time, but with an exponentially increasing power consumption.

## II. Boolean satisfiability

A problem is an NP-complete problem if it is NP-hard and NP at the same time. NP-hard problems are non-deterministic polynomial-time hard, meaning that at least as hard as the hardest problem in NP. NP complete problems are efficiently (polynomial time) checkable, but the worst-case complexity of finding a solution is exponential on Turing machines [5]. Because every NP-complete problem can be transformed into a Boolean satisfiability (*k*-SAT) in polynomial time, it increases the relevance of solving these types of problems [3]. The definition of the *k*-SAT problem is the following: there are given *N* Boolean variables $x_i \in \{0,1\}$ and a propositional formula $\mathcal{F}$ which is a conjugation form of *M* constraints $C_i$:

$$\mathcal{F} = C_1 \wedge \cdots \wedge C_m \wedge \cdots \wedge C_M \tag{1}$$

Each constraint is a disjunctive form of *k* variables $x_i$ or their negations $\bar{x_i}$. The formula can be represented as a connection matrix, where each $C_m$constraint denotes a row of a matrix and each column represent a state: $c_{mi}$, *m=1,...,M and i=1,...,N*. Solving this kind of problem means finding an assignment of the variables where all clauses (constraints) are satisfied. The typical hardness of a *k*-SAT formula can be characterized by the ratio of $\alpha = \frac{M}{N}$. In case of small $\alpha$, with only a few constraints/clauses it is easy to satisfy the formula (easy-SAT phase), and for large $\alpha$ with too many constraints proving the unsatisfiability of the formula is easy (UNSAT). But for the intermediate range, deciding satisfiability and finding a solution can be very hard (hard-SAT), and the worst-case complexity of any known algorithm for *k*-SAT ($k \leq 3$) is exponential in *N*. We have chosen $\alpha$ to be 3, this represent a hard problem according to [6]. Some algorithms solving the *k*-SAT problem can be found in [7],[8],[9].

## III. The circuit model

As this section shows, the dynamics defined in [10] can be implemented by an analogue circuit. The form of the dynamics used in the circuits are very similar to regular cellular neural network dyanmics and are the following:

$$\frac{\mathrm{d}x_i(t)}{\mathrm{d}t} = -x_i(t) + \sum_j w_{ij} f(x_j(t)) + u_i \tag{2}$$

where $x_i$ is the state value (activation potential) of the cell, *f(x)* is the output function of the neuron (usually sigmoid), $u_i$ is the input or bias of the neuron and $w_{ij}$ are connection weights between cells $i$ and $j$.
The Continuous-time recurrent neural network can be defined on a bipartite graph with two type of nodes/cells. One is called the "*s*-type" and represents the variables of *k*-SAT. Their state value will be denoted by $s_i$, *i*=1,...,*N* and the output function is defined as the following:

$$f(s_i) = \frac{1}{2}(\mid s_i + 1 \mid - \mid s_i - 1 \mid) \tag{3}$$

The output of $f(s_i)$ = 1 is assigned to $x_i$ Boolean variable when it is $TRUE$ ($x_i$ = 1) and if the variable is $FALSE$ ($x_i$ = -1), then $f(s_i)$ = -1, but between these two extrema, any continuous value is allowed, meaning *f*($s_i$) ∈ [-1,1]. The self-coupling parameter will be a fixed value $w_{ii}$ = *A* and the input is $u_i$ = 0 ∀*i*.
The other type of the cells represent the constraints of *k*-SAT with value $a_m$, *m*=1, ..., *M* and with the output function of:

$$g(a_m) = \frac{1}{2}(1 + \mid a_m \mid - \mid a_m - 1 \mid) \tag{4}$$

The "*a*-type" cells determine the impact of a clause at a given moment on the dynamics of the state (*s*) variables. When the clause is true, then *g*($a_m$) = 0 and *g*($a_m$) = 1 if it is false. For these cells the self coupling $w_{mm}$ = *B* and the input is $u_m$ = *u* = 1 - *k* where k is the number of variables in the clause, in this case $k = 3$.

The dynamical system is also defined via

$$\dot{s}_i(t) = \frac{\mathrm{d}s_i(t)}{\mathrm{d}t} = -s_i(t) + Af(s_i(t)) + \sum_m c_{mi} g(a_m(t)) \tag{5}$$

$$\dot{a}_m(t) = \frac{\mathrm{d}a_m(t)}{\mathrm{d}t} = -a_m(t) + Bg(a_m(t)) - \sum_i c_{mi} f(s_i(t)) + 1 - k \tag{6}$$

Dóra Eszter. BABICZ, Csaba REKECZKY, András HORVÁTH, "Simulation of an Analogue Circuit Solving Constraint Satisfaction Problems" in *PhD Proceedings Annual Issues of the Doctoral School, Faculty of Information Technology and Bionics, Pázmány Péter Catholic University – 2018.* G. Prószéky, P. Szolgay Eds. Budapest: Pázmány University ePress, 2018, pp. 60–60. This research has been partially supported by the European Union, co-financed by the European Social Fund (EFOP-3.6.3-VEKOP-16-2017-00002).

The dynamics and the simulated circuit both fulfill the following requirements: They have continuous-time dynamics; All states, constraints and variables remain bounded; The derivative of the dynamics is zero if and only if the formula is satisfied; Starting from a chosen initial condition the system converges to a solution without getting trapped

The proof of the last two points along with a more detailed description can be found in [10].

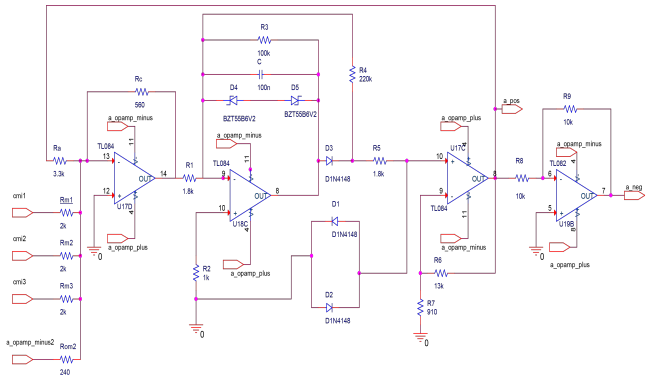

Fig. 1. The circuit design of the "*a*-type" cell. Note that it has three plus one constant inputs (on the left part of the figure) since it is designed for a 3-SAT problem.

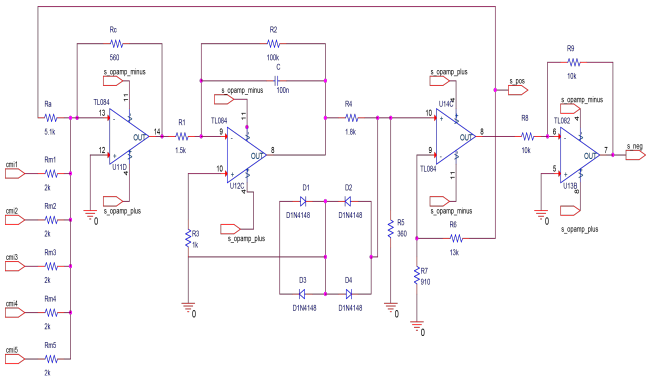

Fig. 2. The circuit design of the "*s*-type" cell. Note that in this example the number of inputs is five meaning that this state variable appears in five constraints. The number of inputs has to be changed according to problem.

The schematic of the circuit model can be seen on figure 1 and figure 2. Both of the circuits are made up of four operational amplifiers, where the first one is responsible for summing the input of other cells, which is a fixed $k$ (plus one input for the constant -2V) in the "*a*-type" cell, because the number of connections is determined by the $k$-SAT problem, and in case of "*s*-type" cells it depends on the number of constraints it is connected to. The main difference between the two cells can be found at the part after the first operational amplifier. As the next step they both realize an integrator, then depending on the corresponding nonlinearity, they clip the signal: for the "*a*-type" cell at $0V$ and $+1V$, while for "*s*-type" cell $-1V$ and $+1V$. The third operational amplifier amplifies the signal ten times to the original value this way it will be more resistant to noise. The last part of both cells is a simple inverter which ensures that both possible connections are feasible: connections with $+1$ and $-1$ weights can be made between a variable and a constraint cell.

## IV. Conclusion

Since NP-complete problems are present in science and technology, the development of efficient solvers is an extremely important task. While CMOS technology reaches its physical limits [11], new ways of computational paradigms must be found. Analog dynamical systems are designed in a way where a number of attractors are interpreted as an output of the computation and the input converges to one of these solutions. The system can be implemented as an analog VLSI device or Cellular Neural/Nonlinear Network (CNN) imitating the nervous system. With the defined dynamics several simulations were ran and experiments were tested to determine whether the system is scalable, is it possible to speed up the process of finding the fix points of the $N$ dimensional space, in other words finding the solution of the NP-complete problem.

## References


[1] Nagel, Laurence William, and Donald O. Pederson. SPICE: Simulation program with integrated circuit emphasis. Electronics Research Laboratory, College of Engineering, University of California, 1973.

[2] Van Leeuwen, Jan. Handbook of theoretical computer science: Algorithms and complexity. Vol. 1. Elsevier, 1990.

[3] Cook, Stephen A. "The complexity of theorem-proving procedures." Proceedings of the third annual ACM symposium on Theory of computing. ACM, 1971.

[4] Ercsey-Ravasz, Maria, and Zoltan Toroczkai. "Optimization hardness as transient chaos in an analog approach to constraint satisfaction." Nature Physics 7.12 (2011): 966-970.

[5] Michael, R. Garey, and S. Johnson David. "Computers and intractability: a guide to the theory of NP-completeness." WH Freeman and Co., San Francisco (1979).

[6] Walsh, Toby. "The constrainedness knife-edge." AAAI/IAAI. 1998.

[7] Schöning, Uwe. "A probabilistic algorithm for k-SAT and constraint satisfaction problems." Foundations of Computer Science, 1999. 40th Annual Symposium on. IEEE, 1999.

[8] Moser, Robin A., and Dominik Scheder. "A full derandomization of schöning's k-SAT algorithm." Proceedings of the forty-third annual ACM symposium on Theory of computing. ACM, 2011.

[9] Marino, Raffaele, Giorgio Parisi, and Federico Ricci-Tersenghi. "The Backtracking Survey Propagation Algorithm for Solving Random K-SAT Problems." arXiv preprint arXiv:1508.05117 (2015).

[10] Molnar, Botond, Zoltan Toroczkai, and Maria Ercsey-Ravasz. "Continuous-time neural networks without local traps for solving Boolean satisfiability." Cellular Nanoscale Networks and Their Applications (CNNA), 2012 13th International Workshop on. IEEE, 2012.

[11] P. Solomon, "Device innovation and material challenges at the limits of CMOS technology," An. Rev. of Materials Science, vol. 30, pp. 681–697, 2000.

# APPENDIX

| PROGRAM 1: Bionics, Bio-inspired Wave Computers, Neuromorphic Models | |
|---|---|
| **Name** | **Supervisor** |
| Luca Anna BORS | Franciska ERDŐ PhD |
| Veronika CSILLAG | Imre FARKAS MD PhD, Zsolt LIPOSITS MD DSc |
| Bianka Vivien FARKAS | Zoltán GÁSPÁRI PhD, Tamás HEGEDŰS PhD |
| Tünde Éva GAIZER | Attila CSIKÁSZ-NAGY PhD |
| Márton Áron GODA | Ferenc KOVÁCS DSc |
| Anna HAJDARA | Sarolta KÁRPÁTI MD DSc, Miklós GYÖNGY PhD |
| Máté HANDBAUER | Zoltán GÁSPÁRI PhD |
| Zita HARMAT | Zoltán GÁSPÁRI PhD |
| Anett HINSENKAMP | Zoltán GÁSPÁRI PhD |
| Kinga KOCSIS | István ULBERT MD DSc |
| Máté MOHÁCSI | Tamás FREUND MHAS, Szabolcs KÁLI PhD |
| György Miklós PERCZEL | László GERENCSÉR DSc, Loránd ERŐSS MD PhD |
| Sára SÁRAY | Tamás FREUND MHAS, Szabolcs KÁLI PhD |
| Beáta Tünde SZABÓ | István ULBERT MD DSc, István WINKLER DSc |
| Csilla SZABÓ | Lucia WITTNER PhD |
| Balázs SZÉKY | Sarolta KÁRPÁTI MD DSc, Miklós GYÖNGY PhD |
| Ádám György SZÉLIG | Kristóf IVÁN PhD |
| Mihály SZÜCS | Kristóf IVÁN PhD |

| PROGRAM 2: Computer Technology Based on Many-core Processor Chips, Virtual Cellular Computers, Sensory and Motoric Analog Computers | |
|---|---|
| **Name** | **Supervisor** |
| Nawar Kadhem AL-HEMEARY | Gábor SZEDERKÉNYI DSc, György CSEREY PhD |
| Áron CSERKASZKY | Péter SZOLGAY DSc |
| Subbareddy DARUKUMALLI | Péter SZOLGAY DSc |
| Márton Zsolt KISS | Ákos ZARÁNDY DSc |
| Zsolt NIKA | Péter SZOLGAY DSc, Miklós RÁSONYI PhD |
| Áron PAPP | György CSEREY PhD |
| Péter POLCZ | Gábor SZEDERKÉNYI DSc |
| Mihály Gergely RADVÁNYI | Péter SZOLGAY DSc, Kristóf KARACS PhD |
| Levente Márk SÁNTHA | Ákos ZARÁNDY DSc, Zoltán NAGY PhD |
| Attila STUBENDEK | Péter SZOLGAY DSc, Kristóf KARACS PhD |
| Gergely SZLOBODNYIK | Gábor SZEDERKÉNYI DSc |

| PROGRAM 3: Feasibility of Electronic and Optical Devices, Molecular and Nanotechnologies, Nano-architectures, Nanobionic Diagnostic and Therapeutic Tools | |
|---|---|
| **Name** | **Supervisor** |
| Krisztián FÜZESI | Miklós GYÖNGY PhD |
| Janka HATVANI | Miklós GYÖNGY PhD |
| Ákos MAKRA | Miklós GYÖNGY PhD |
| Péter MAROSÁN | Miklós GYÖNGY PhD |
| Zsolt MEZRICZKY | Balázs RÓZSA PhD |

| PROGRAM 4: Human Language Technologies, Artificial Understanding, Telepresence, Communication | |
|---|---|
| **Name** | **Supervisor** |
| Máté LŐRINCZ | András OLÁH PhD |
| György SZÖVÉRDFFY | András OLÁH PhD |

| PROGRAM 5: On-board Advanced Driver Assistance Systems | |
|---|---|
| **Name** | **Supervisor** |
| Dóra Eszter BABICZ | Csaba REKECZKY PhD, András HORVÁTH PhD |
| Yahya IBRAHIM | Csaba BENEDEK PhD |
| Ákos KOVÁCS | Tamás BÜKKI PhD, András HORVÁTH PhD |
| Lóránt KOVÁCS | Ákos ZARÁNDY DSc, Levente BALOGH PhD |
| Balázs NAGY | Csaba BENEDEK PhD |
| Franciska Sára RAJKI | András HORVÁTH PhD |